

# Guidelines for Ultrasonic Inspection of Hanger Pins

PUBLICATION NO. FHWA-HRT-04-042

JULY 2004



U.S. Department of Transportation  
**Federal Highway Administration**

Research, Development, and Technology  
Turner-Fairbank Highway Research Center  
6300 Georgetown Pike  
McLean, VA 22101-2296

## **FOREWORD**

In June 1983, a failed hanger pin initiated the tragic collapse of one span of the Mianus River Bridge on the Connecticut Turnpike near Greenwich, CT. This incident resulted in the deaths of three motorists. Following the collapse, there was an immediate increase in interest in the inspection and condition evaluation of bridge hanger pins. Ultrasonic inspection is one of the most reliable methods used to inspect hanger pins, and it has become the primary method of performing a detailed inspection of an in-service hanger pin.

This report provides background information regarding hanger pins in general and discusses the field ultrasonic techniques, including methods, results, and limitations of each method. The report provides a comprehensive document describing the fundamentals of ultrasonic hanger pin inspection and can be used by State transportation agencies that are either inspecting pins themselves or contracting for inspection services. In addition, a limited experimental program was utilized to emphasize, and more completely explain, some important aspects of ultrasonic pin inspection. This report will be of interest to bridge engineers, designers, and inspectors who are involved with the inspection of hanger pin assemblies used in our Nation's highway bridges.

T. Paul Teng, P.E.  
Director, Office of Infrastructure  
Research and Development

## **NOTICE**

This document is disseminated under the sponsorship of the U.S. Department of Transportation in the interest of information exchange. The U.S. Government assumes no liability for its contents or use thereof. This report does not constitute a standard, specification, or regulation.

The U.S. Government does not endorse products or manufacturers. Trade and manufacturers' names appear in this report only because they are considered essential to the object of the document.

Technical Report Documentation Page

1. Report No. HRT-04-042		2. Government Accession No.		3. Recipient's Catalog No.	
4. Title and Subtitle Guidelines for Ultrasonic Inspection of Hanger Pins			5. Report Date July 2004		
			6. Performing Organization Code		
7. Author(s) Mark Moore, P.E., Brent M. Phares, Ph.D., Glenn A. Washer, P.E., Ph.D.			8. Performing Organization Report No.		
9. Performing Organization Name and Address Wiss, Janney, Elstner Associates, Inc. 4165 Shackleford Road, Suite 100 Norcross, GA 30093			10. Work Unit No. (TRAIS)		
			11. Contract or Grant No. DTFH61-98-C-00050		
12. Sponsoring Agency Name and Address Nondestructive Evaluation Validation Center Office of Infrastructure Research and Development Federal Highway Administration 6300 Georgetown Pike McLean, VA 22101-2296			13. Type of Report and Period Covered Final Report January 1998—September 2001		
			14. Sponsoring Agency Code		
15. Supplementary Notes FHWA Contracting Officer's Technical Representative (COTR): Glenn A. Washer, P.E., HRDI-10					
16. Abstract <p>A failed hanger pin initiated the tragic collapse of one span of the Mianus River Bridge in Greenwich, CT on June 28, 1983, resulting in the deaths of three motorists. Following the collapse, there was an immediate increase of interest in the inspection and condition evaluation of bridge hanger pins. Ultrasonic inspection has become the primary method of performing detailed inspection of in-service hanger pins.</p> <p>The document describes the fundamentals of ultrasonic testing and general inspection requirements that can be used by State transportation agencies or by others performing ultrasonic hanger pin inspection. In addition, five hanger pins, with known defects, were inspected to emphasize and more completely explain some important aspects of ultrasonic hanger pin inspection.</p> <p>Items included in the fundamental review are the pulse-echo technique, pitch-catch technique, decibel scale, piezoelectric effect, beam diffraction, beam absorption, beam spread (beam divergence), beam centerline location, and distance amplitude correction. Items included in the general inspection requirement section are cleaning and coupling requirements, interpretation of signals, defect sizing techniques, effect of wear grooves, phenomena of acoustic coupling, inspection documentation, data collection, and inspector qualifications and certifications.</p> <p>Results from the experimental program include beam diffraction graphs, distance amplitude correction curves, sensitivity analysis of straight and angled beams, defect sizing analysis, and verification of the acoustic coupling phenomena.</p>					
17. Key Words Ultrasonic, Bridges, Pin, Nondestructive Evaluation			18. Distribution Statement		
19. Security Classif. (of this report) Unclassified		20. Security Classif. (of this page) Unclassified		21. No. of Pages 107	22. Price

# SI\* (MODERN METRIC) CONVERSION FACTORS

## APPROXIMATE CONVERSIONS TO SI UNITS

Symbol	When You Know	Multiply By	To Find	Symbol
<b>LENGTH</b>				
in	inches	25.4	millimeters	mm
ft	feet	0.305	meters	m
yd	yards	0.914	meters	m
mi	miles	1.61	kilometers	km
<b>AREA</b>				
in <sup>2</sup>	square inches	645.2	square millimeters	mm <sup>2</sup>
ft <sup>2</sup>	square feet	0.093	square meters	m <sup>2</sup>
yd <sup>2</sup>	square yard	0.836	square meters	m <sup>2</sup>
ac	acres	0.405	hectares	ha
mi <sup>2</sup>	square miles	2.59	square kilometers	km <sup>2</sup>
<b>VOLUME</b>				
fl oz	fluid ounces	29.57	milliliters	mL
gal	gallons	3.785	liters	L
ft <sup>3</sup>	cubic feet	0.028	cubic meters	m <sup>3</sup>
yd <sup>3</sup>	cubic yards	0.765	cubic meters	m <sup>3</sup>
NOTE: volumes greater than 1000 L shall be shown in m <sup>3</sup>				
<b>MASS</b>				
oz	ounces	28.35	grams	g
lb	pounds	0.454	kilograms	kg
T	short tons (2000 lb)	0.907	megagrams (or "metric ton")	Mg (or "t")
<b>TEMPERATURE (exact degrees)</b>				
°F	Fahrenheit	5 (F-32)/9 or (F-32)/1.8	Celsius	°C
<b>ILLUMINATION</b>				
fc	foot-candles	10.76	lux	lx
fl	foot-Lamberts	3.426	candela/m <sup>2</sup>	cd/m <sup>2</sup>
<b>FORCE and PRESSURE or STRESS</b>				
lbf	poundforce	4.45	newtons	N
lbf/in <sup>2</sup>	poundforce per square inch	6.89	kilopascals	kPa

## APPROXIMATE CONVERSIONS FROM SI UNITS

Symbol	When You Know	Multiply By	To Find	Symbol
<b>LENGTH</b>				
mm	millimeters	0.039	inches	in
m	meters	3.28	feet	ft
m	meters	1.09	yards	yd
km	kilometers	0.621	miles	mi
<b>AREA</b>				
mm <sup>2</sup>	square millimeters	0.0016	square inches	in <sup>2</sup>
m <sup>2</sup>	square meters	10.764	square feet	ft <sup>2</sup>
m <sup>2</sup>	square meters	1.195	square yards	yd <sup>2</sup>
ha	hectares	2.47	acres	ac
km <sup>2</sup>	square kilometers	0.386	square miles	mi <sup>2</sup>
<b>VOLUME</b>				
mL	milliliters	0.034	fluid ounces	fl oz
L	liters	0.264	gallons	gal
m <sup>3</sup>	cubic meters	35.314	cubic feet	ft <sup>3</sup>
m <sup>3</sup>	cubic meters	1.307	cubic yards	yd <sup>3</sup>
<b>MASS</b>				
g	grams	0.035	ounces	oz
kg	kilograms	2.202	pounds	lb
Mg (or "t")	megagrams (or "metric ton")	1.103	short tons (2000 lb)	T
<b>TEMPERATURE (exact degrees)</b>				
°C	Celsius	1.8C+32	Fahrenheit	°F
<b>ILLUMINATION</b>				
lx	lux	0.0929	foot-candles	fc
cd/m <sup>2</sup>	candela/m <sup>2</sup>	0.2919	foot-Lamberts	fl
<b>FORCE and PRESSURE or STRESS</b>				
N	newtons	0.225	poundforce	lbf
kPa	kilopascals	0.145	poundforce per square inch	lbf/in <sup>2</sup>

\*SI is the symbol for the International System of Units. Appropriate rounding should be made to comply with Section 4 of ASTM E380.  
(Revised March 2003)

## TABLE OF CONTENTS

<b>1. INTRODUCTION</b> .....	1
<b>1.1. BACKGROUND</b> .....	1
<b>1.2. OBJECTIVE</b> .....	1
<b>2. GENERAL INFORMATION</b> .....	3
<b>2.1. ULTRASONIC TESTING EQUIPMENT</b> .....	3
<b>2.1.1. Fundamentals of Ultrasonic Waves</b> .....	3
2.1.1.1. Pulse-Echo Technique.....	6
2.1.1.2. Pitch-Catch Technique.....	10
<b>2.1.2. Decibel Scale</b> .....	12
<b>2.1.3. Transducers</b> .....	12
<b>2.1.4. Ultrasonic Beam Characteristics and Important Formulae</b> .....	15
2.1.4.1. Beam Attenuation.....	15
2.1.4.1.1. <i>Beam diffraction</i> .....	15
2.1.4.1.2. <i>Beam absorption</i> .....	15
2.1.4.2. Beam Spread (Beam Divergence).....	15
2.1.4.3. Beam Centerline Location.....	16
<b>2.1.5. Distance Amplitude Correction</b> .....	17
<b>2.2. GENERAL HANGER PIN INSPECTION REQUIREMENTS</b> .....	19
<b>2.2.1. Cleaning and Coupling Requirements</b> .....	19
<b>2.2.2. Scanning Patterns</b> .....	20
<b>2.2.3. Application and Sensitivity of Straight and Angle Beam Transducers</b> .....	20
<b>2.2.4. Interpretation of Ultrasonic Testing Signals</b> .....	23
<b>2.2.5. Defect Sizing Techniques</b> .....	26
2.2.5.1. Probe Movement Techniques.....	27
2.2.5.1.1. <i>The 6-dB drop technique</i> .....	27
2.2.5.1.2. <i>The 20-dB drop technique</i> .....	27
2.2.5.1.3. <i>The time-of-flight diffraction technique</i> .....	28
2.2.5.2. Amplitude Techniques.....	28
2.2.5.2.1. <i>The comparator block technique</i> .....	28
2.2.5.2.2. <i>The distance amplitude correction technique</i> .....	29
2.2.5.2.3. <i>The distance grain size technique</i> .....	29
<b>2.2.6. Wear Grooves</b> .....	29
<b>2.2.7. Acoustic Coupling</b> .....	30
<b>2.3. INSPECTION DOCUMENTATION</b> .....	31
<b>2.3.1. Physical Measurements</b> .....	32
<b>2.3.2. Visual Assessments</b> .....	33
<b>2.3.3. Ultrasonic Testing Data Collection</b> .....	34
<b>2.4. INSPECTOR QUALIFICATIONS AND CERTIFICATIONS</b> .....	38
<b>3. EXPERIMENTAL PROGRAM</b> .....	41
<b>3.1. INTRODUCTION</b> .....	41
<b>3.2. INSPECTION SPECIMENS</b> .....	41
<b>3.2.1. Side-Drilled Hole Test Block</b> .....	41

**TABLE OF CONTENTS (CONTINUED)**

3.2.2.	Manufactured Cracked Pins.....	43
3.2.3.	Pin/Hanger Mockup.....	46
3.3.	TESTING PROGRAM.....	47
3.3.1.	Beam Diffraction.....	48
3.3.2.	Distance Amplitude Correction.....	48
3.3.3.	Angle and Straight Beam Sensitivity to Cracks.....	48
3.3.4.	Defect Sizing.....	48
3.3.5.	Acoustic Coupling.....	49
4.	EXPERIMENTAL RESULTS.....	51
4.1.	BEAM DIFFRACTION.....	51
4.2.	DISTANCE AMPLITUDE CORRECTION.....	64
4.3.	ANGLE AND STRAIGHT BEAM SENSITIVITY TO CRACKS.....	68
4.4.	DEFECT SIZING.....	79
4.5.	ACOUSTIC COUPLING.....	80
5.	CONCLUDING REMARKS.....	99

## LIST OF FIGURES

Figure 1. Model of an elastic material.....	4
Figure 2. Longitudinal wave .....	4
Figure 3. Shear wave.....	4
Figure 4. Basic principle of pulse-echo technique .....	6
Figure 5. Sketch of a typical ultrasonic A-scan.....	7
Figure 6. Influence of distance on reflected ultrasonic signal.....	8
Figure 7. Influence of shadow effects on ultrasonic signal.....	9
Figure 8. Influence of defect orientation on ultrasonic signal.....	9
Figure 9. Influence of defect size on ultrasonic signal.....	10
Figure 10. Schematic of direct pitch-catch technique .....	11
Figure 11. Schematic of indirect pitch-catch technique .....	11
Figure 12. Piezoelectric effect.....	13
Figure 13. Schematic of a straight beam piezoelectric ultrasonic probe.....	14
Figure 14. Schematic of an angle beam piezoelectric ultrasonic probe .....	14
Figure 15. Concept for generating distance amplitude correction curves.....	18
Figure 16. Typical pin/hanger assembly .....	21
Figure 17. Application of a straight beam transducer .....	22
Figure 18. Application of an angle beam transducer.....	23
Figure 19. Typical physical measurements .....	32
Figure 20. Sample ultrasonic test data.....	36
Figure 21. SDHTB details .....	42
Figure 22. Photograph of the SDHTB.....	42
Figure 23. Typical pin geometry .....	43
Figure 24. Pin 1 defect details .....	44
Figure 25. Pin 2 defect details.....	44
Figure 26. Pin 3 defect details.....	45
Figure 27. Pin 4 defect details.....	45
Figure 28. Pin 5 defect details.....	46
Figure 29. Pin/hanger mockup details.....	47
Figure 30. Beam diffraction results for 8-degree, 5-MHz, 12.7-mm diameter transducer .....	52
Figure 31. Beam diffraction results for 0-degree, 5-MHz, 12.7-mm diameter transducer .....	54
Figure 32. Beam diffraction results for 0-degree, 2.25-MHz, 25.4-mm diameter transducer .....	56
Figure 33. Beam diffraction results for 11-degree, 2.25-MHz, 12.7-mm diameter transducer .....	58
Figure 34. Beam diffraction results for 14-degree, 2.25-MHz, 12.7-mm diameter transducer .....	60
Figure 35. Beam diffraction results for 8-degree, 2.25-MHz, 19-mm square transducer .....	62
Figure 36. Distance amplitude correction curve for 8-degree, 5-MHz, 12.7-mm diameter transducer.....	64
Figure 37. Distance amplitude correction curve for 0-degree, 5-MHz, 12.7-mm diameter transducer.....	65
Figure 38. Distance amplitude correction curve for 0-degree, 2.25-MHz, 25.4-mm diameter transducer.....	65
Figure 39. Distance amplitude correction curve for 11-degree, 2.25-MHz, 12.7-mm diameter transducer.....	66
Figure 40. Distance amplitude correction curve for 14-degree, 2.25-MHz, 12.7-mm diameter transducer.....	66

**LIST OF FIGURES (CONTINUED)**

Figure 41. Distance amplitude correction curve for 8-degree, 2.25-MHz, 19-mm square transducer .....67

Figure 42. Pin 1 testing results .....69

Figure 43. Pin 2 testing results .....71

Figure 44. Pin 3 testing results .....73

Figure 45. Pin 4 testing results .....75

Figure 46. Pin 5 testing results .....77

Figure 47. Photograph of pulse-echo setup using 14-degree transducer.....81

Figure 48. UT scan utilizing pulse-echo technique with a 14-degree transducer .....81

Figure 49. Photograph of pitch-catch setup using 0-degree transducers.....84

Figure 50. UT scan utilizing pitch-catch technique using 0-degree transducers.....84

Figure 51. Photograph of pitch-catch setup using 0-degree receiving and 14-degree transmitting transducers .....90

Figure 52. UT scan utilizing pitch-catch technique using 0-degree and 14-degree transducers...90

## LIST OF TABLES

Table 1.	Defect size data.....	79
Table 2.	Defect sizing error.....	79
Table 3.	Absolute value of defect sizing error.....	80



## **1. INTRODUCTION**

### **1.1. BACKGROUND**

A failed hanger pin initiated the tragic collapse of one span of the Mianus River Bridge in Greenwich, CT, on June 28, 1983, resulting in the deaths of three motorists. The collapse sparked an immediate increase of interest in the inspection and condition evaluation of bridge hanger pins. Ultrasonic inspection has become the primary method of performing detailed inspection of in-service hanger pins.

### **1.2. OBJECTIVE**

The research objective is to develop a document describing the fundamentals of ultrasonic hanger pin inspection that can be used by State transportation agencies that are either inspecting pins themselves or contracting for inspection services. In addition, a limited experimental program is utilized to emphasize, and more completely explain, some important aspects of ultrasonic pin inspection.



## **2. GENERAL INFORMATION**

The following sections summarize the basics of ultrasonic testing. Also, specific requirements and recommendations for ultrasonic pin inspections are presented. Together, this information should be adequate for individual users to develop and execute a successful ultrasonic pin inspection program.

### **2.1. ULTRASONIC TESTING EQUIPMENT**

Ultrasonic testing uses the mechanical sound waves generated in test specimens to assess structural integrity and to make material property measurements. A fundamental understanding of how sound travels through a material is necessary to understanding fully how ultrasonic testing equipment is used.

#### **2.1.1. Fundamentals of Ultrasonic Waves**

Unlike light waves, sound waves move a discrete volume of the material as they pass through a test specimen. This mechanical movement occurs about the material's neutral position and is most commonly described by the number of cycles about the neutral position per second. The number of cycles per second, or frequency, of sound waves is measured in Hertz (Hz) and can be divided into three discrete ranges. Sound with a frequency below approximately 10 Hz is known as subsonic and is inaudible. Likewise, sound with a frequency above 20,000 Hz is known as ultrasonic and is also inaudible.

Assuming that the test material through which sound passes has not been stressed beyond its elastic limit, the material can be modeled as a system of discrete masses connected in a grid-like manner to adjacent masses with elastic springs. This system is depicted in figure 1. If all of the masses on the left side of the model are excited at the same time with the same force to the right, then all of the particles in the first plane are forced to oscillate to the right by the same amount. This oscillation of the first plane of masses changes the length of the spring between the first and second planes. This change in spring length forces the second plane of masses to also oscillate. After the second plane has begun oscillating, forces are induced in the third plane and so on. These oscillations, and the resulting transfer of forces to adjacent masses, result in a regular movement of each particle about its neutral position with respect to the movement of the adjacent masses. This type of planer movement of masses is referred to as a longitudinal wave

because the waves move in the longitudinal direction (i.e., the direction of wave propagation). Figure 2 illustrates a snapshot of a longitudinal wave in a two-dimensional slice of a material. In solid bodies, another kind of wave can also exist; these transverse, or shear, waves occur when particles oscillate at a right angle to the direction of the longitudinal wave propagation. A snapshot of a shear wave is illustrated in figure 3.

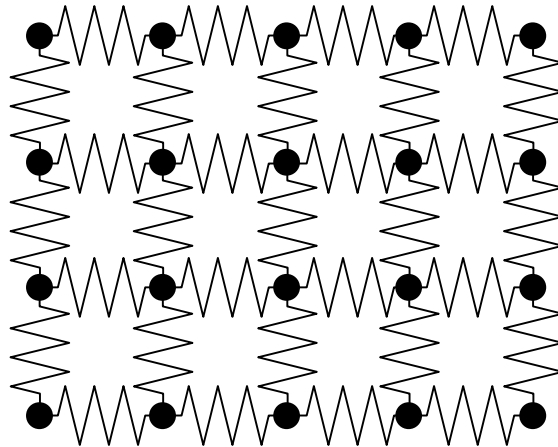


Figure 1. Model of an elastic material.

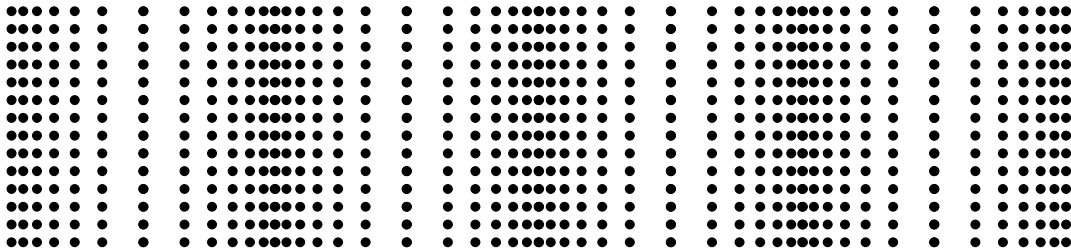


Figure 2. Longitudinal wave.



Figure 3. Shear wave.

A number of important interdependent wave and material property relationships are needed to understand ultrasonic testing fully. The following list defines some of the most frequently cited quantities, their symbols, and their units of measure:

Quantity	Symbol	Unit of Measure
• Frequency	$f$	cycles per second (Hz)
• Wavelength	$\lambda$	meter (m)
• Velocity of sound	$c$	meters per second (m/s)
• Density	$\rho$	kilograms per meter cubed (kg/m <sup>3</sup> )
• Poisson's ratio	$\mu$	not applicable
• Modulus of elasticity	$E$	newtons per meter squared (N/m <sup>2</sup> )
• Shear modulus	$G$	N/m <sup>2</sup>

The following relationship is valid for all wave types (longitudinal and shear):

$$f\lambda = c \quad (1)$$

For longitudinal and shear waves, respectively, the following relationships relate the elastic material constants to the speed of sound in the material:

$$\text{(longitudinal)} \quad c_l = \sqrt{\frac{E}{\rho} \frac{1-\mu}{(1+\mu)(1-2\mu)}} \quad (2)$$

$$\text{(shear)} \quad c_s = \sqrt{\frac{E}{\rho} \frac{1}{2(1+\mu)}} = \sqrt{\frac{G}{\rho}} \quad (3)$$

Combining these equations, the two velocities are related by the following relationship:

$$\frac{c_s}{c_l} = \sqrt{\frac{1-2\mu}{2(1-\mu)}} \quad (4)$$

### 2.1.1.1. Pulse-Echo Technique

Figure 4 demonstrates the basic principle of the pulse-echo ultrasonic testing technique. A transmitter transforms the energy of an electrical voltage into an ultrasonic wave. The ultrasonic wave travels through the material at a velocity dependent upon the material's properties. The ultrasonic wave travels through the material until a discontinuity (i.e., a defect) or the test specimen boundary reflects the signal. The reflected signal travels back through the material to a receiver. The receiver converts the mechanical energy back to electrical energy, which is then amplified. The amplified signal or echo is displayed on the instrument screen as an A-scan, as illustrated in figure 5. The horizontal axis of the display is proportioned to the transit time (often the horizontal axis is calibrated to indicate distance to the reflector) and the vertical axis corresponds to the amplitude of the echo. In summary, in pulse-echo testing, the presence, size, and location of a defect are related to the echo signal amplitude and the time at which the echo signal arrives at the receiver. The primary advantage of the pulse-echo technique is its adaptability to large, irregularly shaped test specimens. The major disadvantage of the pulse-echo technique is the loss of sensitivity near the test surface due to the coupling of the transducer with the test specimen. Prior to entering the test specimen, the ultrasonic signal generally must pass through several materials, which may include couplant, a plexiglass shoe, and a transducer body. Reflected signals produced at each of these material interfaces produces a reflector, which is seen in the A-scan as near-field noise. Typically in ultrasonic pin inspections utilizing the pulse-echo technique, the transmitter and receiver are constructed in a single housing.

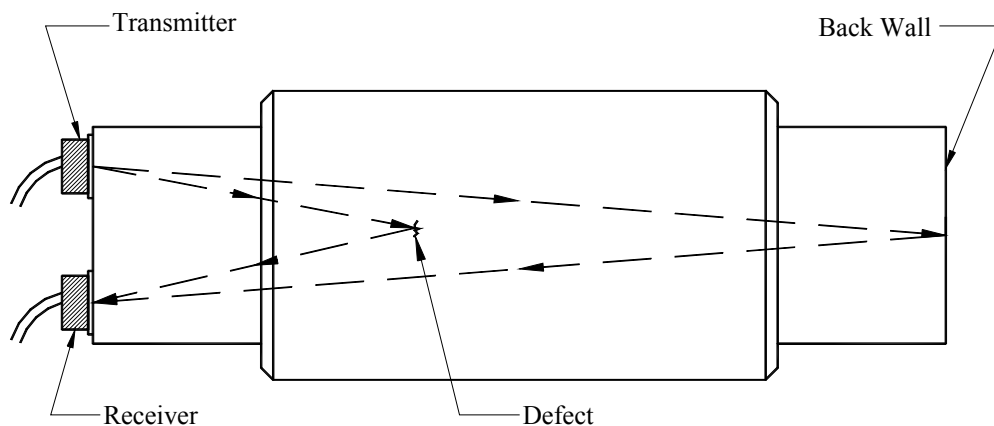


Figure 4. Basic principle of pulse-echo technique.

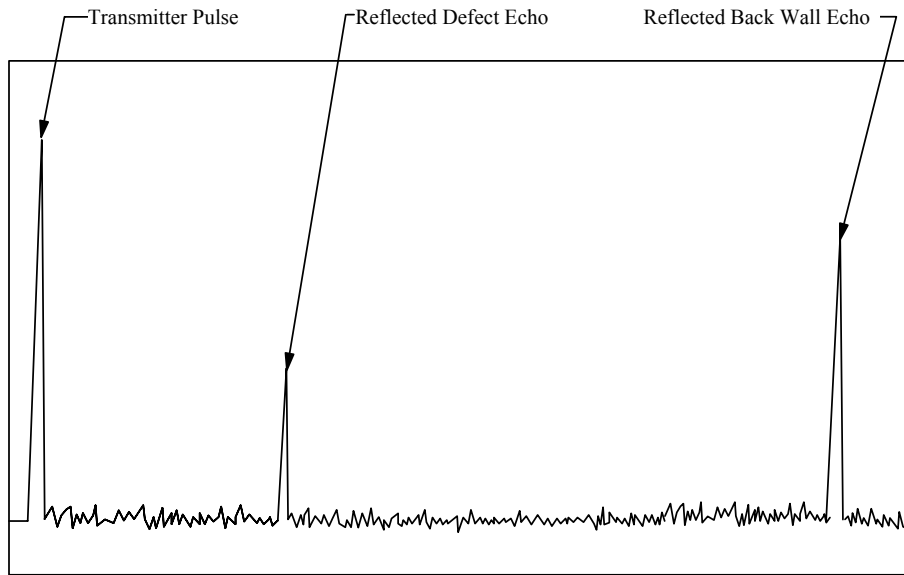


Figure 5. Sketch of a typical ultrasonic A-scan.

The amplitude of the received echo in pulse-echo testing depends on several influencing factors:

- Transmitter power.
- Direction of transmission.
- Size of the reflector.
- Surface qualities of the reflector.
- Position and orientation of the reflector.
- Size and orientation of receiver.
- Loss of signal at receiver due to re-reflection and lack of coupling.
- Attenuation of sound wave due to absorption and scattering.
- Shadow effects.

Figure 6 illustrates the effect of distance on signal amplitude: The signal amplitude from two equivalent defects is reduced for the defect at a greater distance. Figure 7 illustrates shadow effects. In this scan, the presence of the smaller defect is masked by the larger defect, which shields it from the ultrasonic signal. Figure 8 illustrates the effect of defect orientation. Although this figure indicates that no signal would be detected, this really is not the case.

Rather, a much reduced signal would actually be detected as a result of scattering of the beam at the defect. Figure 9 illustrates the influence of defect size. As can be seen, with all else equivalent (for illustrative purposes, the two defects have been shown at slightly different locations here), a larger defect will reflect more ultrasonic energy, yielding a greater amplitude.

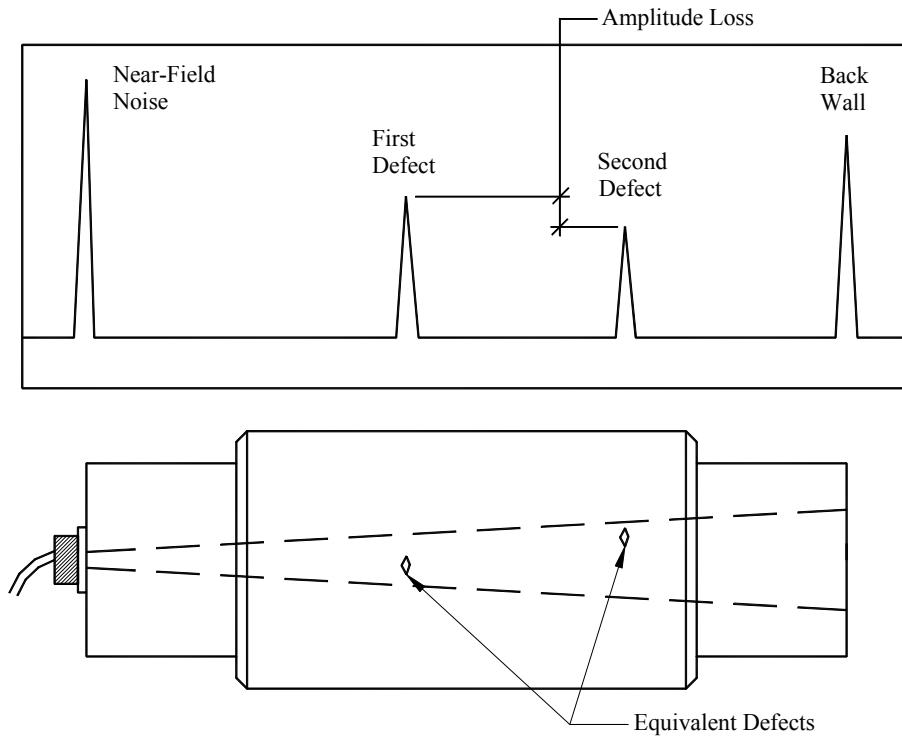


Figure 6. Influence of distance on reflected ultrasonic signal.

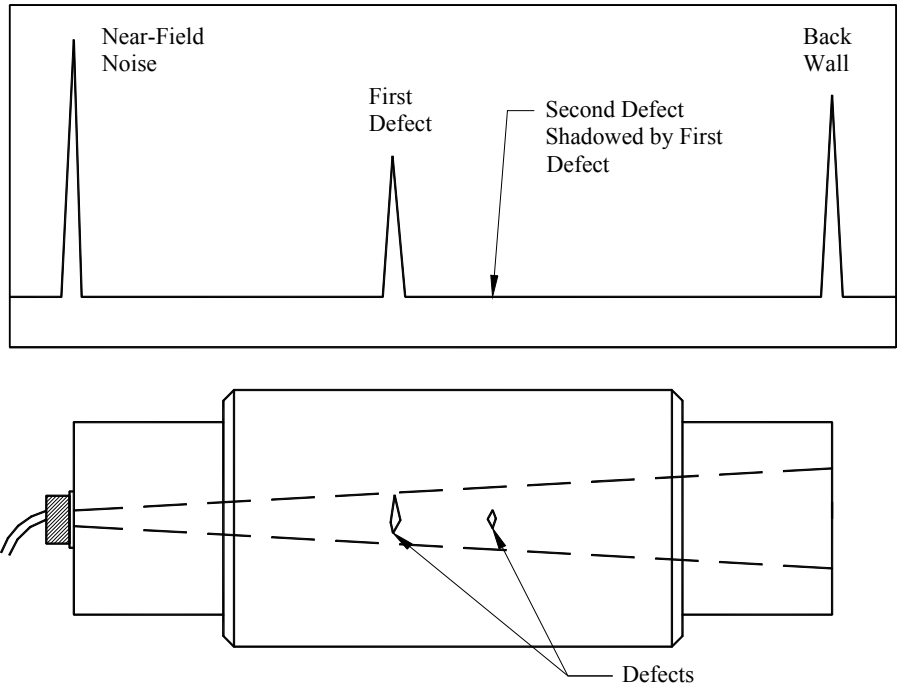


Figure 7. Influence of shadow effects on ultrasonic signal.

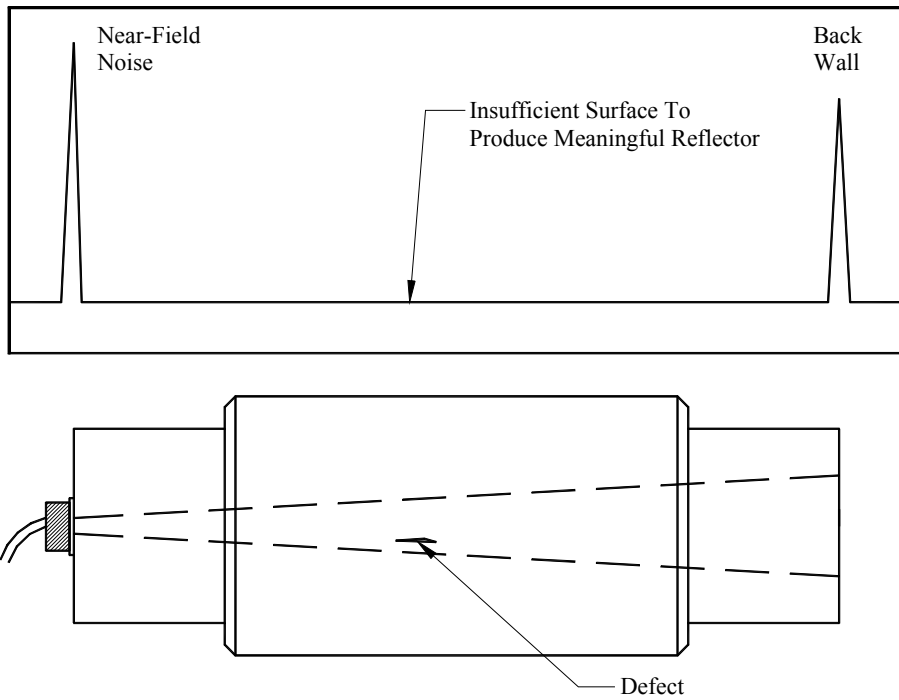


Figure 8. Influence of defect orientation on ultrasonic signal.

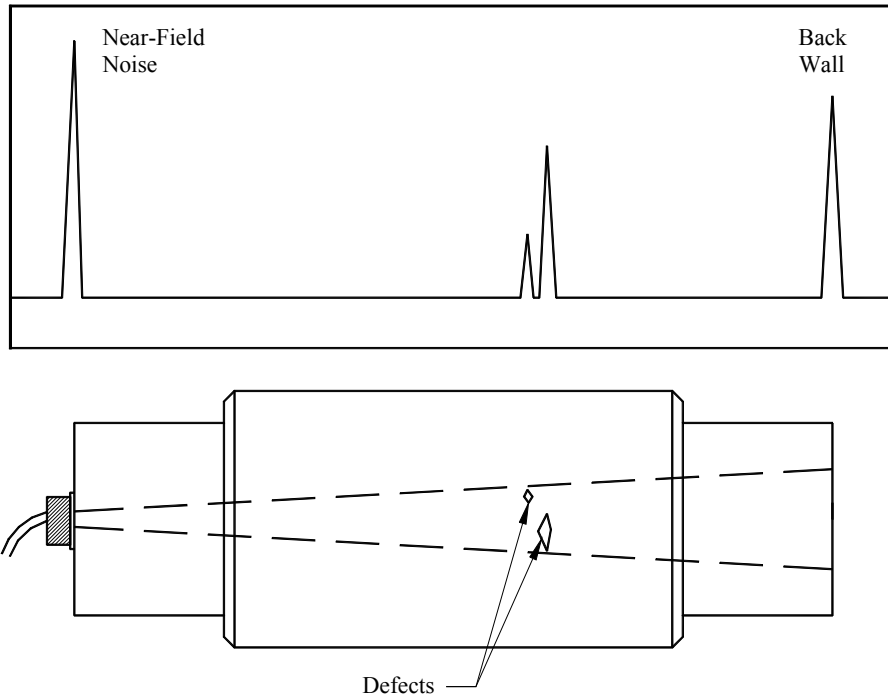


Figure 9. Influence of defect size on ultrasonic signal.

#### 2.1.1.2. Pitch-Catch Technique

The pitch-catch technique is an application of ultrasonic testing where the ultrasonic beam follows a somewhat complex path (i.e., the beam is reflected one or more times before reaching the receiver). The two broad categories of pitch-catch techniques are direct and indirect. For direct pitch-catch, the receiver is placed where the reflected beam is expected if there are no defects. The presence of a defect is found if the signal is not detected where it is expected or if the signal strength is reduced. Conversely, for the indirect pitch-catch technique, the receiver is placed where the reflected beam is expected if a defect does exist. Figures 10 and 11 illustrate the application of the direct and indirect pitch-catch techniques, respectively.

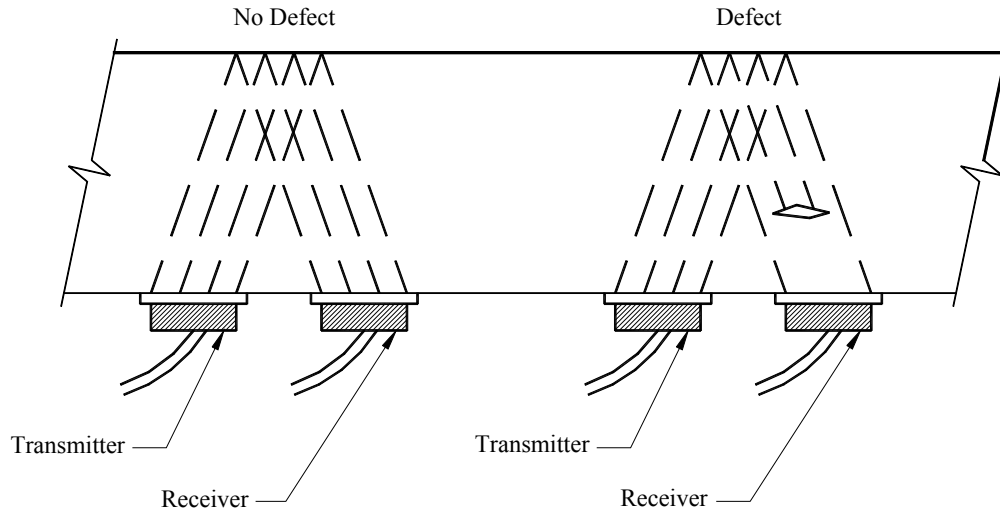


Figure 10. Schematic of direct pitch-catch technique.

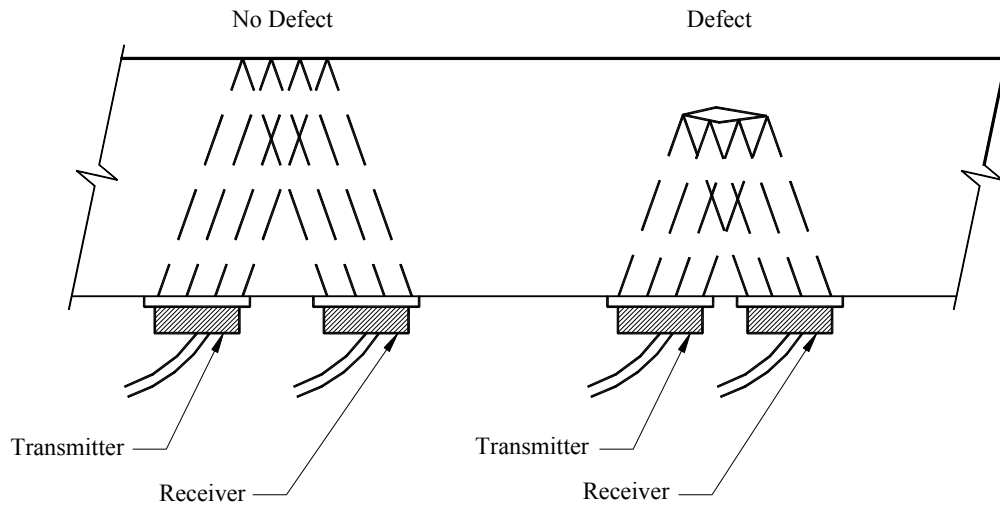


Figure 11. Schematic of indirect pitch-catch technique.

Typically, the direct pitch-catch technique is less prone to error caused by defect orientation and other defect characteristics. On the other hand, the indirect pitch-catch technique is generally faster but may miss some defects because of defect orientation. Both direct and indirect techniques may be used with the transmitter and receiver on the same side or on opposing sides of a test specimen.

### 2.1.2. Decibel Scale

The decibel (dB) is the unit of measure typically referenced by an ultrasonic testing device. The decibel scale is an indication of the ratio between two conditions of the same dimension and is extensively used in electronics. The fundamental decibel is given by the following equation where P is the measured power:

$$dB = 10 \log_{10} \left( \frac{P}{P_0} \right) \quad (5)$$

The power is a square function of the voltage (V) and the decibel relationship could also be written as:

$$dB = 10 \log_{10} \left( \frac{V}{V_0} \right)^2 \quad (6)$$

which in turn translates to:

$$dB = 20 \log_{10} \left( \frac{V}{V_0} \right) \quad (7)$$

Accordingly, a reduction in voltage of one half (i.e., one half the signal strength) corresponds to a drop of approximately 6 dB.

### 2.1.3. Transducers

Transducers are used in a wide variety of applications. By definition, transducers convert energy from one form to another. In the case of ultrasonic testing, electrical energy is converted to ultrasonic energy (pressure energy). Ultrasonic transducers can generally be classified in 6 categories: piezoelectric, electromagnetic, electrostatic, magnetostrictive, optical (e.g., laser), and miscellaneous. For the majority of ultrasonic testing applications, the piezoelectric transducer is the most suitable. Piezoelectricity (pressure electricity) is a property of certain crystals, including quartz. As the name indicates, electricity can be developed in one of these crystals by applying a pressure. Further, the reverse is also true: When an electric field is applied, the crystal rapidly changes shape and, therefore, induces a pressure. This piezoelectric effect is illustrated in figures 12a–d. Figures 12a and 12b illustrate the direct piezoelectric effect where an applied stress induces electric charges on each face. Conversely, figures 12c and 12d

illustrate the opposite piezoelectric effect where an applied electric field induces a mechanical deformation.

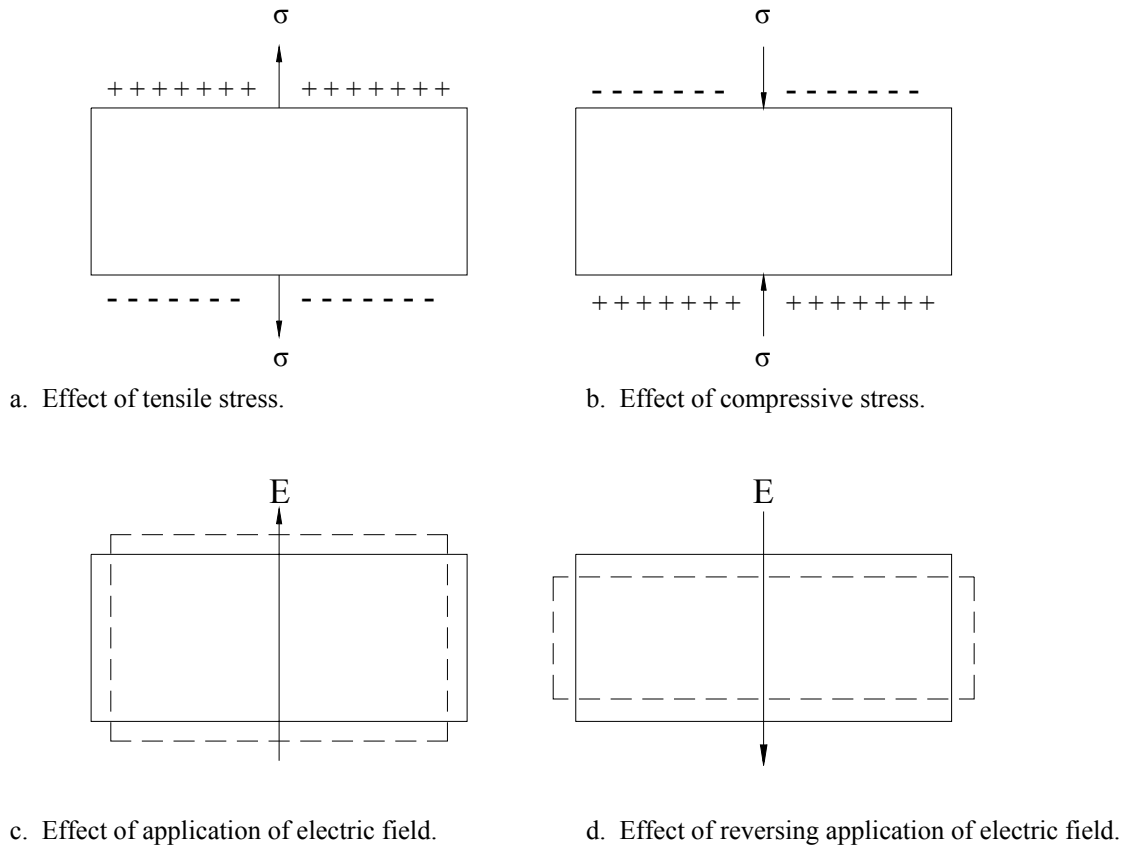


Figure 12. Piezoelectric effect.

Piezoelectric ultrasonic probes take advantage of the piezoelectric effect to perform the testing. The term “probe” refers to the complete assembly of components required to perform ultrasonic testing. Specifically, for a basic straight compression beam, the components include lead wires, a damping block, the housing, a transducer, and a transducer cover. For angle beam probes, the above components are supplemented with an acrylic shoe. Schematics of straight and angle beam probes are illustrated in figures 13 and 14, respectively. The damping block is made from a very high attenuating material and generally has an inclined surface to minimize internal reflections. A protecting hard-wearing cover typically encases the front surface of the transducer. Angle beam transducers have an acrylic wedge, often known as a shoe, shaped in such a way that the direction of the transmitted wave is known. A wide variety of shoe angles are available, offering the inspector significant flexibility in the inspection procedure.

Depending on the angle, angle beam transducers can utilize shear or longitudinal waves. A shear-wave-only test would be accomplished by using a shoe with an angle greater than the first critical angle. This eliminates all longitudinal waves. For longitudinal wave testing, the shoe angle must be less than the first critical angle. Caution must be exercised when using longitudinal waves from an angle beam transducer as shear waves are also present and can make signal interpretation difficult.

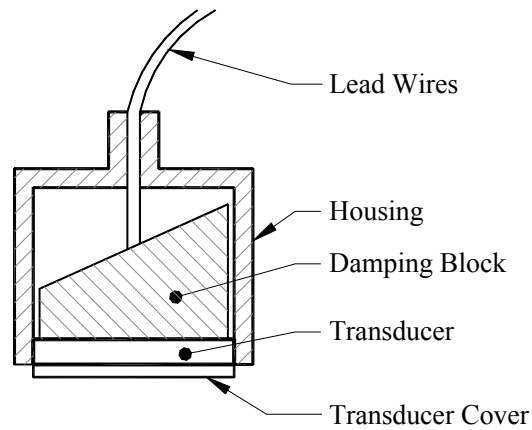


Figure 13. Schematic of a straight beam piezoelectric ultrasonic probe.

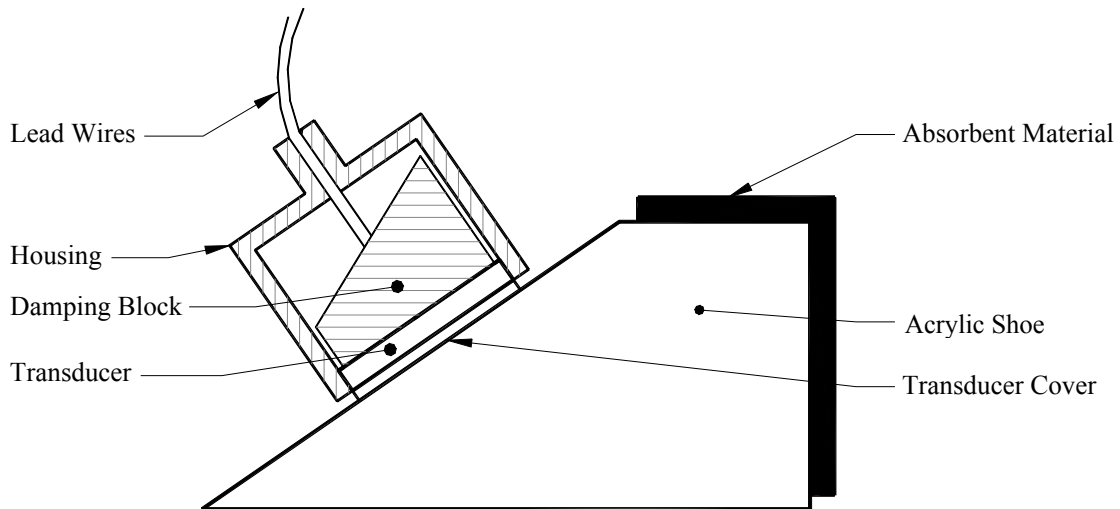


Figure 14. Schematic of an angle beam piezoelectric ultrasonic probe.

#### **2.1.4. Ultrasonic Beam Characteristics and Important Formulae**

To properly identify discontinuities or defects, the location of the ultrasonic beam must be estimated. This estimation includes taking beam attenuation, beam spread, and beam centerline location into account.

##### 2.1.4.1. Beam Attenuation

When sound waves travel through non-idealized (i.e., real) materials, there is a pronounced reduction in the signal strength. This phenomenon, known as attenuation, results primarily from two basic causes: diffraction and absorption.

###### 2.1.4.1.1. *Beam diffraction*

When sound waves encounter a finite boundary, abrupt changes in the direction of propagation of the sound wave may occur. This is known as diffraction. Diffraction occurs when the sound beam encounters a boundary such as a crack tip or member edge. Diffraction also occurs continuously as the beam passes from each grain of material to the next. This important type of diffraction is commonly known as scattering. Scattering of the sound beam occurs as a result of the generally coarse-grained properties of metals. Each grain boundary is a small reflector that emits scattered and reflected signals. For very coarse-grained materials, this can actually lead to detectable echoes, which are commonly referred to as “grass,” that typically present low-amplitude signals on an A-scan.

###### 2.1.4.1.2. *Beam absorption*

The second cause of attenuation is known as absorption. In beam absorption, the sound energy passing through the test material is directly converted to heat. Absorption in crystalline metals can generally be thought of as a process of converting the signal energy to heat through friction. Describing the actual process of beam absorption is well beyond the scope of what is needed here.

##### 2.1.4.2. Beam Spread (Beam Divergence)

Beam spreading occurs in all ultrasonic beams. By definition, beam spread occurs because the beam energy does not stay within the cross section of the transducer. Rather, the

beam starts out as a cylinder and then, after some distance, spreads into a cone. This spreading reduces the intensity of the wave at each discrete point and, as a result, lowers the amount of energy that could be reflected at a defect. This phenomenon is combated through the use of Distance Amplitude Correction (DAC), which is described later. The angle of beam spread ( $\beta$ ) can be approximated using equation 8. This equation gives the angle from the centerline of the beam to the perimeter of the central energy lobe.

$$\beta = \sin^{-1}\left(\frac{0.61\lambda}{a}\right) \quad (8)$$

with:

$\lambda$  = wavelength (m)

$a$  = transducer active radius (m)

#### 2.1.4.3. Beam Centerline Location

Having a good understanding of where the ultrasonic beam is located is key to being able to accurately interpret test signals. For straight beam transducers, this is relatively straightforward: The centerline of the beam is perpendicular to the test plane. However, understanding the location of an angled beam can be slightly more complex.

Computing the beam centerline for an angle beam transducer is relatively easy using basic geometry. In the case of pin inspections, there are two convenient places from which to calculate locations: the end of the pin where the transducer is located, and the longitudinal centerline of the pin. As such, the location system is akin to the cylindrical coordinate system utilized in many mathematical solutions. To use this coordinate system, the operator must measure (or estimate) two quantities related to the transducer position on the face of the pin: distance to index (radial distance from the center of the pin), and the circumferential location (typically quantified in terms of its location on a clock face {e.g., 1:30}). Further, the operator will generate the distance to a reflector (sound path distance) from the ultrasonic test data. From these three quantities and the directional angle of the beam (i.e., the transducer angle), the location of a reflector can be estimated in three dimensions. Because of the effects of beam spread, the location can only be estimated. As a consequence, it is common that the effects of

beam spread be taken into account through additional calculations resulting in a partial-spherical area where the reflector could lie. However, it is also common practice to discount the beam spread in the off-radial-axis of the pin. This allows the operator to interpret the signal based on a single plane rather than a complicated spherical surface with little error. The following equations would be used to locate the centerline of the beam at a reflector as well as the limits of the beam spread at a reflector in the radial plane.

For beam centerline:

$$\text{Axial Distance} = SP \cos(\Theta) \quad (9)$$

$$\text{Radial Distance} = DI + SP \sin(\Theta) \quad (10)$$

For edge of beam spread:

$$\text{Axial Distance} = SP \cos(\Theta \pm \beta) \quad (11)$$

$$\text{Radial Distance} = DI + SP \sin(\Theta \pm \beta) \quad (12)$$

with:

- $SP$  = Sound path
- $DI$  = Distance to index
- $\Theta$  = Transducer angle
- $\beta$  = Beam spread angle (equation 8)

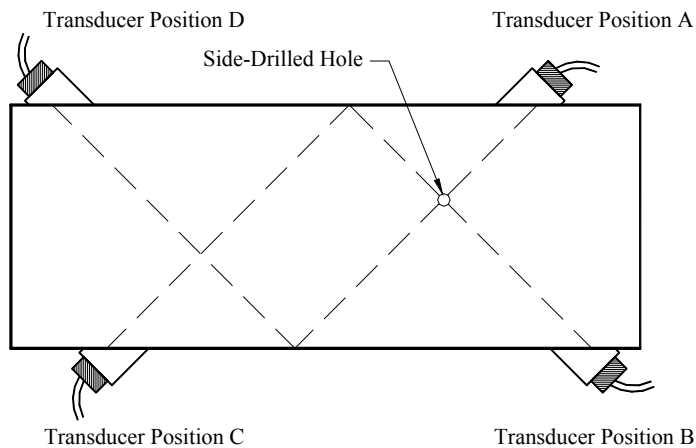
### 2.1.5. Distance Amplitude Correction

As mentioned previously, as a result of beam spread and attenuation, echo heights observed from equivalent defects decrease with increased distance. Consequently, a technique known as distance amplitude correction (DAC) is commonly employed to adjust signals generated at different distances for comparison purposes. This technique consists of generating a DAC curve that essentially indicates that a smaller echo at a greater distance may have similar properties to a larger echo at a lesser distance.

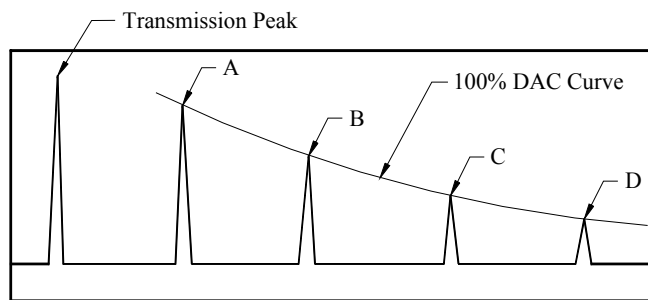
With straight beam transducers, blocks with flat bottom-hole specimens typically are used to generate the DAC curve. However, generating the same curve with an angle transducer

is typically completed using a specimen with side-drilled holes. Regardless of the technique used to generate a DAC curve, the material used in the calibration block should be the same as the material in the test specimen due to potential differences in attenuation characteristics.

Figures 15a and 15b conceptually illustrate how a DAC curve would be generated for an angle beam transducer. In figure 15a, a side-drilled hole is shown in a test block that can be scanned with four different scanning patterns. Note that one could double the number of points on the DAC curve by using a second equivalent side-drilled hole at a different depth. When the echo signals are plotted together, the DAC curve shown in figure 15b results. This curve is referred to as “100 percent DAC.” This means that for an equivalent defect in the test specimen, the echo signal will fall on this line. Smaller or larger defects in the test specimen will lie below or above the 100 percent DAC curve, respectively. The most accurate way to assess these defects is to repeat the DAC curve generation with a series of diameter holes. The result will be a series of curves that should allow for more accurate defect assessment.



a. Transducer and hole location for generating DAC curve.



b. Resulting DAC curve.

Figure 15. Concept for generating distance amplitude correction curves.

## **2.2. GENERAL HANGER PIN INSPECTION REQUIREMENTS**

Factors affecting the reliability of hanger pin inspections include cleaning of and coupling to the test surface, comprehensive scanning patterns, selection of appropriate transducers, proper signal interpretation, and proper defect sizing techniques. In addition, wear grooves and acoustic coupling can affect inspection results.

### **2.2.1. Cleaning and Coupling Requirements**

Many aspects of the use of ultrasonics may influence the reliability of the inspection. However, the condition of the test surface is of decisive importance. Without proper surface preparation, reliable and consistent flaw detection is simply not possible. Regardless of the specific ultrasonic technique and procedures used, all ultrasonic inspections require uniform surface conditions. Specifically, for the direct-contact method, where the probe is coupled to the specimen by a thin film of couplant, anything causing variability in the couplant thickness alters the transmission characteristics.

Prior to pin inspection, it is of primary importance to remove all paint, dirt, and loose scale from the exposed pin ends. Equally important is the removal of surface irregularities that may create unequal couplant thickness. Surface irregularities that produce variable surface amplitudes, such as corrosion pitting, machining grooves, saw cutting, or hammer marks must be removed. This is done most effectively by using a handheld grinder in a two-step process. First, a 24-grit metal grinding wheel is used to remove all paint, surface contaminants, rust, and larger amplitude surface irregularities from the pin ends. Following this, a 200-grit sandpaper “flapper” wheel should be used to refine the cleaning. During both steps, extreme care should be exercised to prevent the creation of local concave spots or rounded corners on pin edges. If local concave spots are discovered during the cleaning process, the grinding wheel and “flapper” wheel should be used to feather these depressions. The finished surface should also be as close to perpendicular to the longitudinal pin axis as possible. Immediately prior to testing, the ultrasonic test operator may wish to use an emery cloth to remove any surface corrosion that may have developed. Although uniform surface conditions are essential to ultrasonic test reliability, testing on polished flat surfaces can be troublesome, because transducers will stick to the highly polished surfaces as a result of suction developed in the couplant. This suction makes it difficult to slide the transducer along the surface.

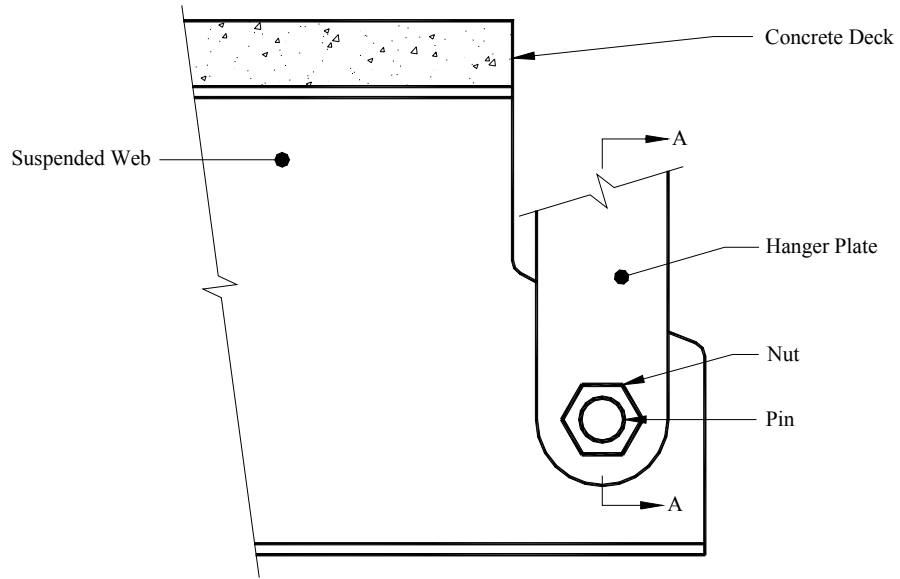
Using couplant permits the transmission of ultrasound from the transducer to the test material. Typical couplants include water, cellulose gel, oil, and grease. A couplant must be selected that will not be detrimental to the test material or the procedure. Further, the couplant used during testing must be the same as was used during calibration. During testing, the thickness of the couplant between the transducer and the test surface must be constant. Inconsistency in couplant thickness will result in sensitivity variations. Further, the couplant selected should have a viscosity that is appropriate for the surface finish of the test material. Specifically, rougher materials require a more viscous couplant. Consideration should also be given to couplant selection and/or cleaning procedures for the post-test treatment of pin ends for corrosion protection purposes.

### **2.2.2. Scanning Patterns**

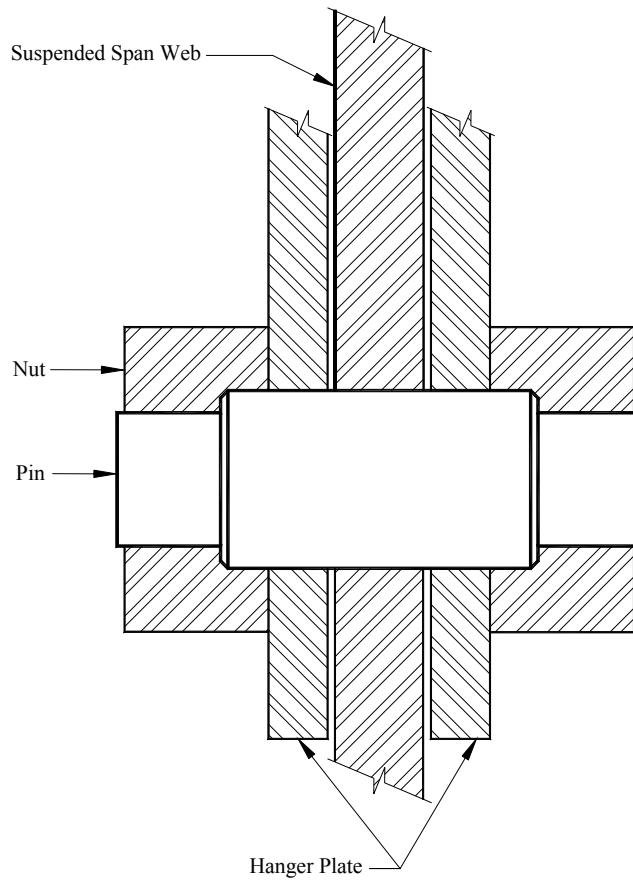
Although no specifications exist for scanning patterns, the general rule is that the scan should be performed by advancing the transducer radially for the full pin circumference. Further, when a reflector is identified, it is common practice to “wobble” the transducer to assess the reflector from a variety of viewpoints (i.e., alter the angle of incidence). When using angled beam transducers, care should be taken to direct the ultrasonic beam toward the pin surface. In short, no standard scan pattern exists; however, the scan pattern that is utilized must be thorough and capable of detecting reflectors at the critical locations (i.e., planes of high shear).

### **2.2.3. Application and Sensitivity of Straight and Angle Beam Transducers**

A typical pin assembly is shown in figures 16a–b. Typically, an ultrasonic inspection of the pin would include the use of both straight and angle beam transducers. Straight beam testing, as illustrated in figure 17, is completed for two reasons: to confirm the total pin length, and to identify total pin failure or very large cracks. Angle beam testing, illustrated in figure 18, is completed to capture and/or enhance the reflection from the reflectors at the pin surface (e.g., cracks, wear grooves, corrosion). Angle beam transducers allow the signal to be directed around obstacles, and they also direct a greater amount of the sound energy at the critical locations. This should allow for greater accuracy in assessing reflectors.



a. Elevation.



b. Cross section A-A.

Figure 16. Typical pin/hanger assembly.

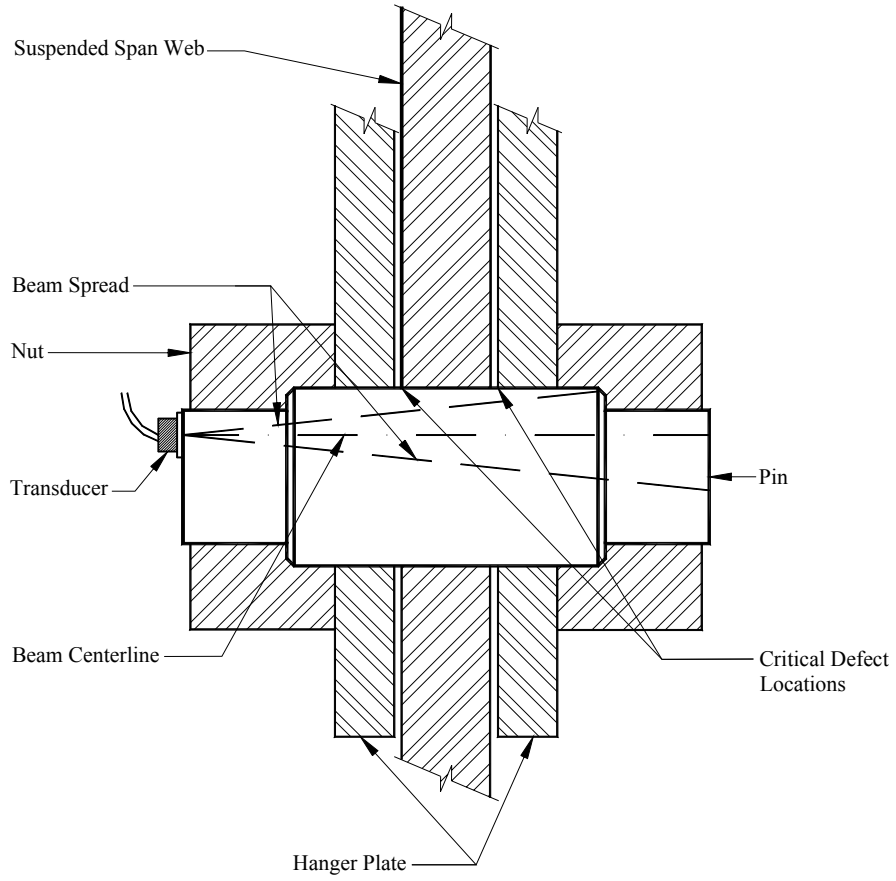


Figure 17. Application of a straight beam transducer.

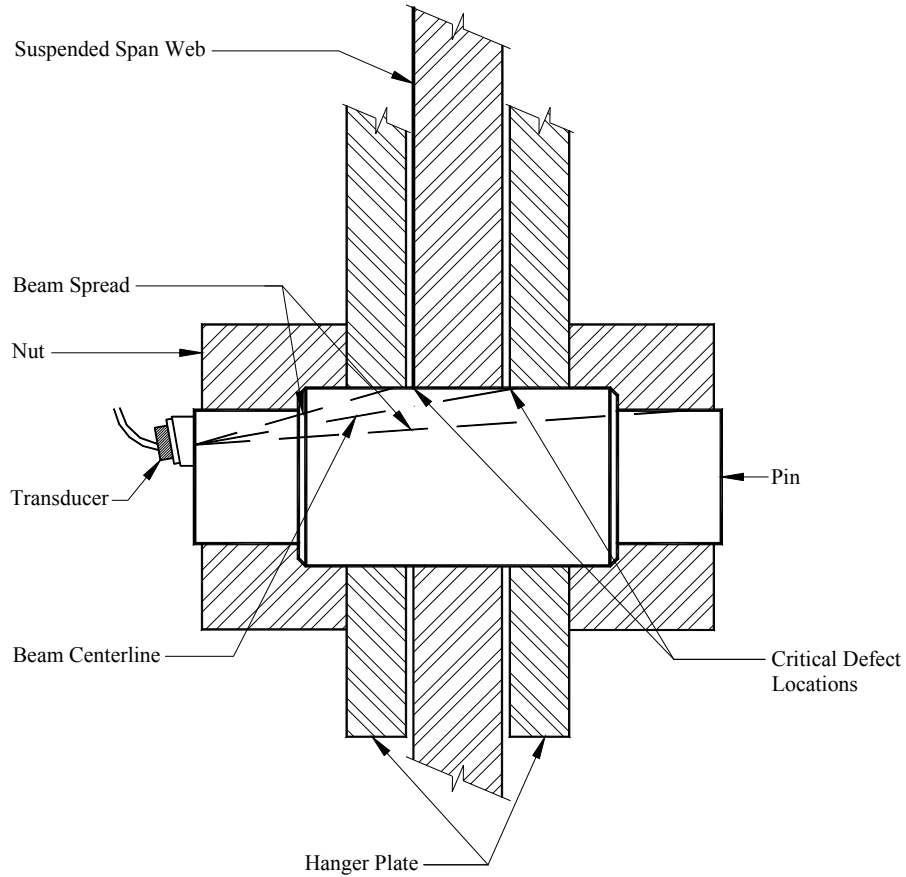


Figure 18. Application of an angle beam transducer.

#### 2.2.4. Interpretation of Ultrasonic Testing Signals

Ultrasonic examination of bridge connecting pins is typically accomplished with the use of standard portable instruments designed for field use. Currently available instruments utilize digital circuitry and are capable of storing multiple displays and instrument calibrations that permit the use of multiple transducers and instrument calibrations for evaluation of the pin with relative convenience. A “view” into the body of the pin may be achieved by a skilled ultrasonic technician through the time baseline and signal amplitude based presentation of the A-scan display.

Presentation of ultrasonic indications is dependent primarily upon appropriate transducer and incident angle selection, accurate calibration of the test apparatus, and an effective transducer scan pattern conducted with corresponding attention to the respective instrument display. It is imperative that the connection assembly and pin configuration are subjected to

adequate study, prior to development of the inspection procedure, to determine parameters that are fundamental to the examination.

In conjunction with applicable inspection procedures and test apparatus, interpretations of ultrasonic indications also require knowledge of the principles of ultrasonic wave propagation, as well as the operation and nuances of pin assemblies. A comparison of indications produced from pins of like connections also may contribute to their interpretation and characterization, as “signature” display patterns often become apparent for similar assembly configurations.

Initial interpretation of the ultrasonic signal presentation is based on the magnitude of the indication, and the linear sound path distance from the transducer. Indications that appear within the vicinity of connection shear planes are of primary importance; however, the significance of all reasonably defined trace defects must be evaluated. Indications that exhibit a low signal-to-noise ratio may be confusing, but should not be ignored when they are consistent and repeatable. The linear distance from the transducer to the apparent indication source requires conversion to the axial location for comparison to the measured distances to shear planes when using angle beam transducers. The sound path distance to surface-oriented discontinuities, however, may also occur at an angle with the diverted wave propagation from the straight beam transducer.

A straight beam transducer is effective for determining length and sound path distance to the far side shoulder of the pin. For some connections, pins may be adequately inspected using only the straight beam transducer. Provided that the shoulder step is not too great and the distance to the shear plane is not too short, the spread portion of the beam may be used to detect surface-oriented discontinuities. It should be noted that interpretative evaluations of reflectors detected using beam spread should be executed carefully, as signal amplitudes are greatly influenced by distance from the radial signal centerline.

For geometric configurations that do not permit access to critical shear plane regions of the pin when using an inspection procedure in which the propagated wave is normal to the plane of entry, a low angled longitudinal beam transducer is often necessary for adequate inspection. A study of pin configuration and proximity of connection shear planes determines the appropriate angle of incidence to accomplish the inspection. Because of its greater sensitivity to barrel surface discontinuities, the angled transducer is generally preferred for interrogation purposes. Although the angled search unit is not accurate for direct measurement of axial distance without adjustment to the horizontal linearity, the incident angle of the sound beam with

respect to the barrel surface is more definitive for approximation of the radial location of the discontinuity. In addition, some of the acoustic interference associated with the boundary surface may also be reduced. The increased sensitivity of the angled beam, however, is more susceptible to the detection of shallow and rounded wear grooves, and may also enhance discernible acoustic sound transfer across mating surfaces of adjoining components. While some ultrasonic indications produced when using the angle beam transducer may complicate the interpretation, this is offset by an increased potential for detection of cracks or other minute discontinuities.

It is advisable to perform ultrasonic examinations from both ends of each pin. Restrictions to the sound beam from geometric obstructions within the pin (such as section changes at threaded ends, cotter pin holes, and machined turning centers at end surfaces) may be mitigated more easily. Where access to only one end is possible, the inspection for a portion of the critical area of the pin may be limited. A comparison of scans from each end of the pin may also be beneficial in the interpretation of indications, especially for indications with large signal magnitude, or at the pin end surfaces. In general, indications registered from both sides of the pin can suggest the presence of cracks or severe grooves. Conversely, an absence of corresponding indications when comparing opposite end scans suggests an alternate reflector source such as intercomponent acoustic sound transfer, or shallow wear grooves.

Interpretation of ultrasonic indications and subsequent evaluation of connecting pins demand thoughtful consideration of the various data contributions. Indications that are determined to originate from geometric features of the pin, such as cotter pin holes, threaded ends, or section changes (e.g., shoulders) may be disregarded. Except for potential ultrasonic multiple reflections, indications from intercomponent acoustic transference will occur at planes of the assembly. Shear plane regions must be scrutinized carefully to avoid confusion between indications from actual discontinuities and reflections achieved through acoustic transference.

Through observation of shape, amplitude, and baseline width, the signal trace characterization may suggest the nature of the discontinuity or indication source. Cracks, deep grooves, and acoustic transference reflections may produce relatively sharp indications. Shallow wear grooves and corrosion pitting tend to generate a more broad-based and rounded signal. Indications of this type generally produce relatively low-amplitude responses and correspond to linear areas of the pin that may be associated with the suspected condition. The variability

associated with the corrosion surface, which includes angular-to-rounded profile pitting, creates beam scatter, which ultimately reduces the beam's return energy.

The dynamic ultrasonic signal trace, in comparison with the saved screen display, presents substantially greater information for the evaluation of connecting pins. Continuous comparison of signals generated from the various areas of the pin during movement of the transducer may often clarify the indication source. Intercomponent acoustic transference may also be substantiated through observation of the dynamic signal when significant load variations result in fluctuation of the trace deflection.

Ultimately, evaluation for the disposition of connecting pins of bridge structures includes the analysis and interpretation of the cumulative acquisition of data including consideration of pin geometry, bearing forces, location and orientation of indications, signal magnitude, and characteristics of trace deflections. Additional transducer angles and test frequencies or alternate scan patterns may be advisable to confirm uncertain conditions.

The interpretation of indications detected in the inspection of connecting pins may be successful with skilled operators using appropriate inspection procedures. Characteristics of significant cracks may generally be identified and appropriate explanations may be provided for many of the indications. When inspections are performed at appropriate intervals, observed conditions may be monitored for change without significant risk of large, undetected crack growth. Care must always be used to observe the sometimes-subtle differences between indications from acoustic transference or wear grooves and cracks.

#### **2.2.5. Defect Sizing Techniques**

The two principal categories of defect sizing techniques are probe movement techniques and amplitude techniques. Although not a standard, defects are generally referred to as either large or small depending on whether they are larger or smaller than the cross-sectional area of the beam at the point of incidence. In general, small flaws may be sized by either sizing technique. However, large flaws can only be sized using probe movement. Regardless of the specific technique used, it is important to take into account the fact that the beam is divergent in the far field. The following will briefly describe common ultrasonic defect sizing techniques.

## 2.2.5.1. Probe Movement Techniques

### 2.2.5.1.1. *The 6-dB drop technique*

The 6-dB drop technique is the easiest technique for sizing large, planar defects. It is based on the principal that when half of the ultrasonic beam is not reflected by a defect, the echo is 6 dB less than when the entire beam is reflected. It is then assumed that when half of the beam is returned, the transducer centerline is directly over the edge of the defect. Unfortunately, this only occurs in a defect with straight edges and only when the transducer is away from a defect corner. Because this type of defect very rarely occurs, the 6-dB technique only gives an approximation of the defect size. The following describes the general procedure:

1. Locate the flaw.
2. Maximize the echo and note the signal amplitude.
3. Translate the probe until the signal amplitude is reduced by 6 dB from the maximum.
4. Mark the probe position.
5. Repeat steps 1 through 4 as necessary to completely describe the shape of the defect.

### 2.2.5.1.2. *The 20-dB drop technique*

The 20-dB drop technique often is used to size small defects in welds using angle probes. As such, this technique typically is not used in ultrasonic inspection of pins and is presented here for completeness only. This technique actually requires the operator to generate a beam profile plot with a beam calibration block containing several holes at different depths (e.g., BS 2704 A5) before sizing any defects. The beam profile plot is generated as follows:

1. Locate a hole and maximize the echo amplitude (location O).
2. Move the probe forward until the echo is reduced by 20 dB and note the location.
3. Move the probe backward from location O until the echo is reduced by 20 dB and note the location.
4. Repeat steps 1 through 3 for different hole depths and sizes.

With this information, a beam profile plot is generated. The following procedure is used to size actual defects using the 20-dB drop technique:

1. Locate the flaw.
2. Maximize the echo noting the amplitude and location.
3. Move the probe forward and backward noting the 20-dB drop positions.
4. Use the beam profile plot to determine the depth and size of the defect.

#### 2.2.5.1.3. *The time-of-flight diffraction technique*

The time-of-flight diffraction technique, first used to measure crack depths in concrete, is based on the phenomena of diffraction at edges of discontinuities. Recently, however, it has been applied to ultrasonic inspection of metal structures. Unfortunately, the geometry of most pin/hanger connections is such that the ultrasonic operator cannot obtain a scan that is thorough enough to determine crack size with this technique. As a result, this technique is very rarely used for sizing defects in pins.

#### 2.2.5.2. Amplitude Techniques

##### 2.2.5.2.1. *The comparator block technique*

The use of a comparator block is the most straightforward, easy, and possibly most accurate technique for sizing reflectors. The technique consists of comparing the echo from an artificial target in a fabricated test block to echoes found in the field-installed pin. The test block must be of similar material to the test specimen. In addition, the artificial target must be in approximately the same location (referenced to the test surface) as the actual defect. This requires that the test block be fabricated with prior knowledge of likely locations for defects. Fortunately in the case of pins, the location of the shear planes can be estimated with sufficient accuracy (as described later). In the case of pin inspections, the preparation of the test block also allows the operator to verify that a particular transducer will be able to detect defects at critical locations (i.e., defects will likely not be obscured by pin shoulders, cotter pin holes, etc.).

#### 2.2.5.2.2. *The distance amplitude correction technique*

When the location of a defect is not well-known, the use of the DAC curves described previously provides a tool for estimating defect sizes. The process is similar to the comparator block technique; multiple defect depths are used to generate the DAC curves.

#### 2.2.5.2.3. *The distance grain size technique*

The distance grain size technique is a graphical representation of the various echoes produced by various size defects at various distances. Distance grain graphs are produced for each probe by testing a large number of manufactured defects at various depths and plotting the results as a series of curves for various flaw sizes. Unfortunately, this technique is only valid for defects smaller than the cross-sectional area of the beam at the defect depth and is only accurate for circular defects. Typically, this type of defect does not occur in bridge pins, so this technique is rarely used.

### **2.2.6. Wear Grooves**

By definition, the term “groove” suggests a linear intrusion into the affected subject material. For bridge connection pins, a groove may originate from wear related to the direct bearing forces of the interlinked components, or from corrosion attack at the barrel surface. Mating surfaces between bearing components generally exhibit a uniform pattern of wear, except when corrosive activity or abrasive foreign debris has been introduced to the process. With uniformity of wear, grooves are typically shallow, with only minor loss of section at the contact surface. Corrosion-induced grooving, however, characteristically produces pitting within a relatively narrow radial band in the vicinity of the barrel surface. This band corresponds to the spaces between adjoining members of the connection assembly.

Wear grooves that develop from bearing surfaces of interlinked components, although very shallow, may be well-defined. Wear may be expected to occur at contact surfaces of all interconnected components, therefore the hole of the web or interlinking plate may also become slightly enlarged. With the mutual “wearing-in,” or “seating” between components, the area of contact and associated wear may become greater. However, actual section loss to mating parts is usually very minor for bridge joints that do not suffer from an abrasive or corrosive environment.

Occasionally, a pin will continuously rotate as the bridge repeats regular thermal cycles; however, movement is more often limited to minor cyclic rotation of a few degrees in each direction. Rotating pins may develop grooves throughout the full pin circumference.

In axial examination, an ultrasonic beam that is propagated through the volume of the pin may be impeded from any interruption in the path of the wave. Within the homogeneous material of the pin, a portion of the sound beam that reaches the affected area may be reflected from the groove. The quantity of reflected sound that is detected with the ultrasonic system is dependent largely upon the size and surface condition of the wear groove and relative angle of incidence.

### **2.2.7. Acoustic Coupling**

Based on observations made while conducting ultrasonic tests of pinned connections in bridge structures, a condition sometimes referred to as “acoustic coupling” has been theorized. The phenomenon, possibly directly related to the local bearing forces between the pin and the connected components, is important because indications generated from this condition are often of sufficient signal magnitude that they may be confused with or mistaken for significant discontinuities within the pin.

The origin of the acoustic coupling theory resulted from observed indications that exhibited patterns that were inconsistent with the anticipated response from either cracks or wear grooves. Specifically, these inconsistent display patterns include:

- Dissimilar patterns in pins of like type.
- Typically moderate-to-weak indication levels.
- Indications coincident with bearing surfaces.
- Signal amplitude fluctuations under traffic loads.
- Indications at interfaces of connected components, including major shear planes.

To investigate these indications, the ultrasonic test data were represented graphically on inspection data sheets to define their relative radial orientation. From these graphical representations, the acoustic coupling phenomenon was further reaffirmed.

Study of historical inspection data indicated a potential relationship between imposed loads on the connection components and signal generating conditions. In typical pin/hanger

connections, indications corresponding to the linear distance of hanger link plates from the ultrasonic transducer were frequently observed, but only in the “upper hemisphere” of upper pins, and only in the “lower hemisphere” of lower pins. Indications were sometimes observed that corresponded to the distance of the girder web plate, although the orientation was opposite to that observed for hanger link plates. When traffic is active on a bridge span where testing of a related pin is in progress, fluctuations in the signal intensity have been observed. The fluctuations are most prominent when larger, heavier trucks traverse the span.

Based on field observations, it is apparent that with sufficient bearing force between adjoining components, sound transference may occur. The ultrasonic wave will be conducted at the point or points of contact between the pin and the connection assembly. The contact area may typically range from a single point at the outside radius of the pin to a broad contact area exceeding a third of the circumference. In some cases, contact may be semicontinuous within a limited area, and the magnitude of reflected signal may vary within the contact area.

Indications that are generated from acoustic coupling have been observed individually and in multiple groups. In some instances, each indication is unique, reflecting from one of the elements of the hanger or girder that is in contact with the radial surface of the pin. In other cases, multiple indications may be internal multiples from individual plates within a bearing assembly. The potential occurrence of this condition is suggested when observed indication multiples are exactly concurrent in the course of radial transducer travel, and when the later signal is consistently attenuated with respect to the earliest of the concurrent indications.

Minor variations in bearing contact with the barrel surface of the pin may significantly affect intercomponent acoustic transfer. These may include bearing load, mismatch between nonconcentric bearing surfaces, skewed fit, or other surface conditions or irregularities.

Pin assemblies that incorporate the use of bronze bushings often do not produce indications from intercomponent acoustic transfer. This is most likely the result of the acoustic mismatch of the materials, resulting in either refraction or attenuation of the sound wave, which may prevent sufficient discernible energy from returning to the transducer.

### **2.3. INSPECTION DOCUMENTATION**

Regardless of how well ultrasonic testing is performed, the results may not be very useful without proper documentation. Because the inspection of each pin/hanger connection is unique,

the following discussion will provide general information concerning the type of documentation that should typically be required. However, specific requirements for documentation must be determined on an inspection-by-inspection basis.

### 2.3.1. Physical Measurements

Without full understanding of the geometry of pin/hanger connections, proper assessment of the test results cannot be made. Specifically, it is important to locate all potential shear planes. Unfortunately, nearly the entire pin is obscured by the connecting elements. As a result, the location of potential shear planes can only be approximated with physical measurements made in the field and/or the original design dimensions. Figure 19 shows a typical pin/hanger cross section with physical measurements. Each potential shear plane can be located using a variety of measurement combinations. Equations 13 through 16 illustrate several ways to locate the rightmost shear plane. Equation 17 averages equations 13 through 16 to minimize any error in the constituent measurements. This method should be repeated until all shear planes are located.

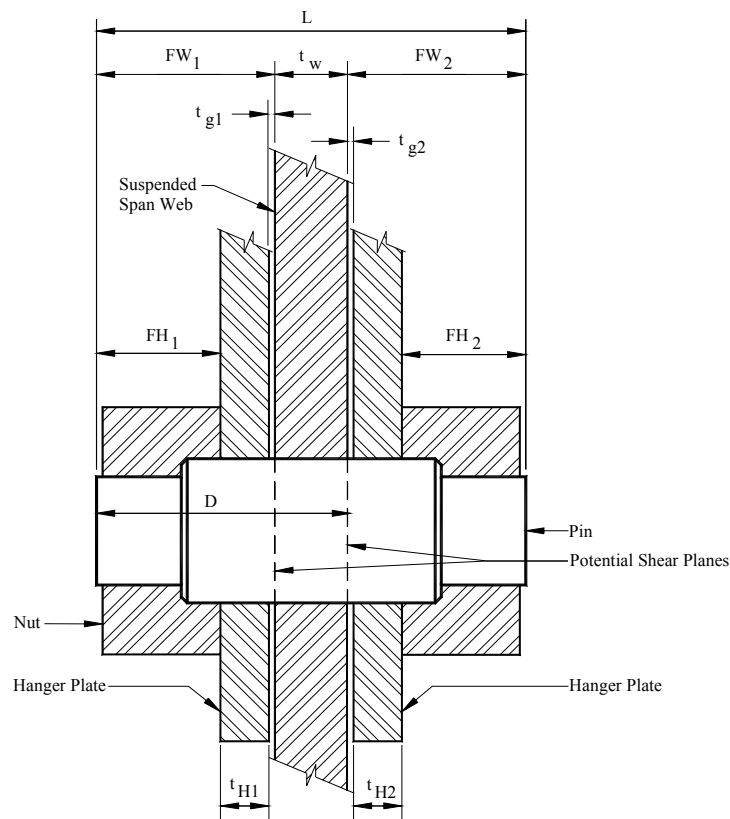


Figure 19. Typical physical measurements.

$$D_1 = FH_1 + t_{H_1} + t_{g_1} + t_w \quad (13)$$

$$D_2 = FW_1 + t_w \quad (14)$$

$$D_3 = L - [FH_2 + t_{H_2} + t_{g_2}] \quad (15)$$

$$D_4 = L - FW_2 \quad (16)$$

$$D = \frac{D_1 + D_2 + D_3 + D_4}{4} \quad (17)$$

with:

D	= Distance to potential shear plane
FH <sub>n</sub>	= Distance from face of pin to face of hanger
FW <sub>n</sub>	= Distance from face of pin to face of web
t <sub>g</sub>	= Measured gap width
t <sub>H</sub>	= Measured thickness of hanger
t <sub>w</sub>	= Measured thickness of web
L	= Length of pin (measured or design)

### 2.3.2. Visual Assessments

Since the first pin/hanger connection failure, significant emphasis has been placed on ensuring connection integrity. As such, newer and rehabilitated pin/hanger connections have been developed that incorporate the fundamentals of alternate load paths. By these fundamentals, the bridge is designed with redundancy such that if one pin fails, the load will be distributed to other structural members, thus avoiding a total collapse. However, if the secondary members that should redistribute the loads are in poor condition, the entire system may not perform as intended. To avoid this, a complete pin inspection must include a visual examination of the area immediately surrounding the connection. Specifically, the members that would be necessary to distribute the load in the case of a pin failure must be thoroughly

examined. The typical area of concern is the area within approximately 3 meters (m) (9.8 feet (ft) longitudinally of the pin connection.

The visual inspection should note all areas of corrosion, rubbing of elements, thickness loss, cracking, and any other important observations. When necessary, detailed measurements should be taken of members so that a detailed structural analysis may be completed.

### **2.3.3. Ultrasonic Testing Data Collection**

Without an effective means of summarizing the test results, the inspection is virtually useless. Accordingly, a minimum amount of data must be collected and presented in a pin-by-pin format. The following summarizes what should be considered the minimum documentation required for ultrasonic testing. Generally, the collected data can be loosely grouped in three categories: basic data, geometrical data, and ultrasonic testing data. A sample form that could be used to collect and summarize ultrasonic testing results is presented in figure 20. Figure 20 includes sample data to illustrate how the form would be used. This data sheet is generated in a spreadsheet and various calculations are completed to give the specific data shown.

The basic information that must be collected includes the bridge designation, the location of the assembly being tested, and the date of inspection. Other information might include specific and general information on weather conditions (e.g., temperature, cloud cover), and access equipment (see the uppermost portion of the data sheet given in figure 20).

The second type of data that must be summarized on the sheet is information related to the geometry of the connection assembly. This would include both summarizing the physical measurements described previously, calculated location of shear planes (see equation 17), and fundamental design information. It is important to summarize this information so that engineering assessments of the ultrasonic test results can be made as the inspection is being completed. Without this information, the operator would simply be noting indications without regard for the potential implication or cause.

Finally, the actual ultrasonic test results must be collected. The same set of information must be collected for each reflector identified within each pin in a connection. The minimum data that should be collected for each indication (referred to as a “NOTE” in figure 20) is as follows. First, to determine of the location of a specific reflector, the ultrasonic scan angle must be known. The magnitude of the reflected signal is also very important. However, without some

idea of how large the signal is, the amplitude of the echo loses significant value. Accordingly, the reference indication level must also be recorded. The reference indication level is typically the magnitude of the echo that was generated in a pin mockup (i.e., a comparator block). Together, these data allow the operator to discern individual indications as either low level or significant. Two pieces of physical data must be recorded when a significant indication is identified. First, the location of the transducer on the pin face is recorded with respect to the transducer location on a clock face (e.g., 12:30, 5:30). Second, the distance from the center of the pin to the center of the transducer (distance to index) in the radial direction must be recorded. With these data and the distance to the indication determined from the ultrasonic testing, the approximate location of the reflector can be determined with the equations presented previously (i.e., axial and radial distance). Because a specific indication rarely is present in a single location, it is also common to record the range over which the signal extends (again, in reference to the clock face (e.g., 1:30–6:30)).

When the results of the ultrasonic test data are combined with the geometric information, the operator can determine the locale of each echo. This information is most easily understood in a graphical presentation similar to the one given in figure 20.

## ULTRASONIC INSPECTION OF PIN AND HANGER ASSEMBLIES

BRIDGE:	70-77-2386 AND 70-77-2420		
ASSEMBLY LOCATION:	Interstate I-70, Bent 17, Girder 1	DATE:	7/15/00

PIN LOCATION	REF. PLANE	STICK-OUT, inch	FACE OF HANGER, inch	FACE OF WEB, inch	WEB THICKNESS, inch	HANGER THICKNESS, inch	UT LENGTH, inch	DIST. TO SHEAR PLANE, inch
TOP	NORTH	0.59	2.09	2.84	1.38	0.75	7.00	4.23
BOTTOM	NORTH	0.28	1.78	2.66	1.31	0.75	7.05	4.04
TOP	SOUTH	0.31	1.94	2.75	1.38	0.69	7.00	4.14
BOTTOM	SOUTH	0.44	1.91	2.94	1.31	0.69	7.05	4.32

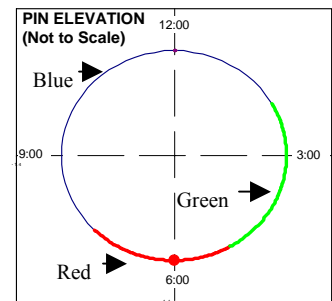
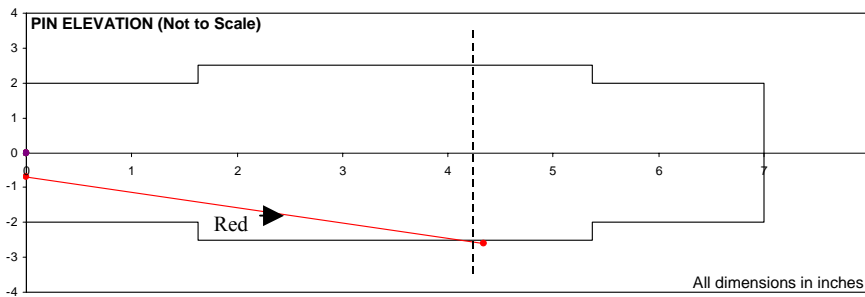
NOMINAL PIN DIMENSIONS, inch		NOMINAL HANGER DIMENSIONS, inch		NOMINAL WEB DIMENSIONS, inch	
THREADED DIAMETER	4.00	WIDTH		THICKNESS	1.38
BARREL DIAMETER	5.00	THICKNESS	0.75		
BARREL LENGTH	3.75				
TOTAL PIN LENGTH	7.00				

1 inch = 25.4 millimeters (mm)

### a. Basic pin information.

LOCATION:	TOP	REF. PLANE:		NORTH										
NOTE	UT SCAN ANGLE, deg.	INDICATION LEVEL, dB	REF. LEVEL, dB	ATTEN	IND. LEVEL +/- REF, dB	READING RADIAL LOCATION, hh:mm	RADIAL LOCATION 1, hh:mm	RADIAL LOCATION 2, hh:mm	DISTANCE TO INDEX, inch	SOUND PATH DISTANCE, inch	AXIAL DISTANCE, inch	RADIAL DISTANCE, inch	ACOUSTIC COUPLING	
1	24	50	43		7	6:00	5:00	7:30	0.69	4.75	4.34	2.62	<input checked="" type="checkbox"/>	
2	24	Low level	43				2:00	5:00					<input type="checkbox"/>	
3													<input type="checkbox"/>	
4													<input type="checkbox"/>	
5													<input type="checkbox"/>	

Red →



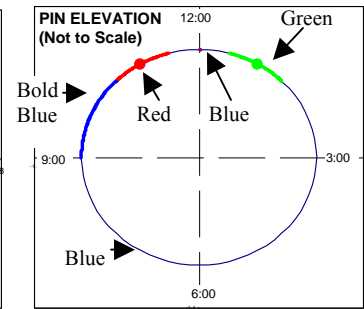
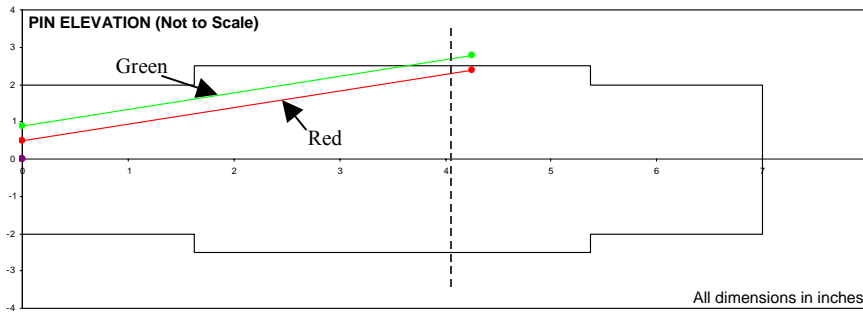
1 inch = 25.4 mm

### b. Top of pin results.

Figure 20. Sample ultrasonic test data.

LOCATION: BOTTOM		REF. PLANE: NORTH													
NOTE	UT SCAN ANGLE, deg.	INDICATION LEVEL, dB	REF. LEVEL, dB	ATTEN	IND. LEVEL +/- REF, dB	READING RADIAL LOCATION, hh:mm	RADIAL LOCATION 1, hh:mm	RADIAL LOCATION 2, hh:mm	DISTANCE TO INDEX, inch	SOUND PATH DISTANCE, inch	AXIAL DISTANCE, inch	RADIAL DISTANCE, inch	ACOUSTIC COUPLING		
6	24	53	43		10	11:00	10:30	11:30	0.50	4.65	4.25	2.39	<input type="checkbox"/>		
7	24	53	43		10	1:00	12:30	1:30	0.88	4.65	4.25	2.77	<input type="checkbox"/>		
8	24	Low level	43				9:00	10:30					<input type="checkbox"/>		
9													<input type="checkbox"/>		
10													<input type="checkbox"/>		

Red →  
Green →



1 inch = 25.4 mm

c. Bottom of pin results.

Figure 20. (Continued) Sample ultrasonic test data.

## 2.4. INSPECTOR QUALIFICATIONS AND CERTIFICATIONS

The effectiveness of any nondestructive evaluation technique depends on the capabilities of the personnel performing the inspection. The American Society for Nondestructive Testing (ASNT) has developed a set of guidelines for the training and certification of testing personnel that are summarized in the ASNT document SNT-TC-1A.<sup>1</sup>

ASNT outlines three basic levels of qualification. A fourth classification, “trainee,” should be assigned while an inspector is being trained initially. The three basic levels are:

- **Level I.** A Nondestructive Testing (NDT) Level I individual should be qualified to perform specific calibrations properly, specific NDT, and specific evaluations for acceptance or rejection determinations according to written instructions and to record results. The NDT Level I should receive the necessary instruction or supervision from a certified NDT Level II or III individual.
- **Level II.** An NDT Level II individual should be qualified to set up and calibrate equipment and to interpret and evaluate results with respect to applicable codes, standards, and specifications. The NDT Level II should be thoroughly familiar with the scope and limitations of the methods for which he or she is qualified and should exercise assigned responsibility for on-the-job training and guidance of trainees and NDT Level I personnel. An NDT Level II should be able to organize and report the results of NDT.
- **Level III.** An NDT Level III individual should be capable of establishing techniques and procedures; interpreting codes, standards, specifications, and procedures; and designating the particular NDT methods, techniques, and procedures to be used. The NDT Level III should be responsible for the NDT operations for which he or she is qualified and assigned, and should be capable of interpreting and evaluating results in terms of existing codes, standards, and specifications. The NDT Level III should have sufficient practical background in applicable materials, fabrication, and product technology to establish techniques and to assist in establishing acceptance criteria when none are otherwise available. The NDT Level III should have general

<sup>1</sup>*Recommended Practice No. SNT-TC-1A, 2001 Edition* is available from ASNT at <http://www.asnt.org>.

familiarity with other appropriate NDT methods as demonstrated by the ASNT Level III basic examination or other means. The NDT Level III, in the methods in which he or she is certified, should be capable of training and examining NDT Level I and II personnel for certification in those methods.

The ASNT guidelines also give criteria for minimum education and experience that the various NDT levels must have. The requirements specific to ultrasonic testing are:

- **Level I.** Minimum of 3 months of experience and 30 to 40 hours of training depending on education. (individuals who have passed at least 2 years of engineering or science study in a university, college, or technical school are required to have 30 hours of training, while individuals with a high school diploma are required to have 40 hours of training.)
- **Level II.** Minimum of 9 months of experience and 40 hours of training.
- **Level III.** Meet one of the following criteria:
  - Graduated from a minimum 4-year college or university curriculum with a degree in engineering or science, plus 1 year of experience in NDT in an assignment comparable to that of an NDT Level II in the applicable NDT method.
  - Completed at least 2 years of engineering or science study with passing grades at a university, college, or technical school, plus 2 years of experience in NDT in an assignment at least comparable to that of NDT Level II in the applicable NDT method.
  - Completed 4 years in an NDT assignment at least comparable to that of an NDT Level II in the applicable NDT method.

In addition to having a qualified NDT inspector, it is good practice, although not required, to have a qualified structural engineer assist the NDT inspector. Engineering assessments of the NDT results can be made with the combined expertise of the two professionals.



### **3. EXPERIMENTAL PROGRAM**

#### **3.1. INTRODUCTION**

A laboratory experimental program was initiated to gain an understanding of some of the key issues presented previously. The experimental program included testing of a steel block to illustrate the principles of beam diffraction and distance amplitude correction. Also, pins with manufactured cracks were tested to study angle and straight beam sensitivity to cracks, defect sizing, and the acoustic coupling phenomenon.

#### **3.2. INSPECTION SPECIMENS**

To accomplish the experimental program described here, 7 specimens were used. This consisted of a test block with a side-drilled hole, 5 pins with implanted cracks, and a pin/hanger mockup. Each specimen is described briefly below.

##### **3.2.1. Side-Drilled Hole Test Block**

The side-drilled hole test block (SDHTB) is shown in figures 21 and 22. The test block is a 305-mm x 305-mm x 51-mm (12-inch x 12-inch x 2-inch) steel plate with a 6-mm (0.2-inch) hole drilled through the thickness.

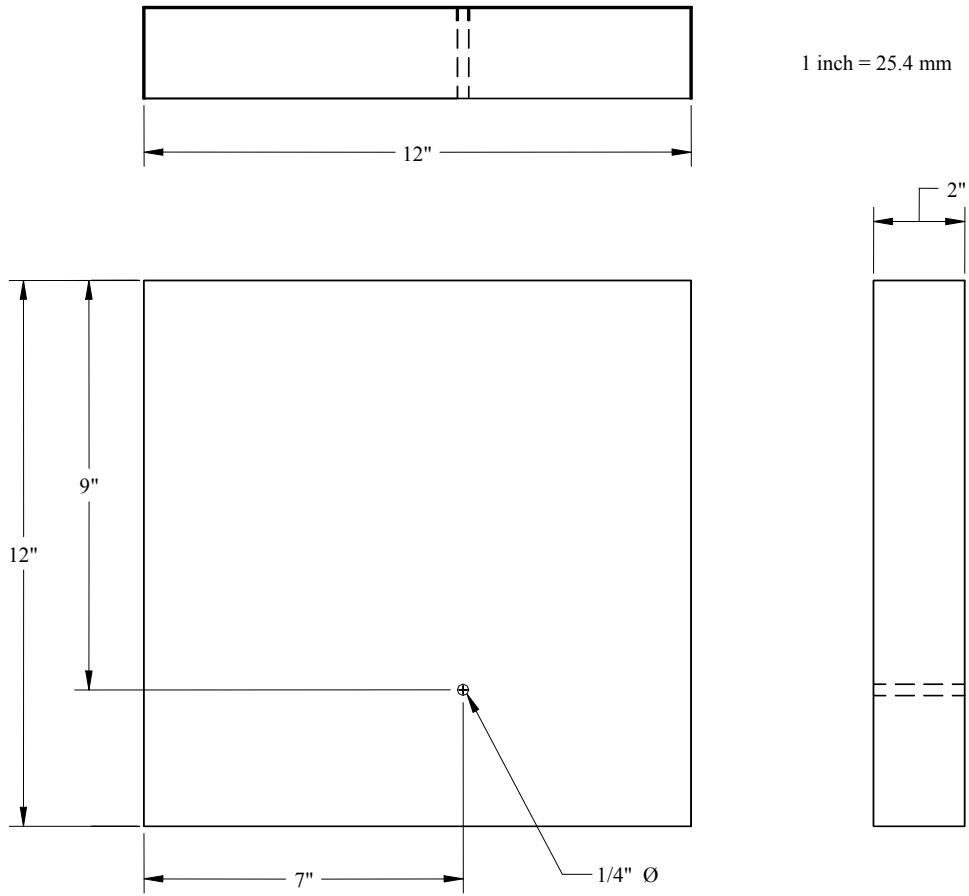


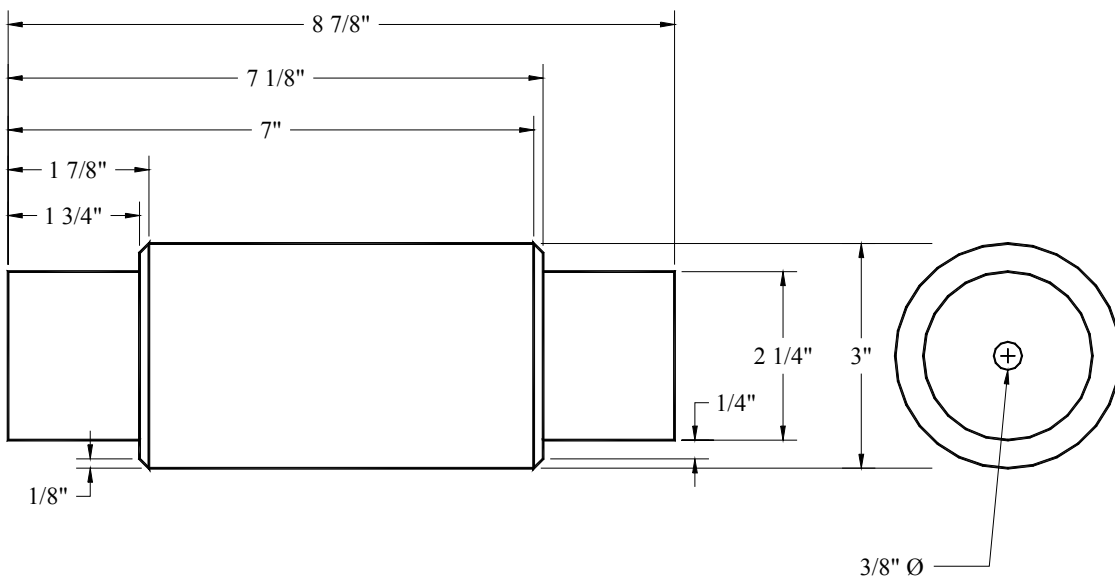
Figure 21. SDHTB details.



Figure 22. Photograph of the SDHTB.

### 3.2.2. Manufactured Cracked Pins

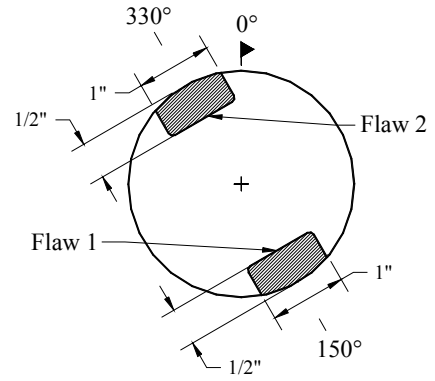
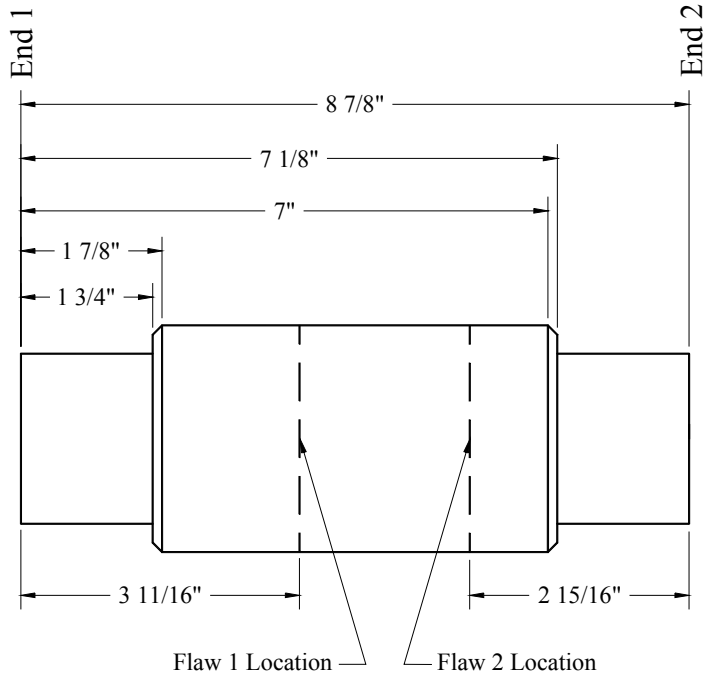
Five pins, removed from service in 1999, had a total of 7 cracks implanted at various locations. The typical geometry of the pins is shown in figure 23. All cracks were surface breaking and were oriented such that the defect was perpendicular to the length of the pin. Figures 24 through 28 illustrate the location and approximate size and shape of the cracks. As can be seen from these figures, the cracks represent a wide cross section of defect sizes and shapes. Further, these defects are representative of the range of defects one might expect to exist in actual pin and hanger connections.



1 inch = 25.4 mm

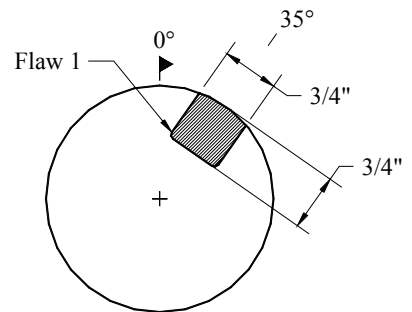
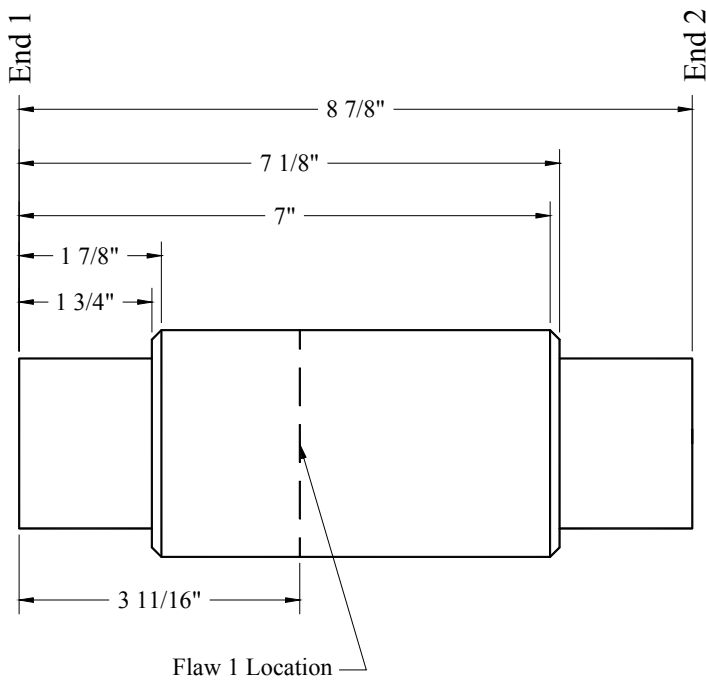
Figure 23. Typical pin geometry.





1 inch = 25.4 mm

Figure 26. Pin 3 defect details.



1 inch = 25.4 mm

Figure 27. Pin 4 defect details.

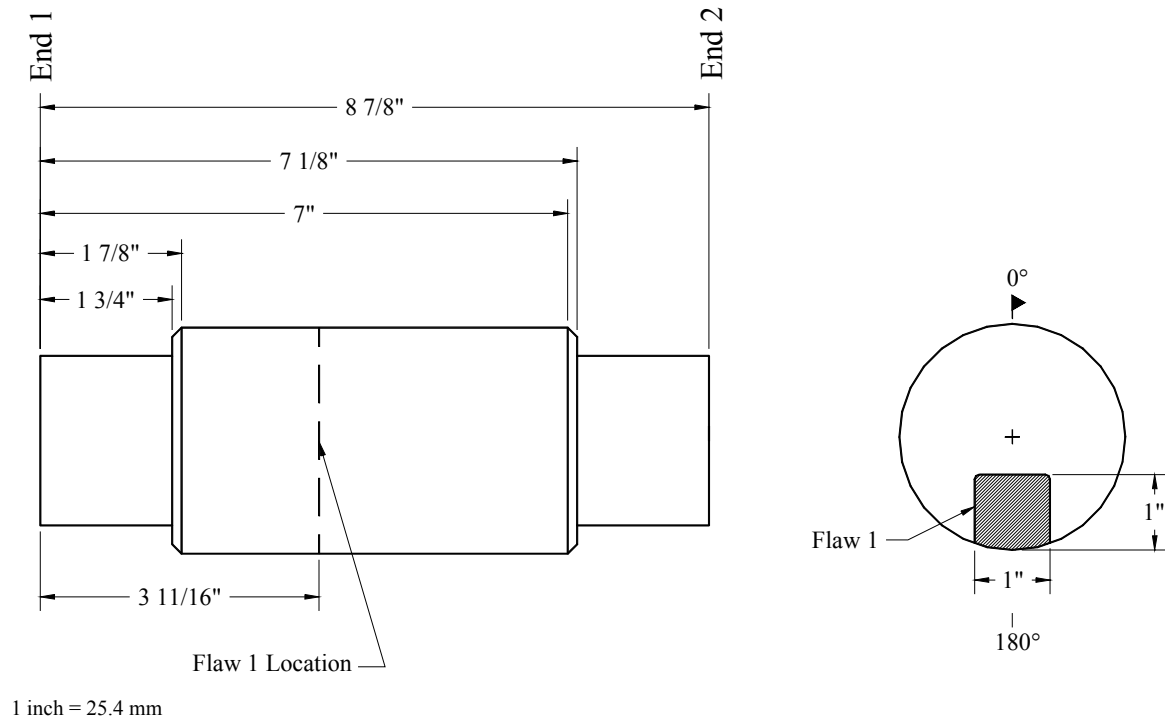
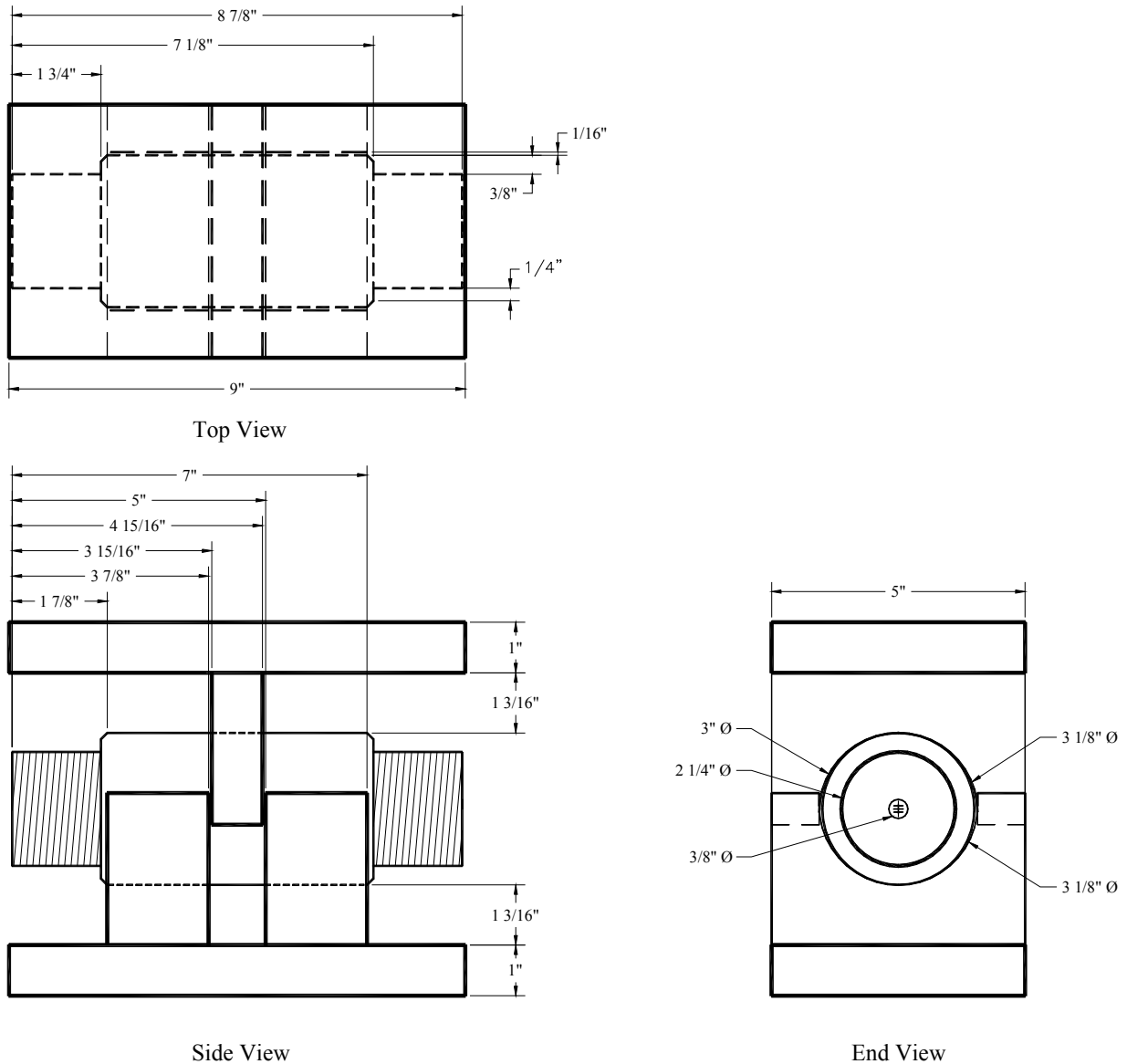


Figure 28. Pin 5 defect details.

### 3.2.3. Pin/Hanger Mockup

As was discussed previously, the phenomenon known as acoustic coupling has recently been a topic of significant debate. The ability to generate acoustic coupling in a pin/hanger connection requires two elements: a realistic connection geometry, and realistic load levels. To simulate these conditions, a pin/hanger connection mockup based on actual field geometry was developed. The mockup is shown schematically in figure 29. The pin used in the mockup has the same geometrical characteristics as the other pins used in this study. The rest of the mockup consists of three plates and two load platens. The three plates represent the suspended span web and two hanger plates found in a typical connection.



1 inch = 25.4 mm

Figure 29. Pin/hanger mockup details.

### 3.3. TESTING PROGRAM

The specific details of the testing program are described in the following five sections. For each test type, the number of tests conducted and the specimens used are described. In addition, where applicable, details about the specific transducers used are presented.

### **3.3.1. Beam Diffraction**

Beam diffraction testing was completed on the SDHTB specimen. Six different transducers were used with angles of 0.00, 8.02, 10.89, and 13.15 degrees and frequencies of 2.25 and 5 MHz. During this testing, each transducer was translated along each edge of the SDHTB in 3-mm (0.1-inch) increments with the return signal level for 80 percent screen height from the side-drill hole noted at each location. From this, a profile of return signal strength was generated. This type of test illustrates the amount of beam spread present in each transducer and how the depth of penetration influences the beam spread.

### **3.3.2. Distance Amplitude Correction**

Similar to the beam diffraction testing, the distance amplitude correction testing was also completed with the SDHTB. For this testing, the transducer was placed on each edge of the SDHTB such that the return signal was maximized. Four different signal amplitudes with accompanying sound path distances could be generated with this setup. With these four data points for each transducer, the DAC curve could be generated.

### **3.3.3. Angle and Straight Beam Sensitivity to Cracks**

To investigate the sensitivity levels for angle and straight beam transducers with respect to cracks, “normal” pin inspections were completed on the manufactured cracked pin samples described previously. This means that each pin was inspected following the general procedures outlined previously with the goal of locating any defects. A single angle beam transducer, which had been optimized for the shear plane location, was used for the angle beam testing. For the subject cracked pin specimens, the selected transducer had an incident angle of 13.15 degrees with a frequency of 5 MHz with a 13-mm (0.5-inch) diameter beam. The straight beam transducer was 13 mm (0.5 inch) in diameter with a frequency of 5 MHz. Through this type of testing, one can study, qualitatively, the ability of each transducer to detect cracks of various sizes.

### **3.3.4. Defect Sizing**

For this testing, each defect in the manufactured cracked pin specimens was sized using ultrasonic contact and immersion tank techniques. The manual ultrasonic sizing utilized a

combination of straight and angle beam transducers. The technique used was most similar to the 6-dB drop method described previously. The immersion tank sizing was completed solely with a straight beam transducer and varying gain levels. The immersion tank testing was completed following established techniques for these types of inspections.

### **3.3.5. Acoustic Coupling**

To verify the presence of acoustic coupling, the pin/hanger connection mockup described previously was used in combination with a hydraulic load frame. During this testing, various combinations of transducers were used to verify the presence of acoustic coupling under varying load conditions. The hydraulic load frame had the capability of applying 20 kips (1 kip is equal to 1,000 pounds) compression to the pin/hanger connection mockup which is equivalent to the load level experienced in a lightly loaded bridge. This type of setup allowed the presence of acoustic coupling to be verified in both the pitch-catch and pulse-echo formats; it will be described later.

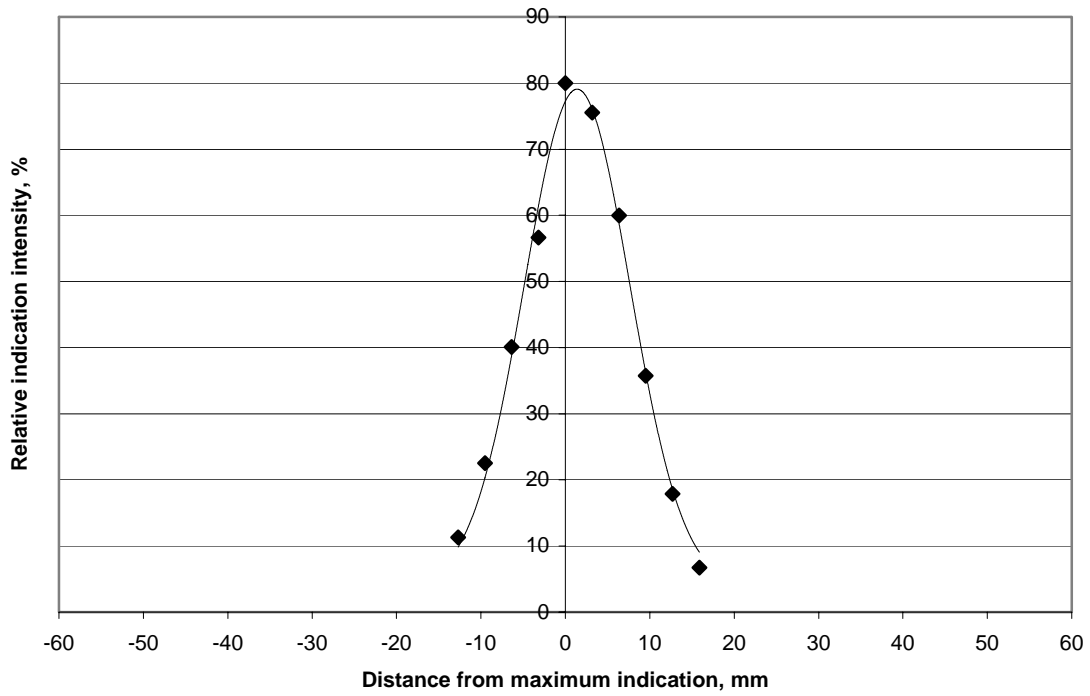


## **4. EXPERIMENTAL RESULTS**

The following sections summarize the results from the experimental portion of this investigation. Results will be presented in five sections. First, the results from testing related to beam diffraction will be summarized. Next, results from the distance amplitude correction testing will be presented. Third, results from testing related to angle and straight beam sensitivity to cracks will be presented. Fourth, results from the defect sizing testing will be presented. Finally, testing related to the acoustic coupling phenomenon will be summarized.

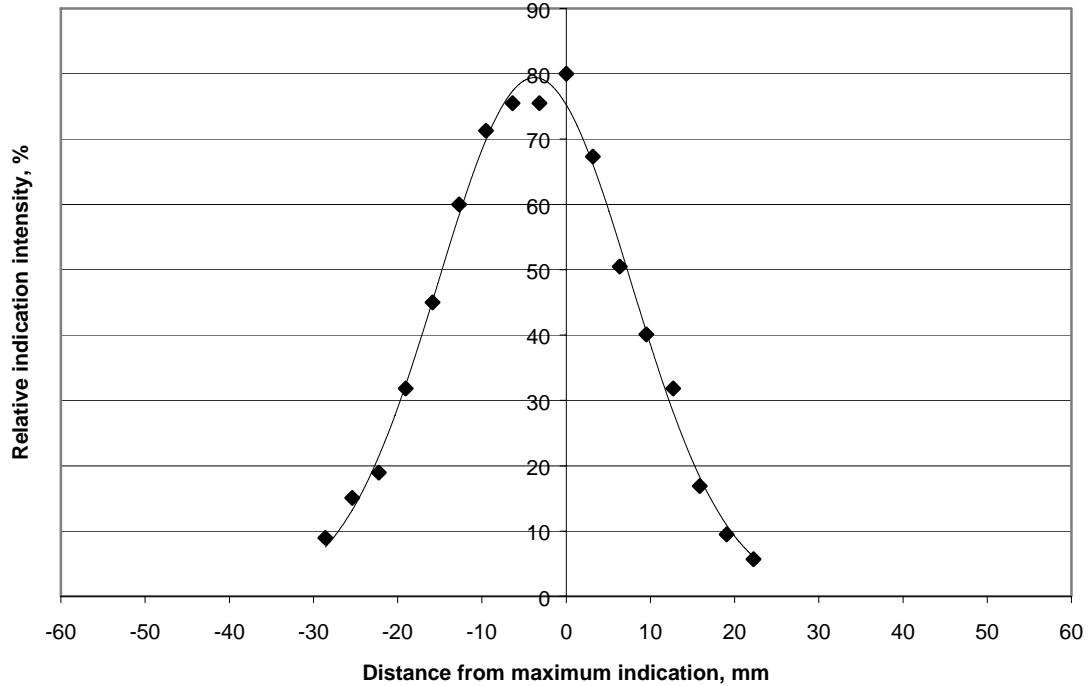
### **4.1. BEAM DIFFRACTION**

Six transducers were used in the beam diffraction study and represent typical transducers that might be used during a pin/hanger inspection. An indication level at 80 percent screen height was collected for each transducer at each penetration depth. Figures 30 through 35 summarize the experimental beam diffraction testing results. In addition, a best-fit Gaussian distribution is also shown for each test. As can be seen from these data, as the depth of penetration increases, so does the breadth of the beam diffraction, which would be expected given the nature of ultrasonics. Note the good agreement, within the sensitivity of the test, between the Gaussian distribution and the experimental data. Again, this is expected, given the manner in which ultrasonic waves propagate through a test specimen. Note, however, that the secondary acoustic lobes known to exist in ultrasonic signals could not be identified consistently during this testing. This is most likely because these lobes are often very small, and the sensitivity of this testing was such that these could not be monitored.



1 mm = .039 inch

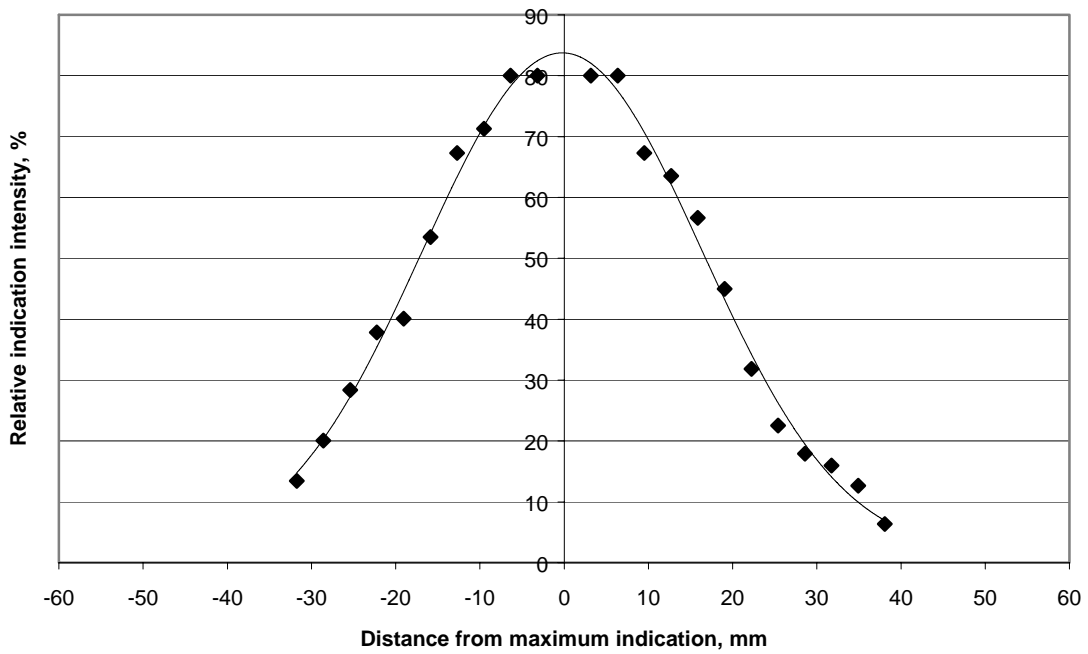
a. 76.2-mm penetration.



1 mm = .039 inch

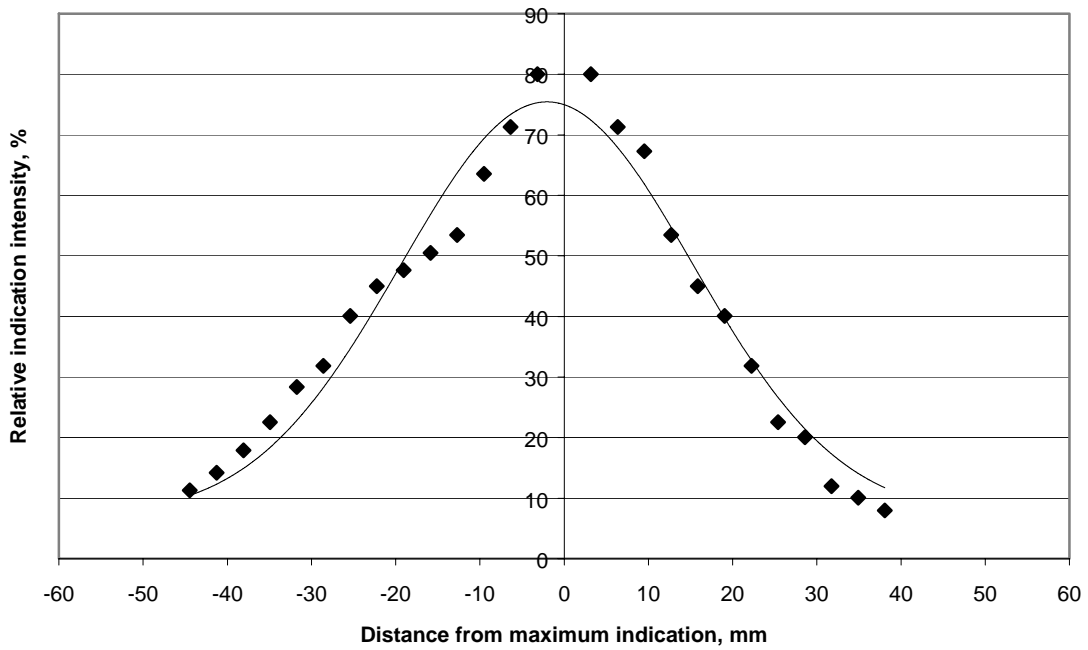
b. 127-mm penetration.

Figure 30. Beam diffraction results for 8-degree, 5-MHz, 12.7-mm diameter transducer.



1 mm = .039 inch

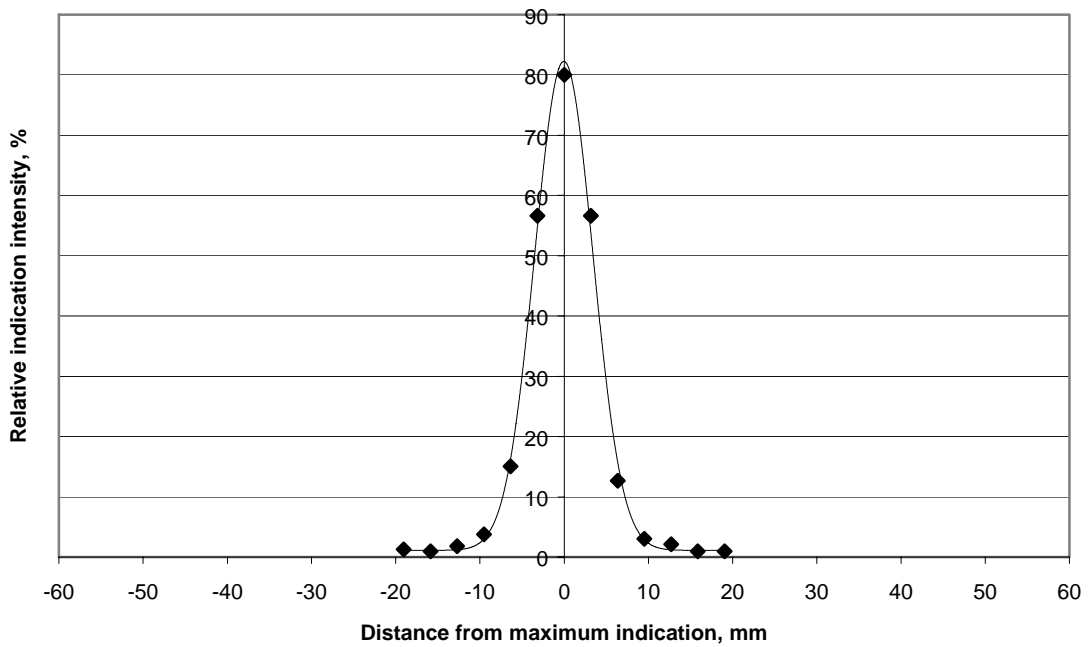
c. 177.8-mm penetration.



1 mm = .039 inch

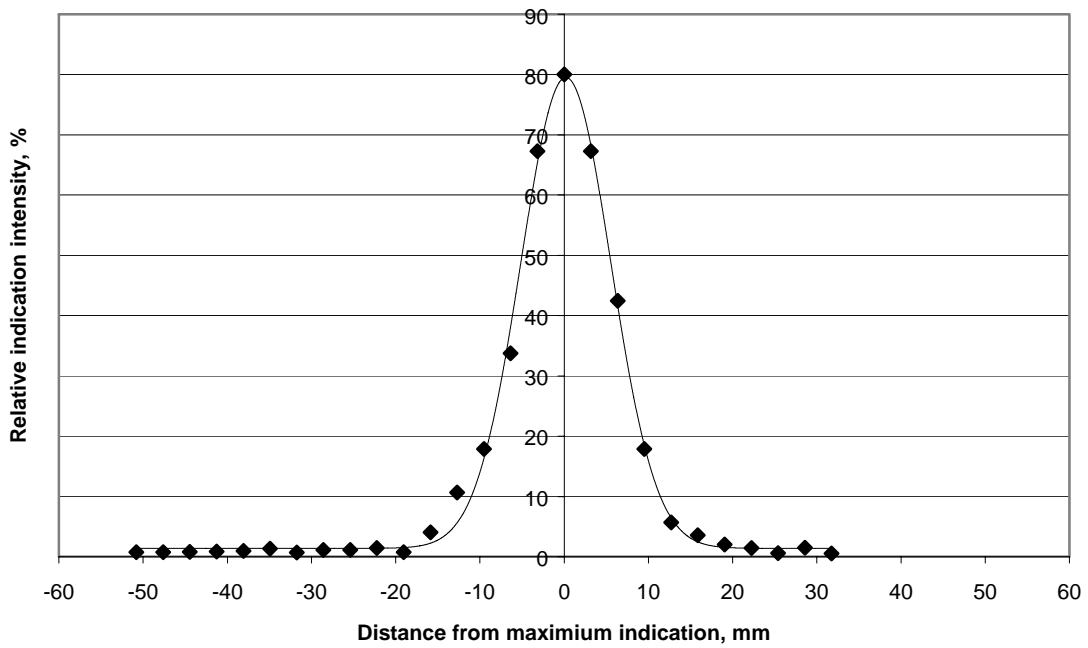
d. 228.6-mm penetration.

Figure 30. (Continued) Beam diffraction results for 8-degree, 5-MHz, 12.7-mm diameter transducer.



1 mm = .039 inch

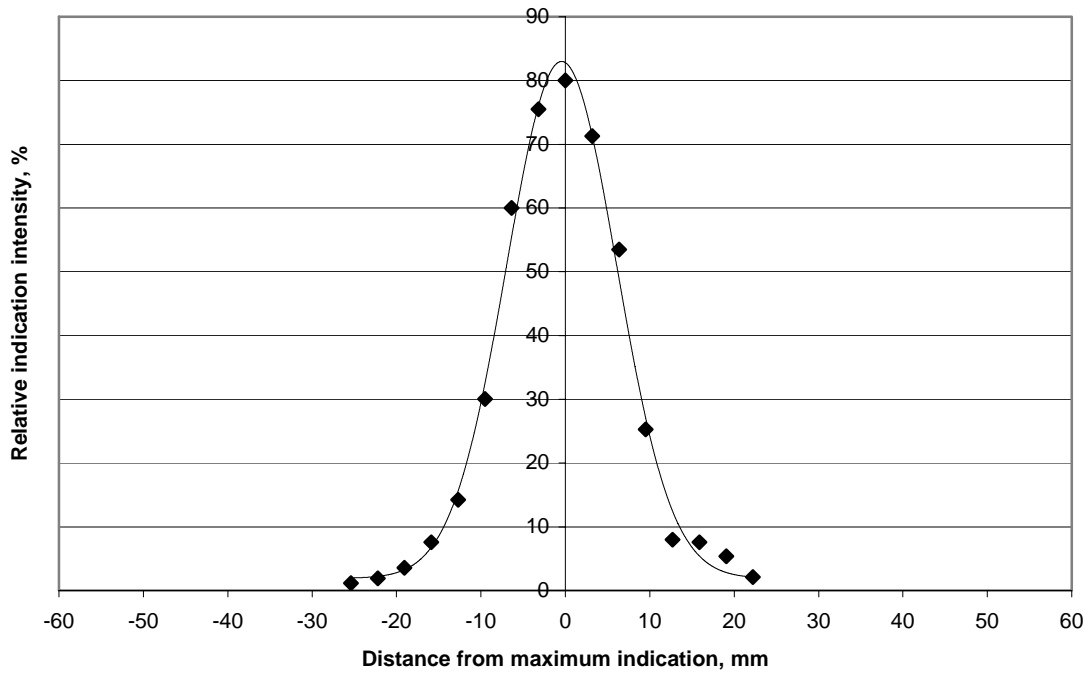
a. 76.2-mm penetration.



1 mm = .039 inch

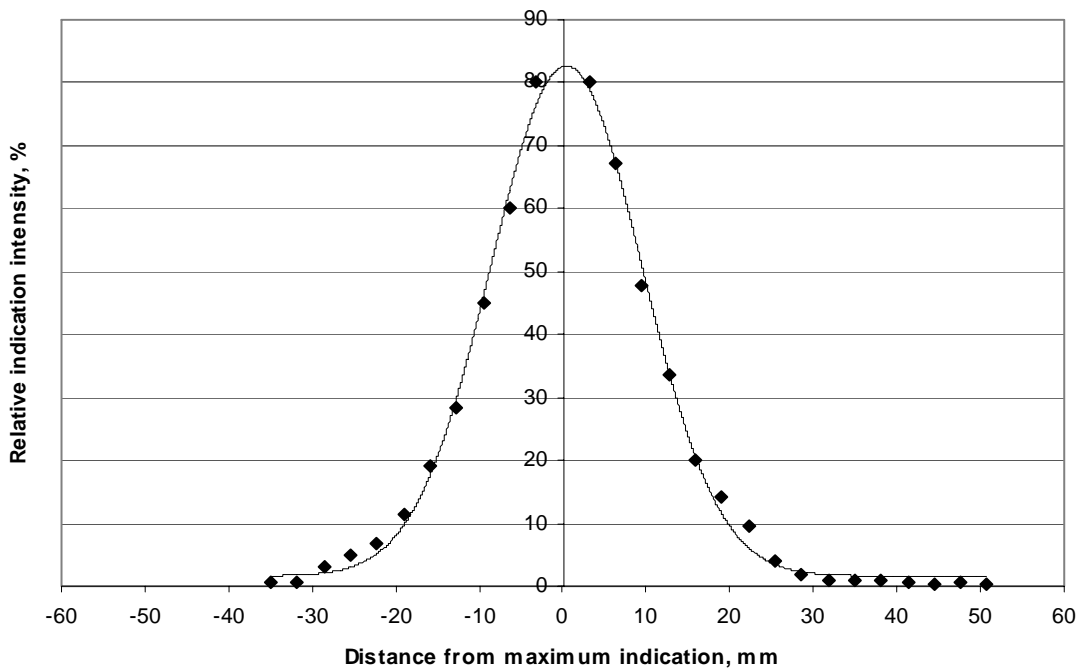
b. 127-mm penetration.

Figure 31. Beam diffraction results for 0-degree, 5-MHz, 12.7-mm diameter transducer.



1 mm = .039 inch

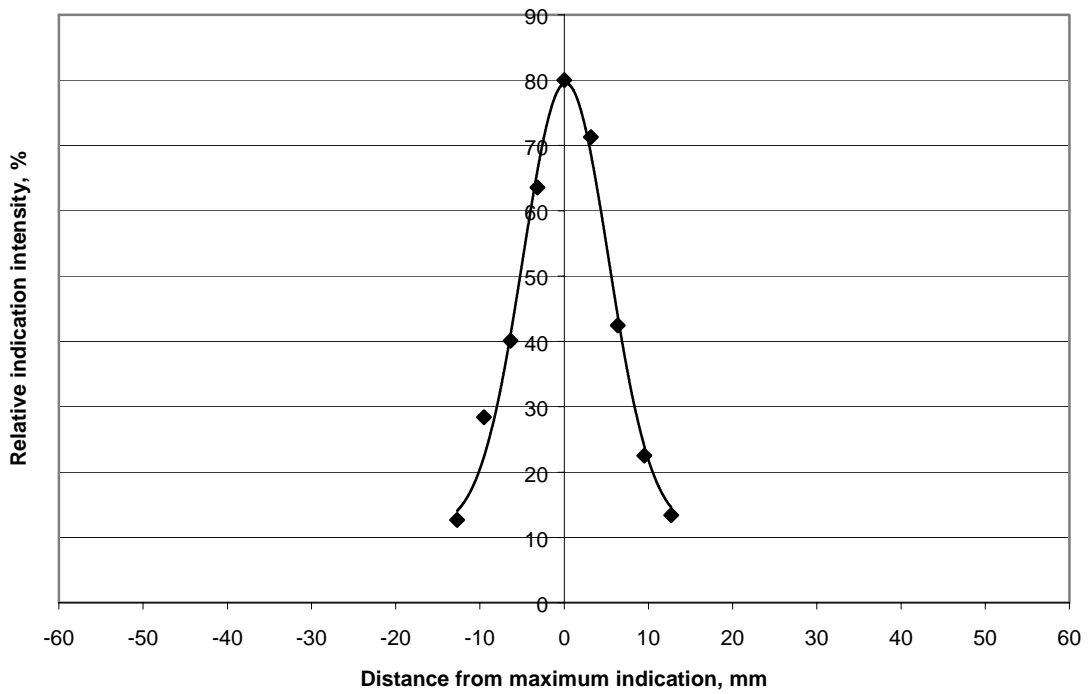
c. 177.8-mm penetration.



1 mm = .039 inch

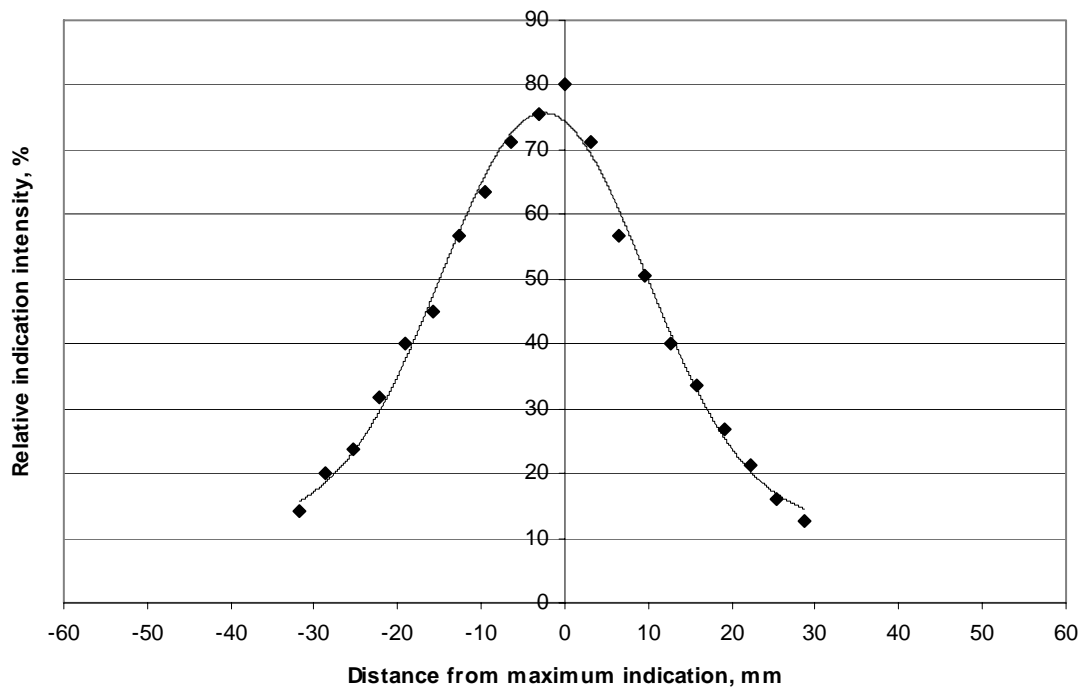
d. 228.6-mm penetration.

Figure 31. (Continued) Beam diffraction results for 0-degree, 5-MHz, 12.7-mm diameter transducer.



1 mm = .039 inch

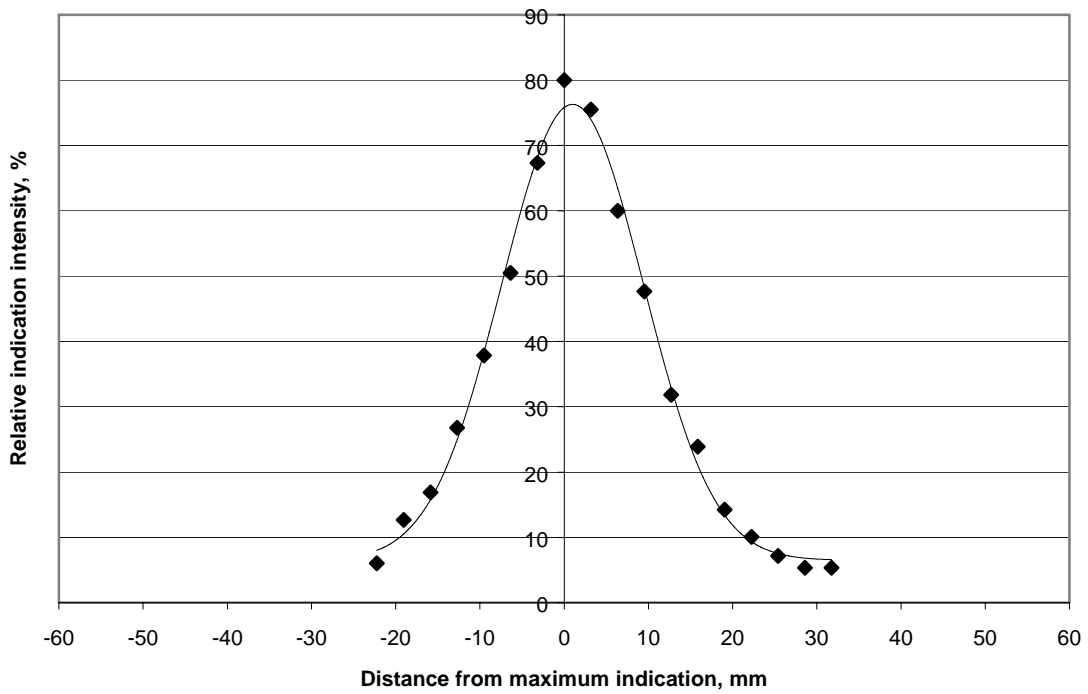
a. 76.2-mm penetration.



1 mm = .039 inch

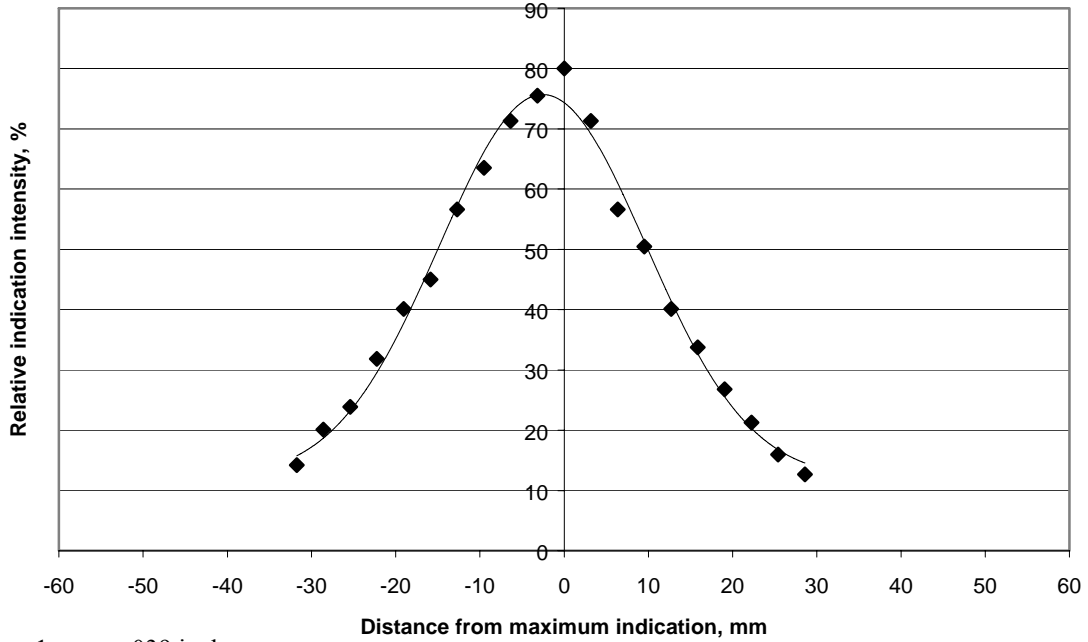
b. 127-mm penetration.

Figure 32. Beam diffraction results for 0-degree, 2.25-MHz, 25.4-mm diameter transducer.



1 mm = .039 inch

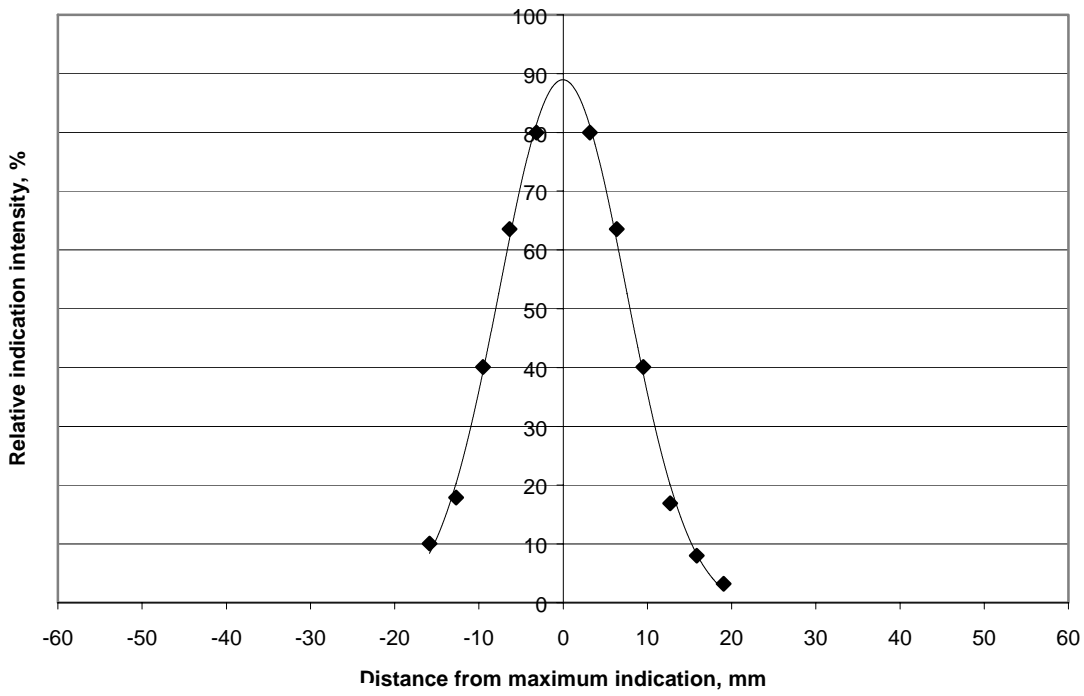
c. 177.8-mm penetration.



1 mm = .039 inch

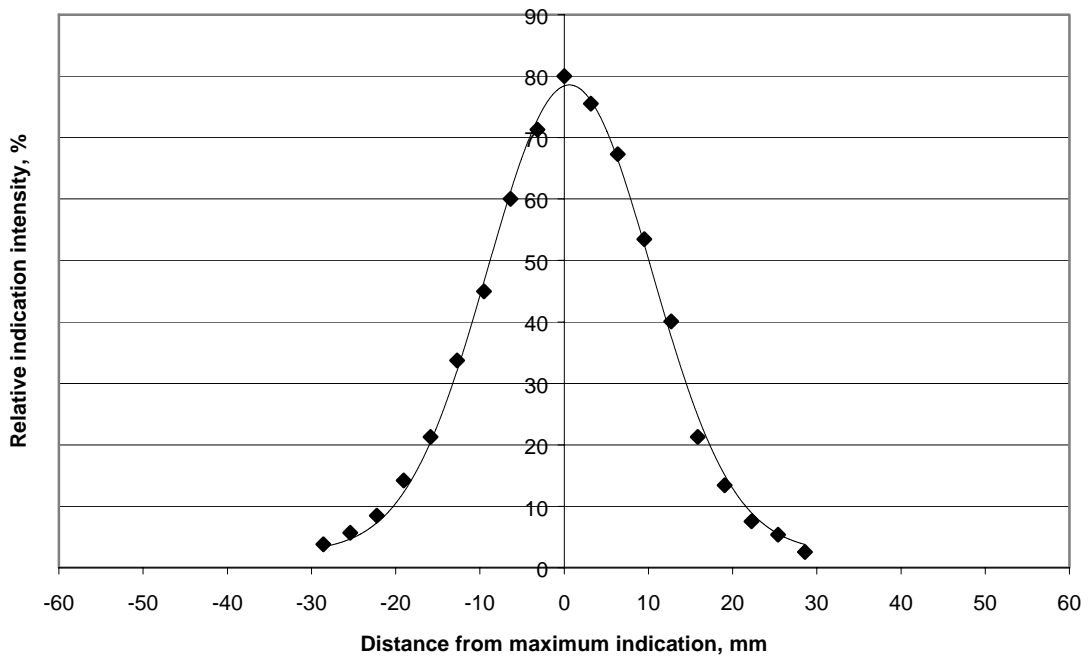
d. 228.6-mm penetration.

Figure 32. (Continued) Beam diffraction results for 0-degree, 2.25-MHz, 25.4-mm diameter transducer.



1 mm = .039 inch

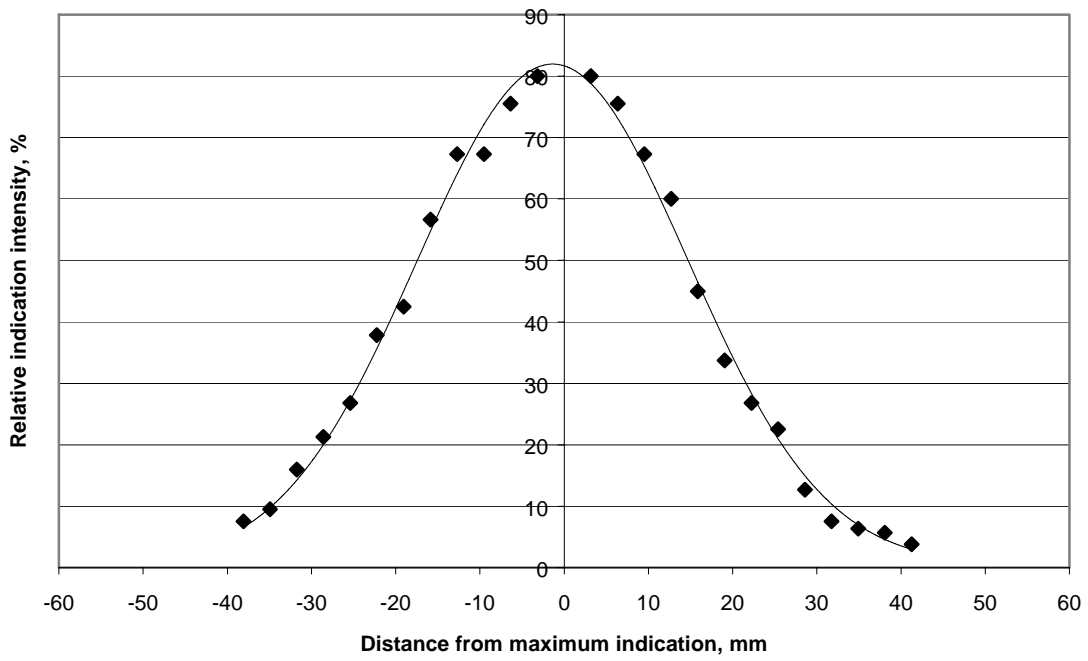
a. 76.2-mm penetration.



1 mm = .039 inch

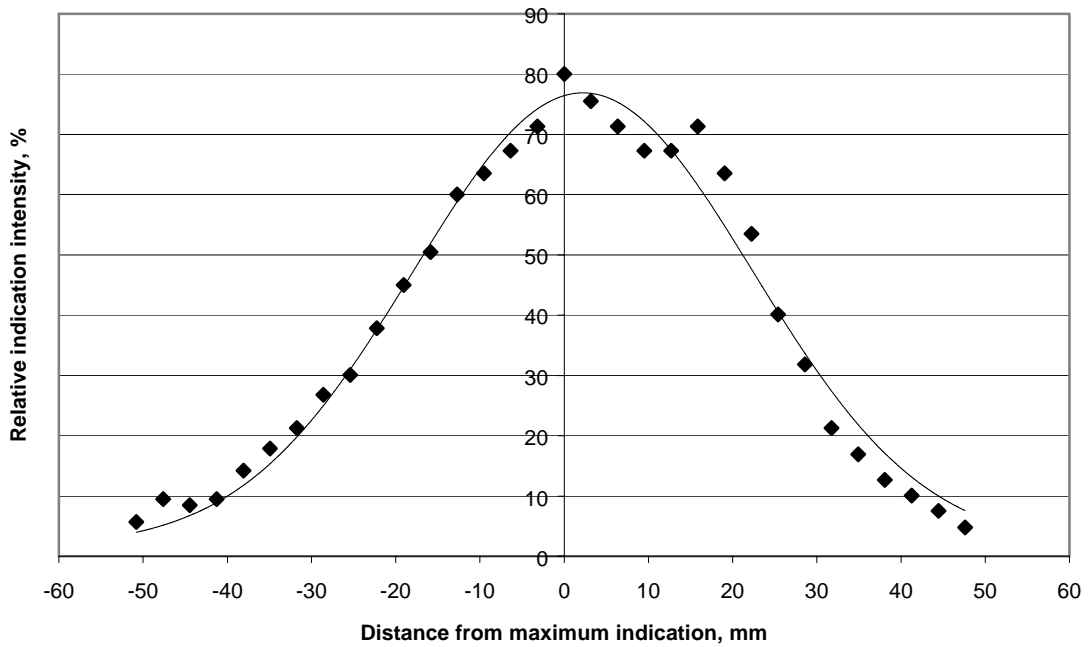
b. 127-mm penetration.

Figure 33. Beam diffraction results for 11-degree, 2.25-MHz, 12.7-mm diameter transducer.



1 mm = .039 inch

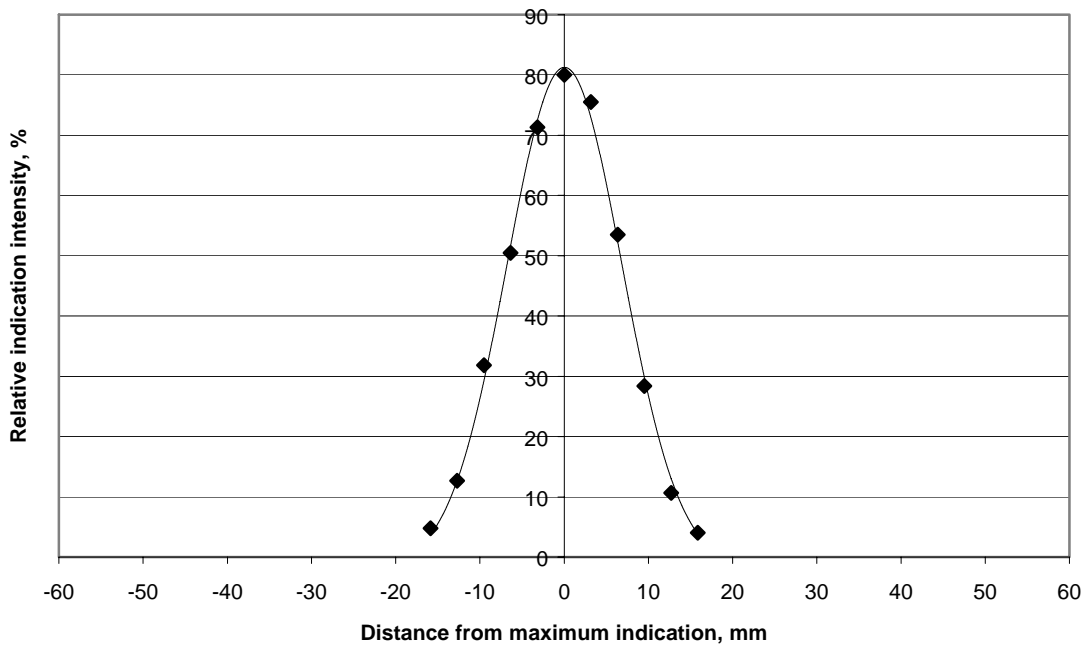
c. 177.8-mm penetration.



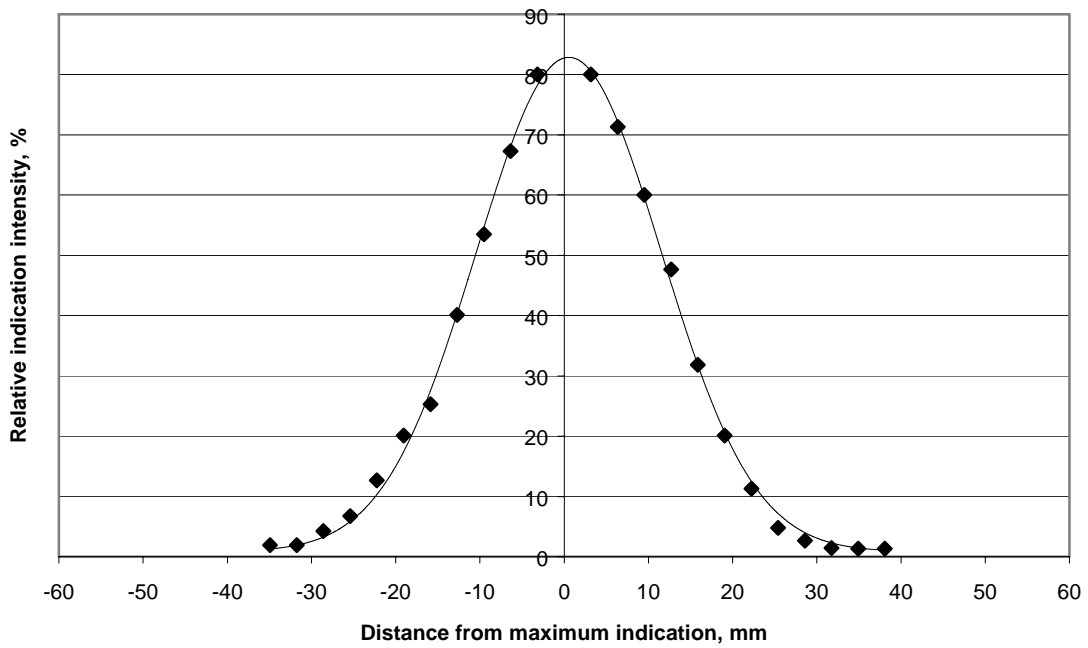
1 mm = .039 inch

d. 228.6-mm penetration.

Figure 33. (Continued) Beam diffraction results for 11-degree, 2.25-MHz, 12.7-mm diameter transducer.

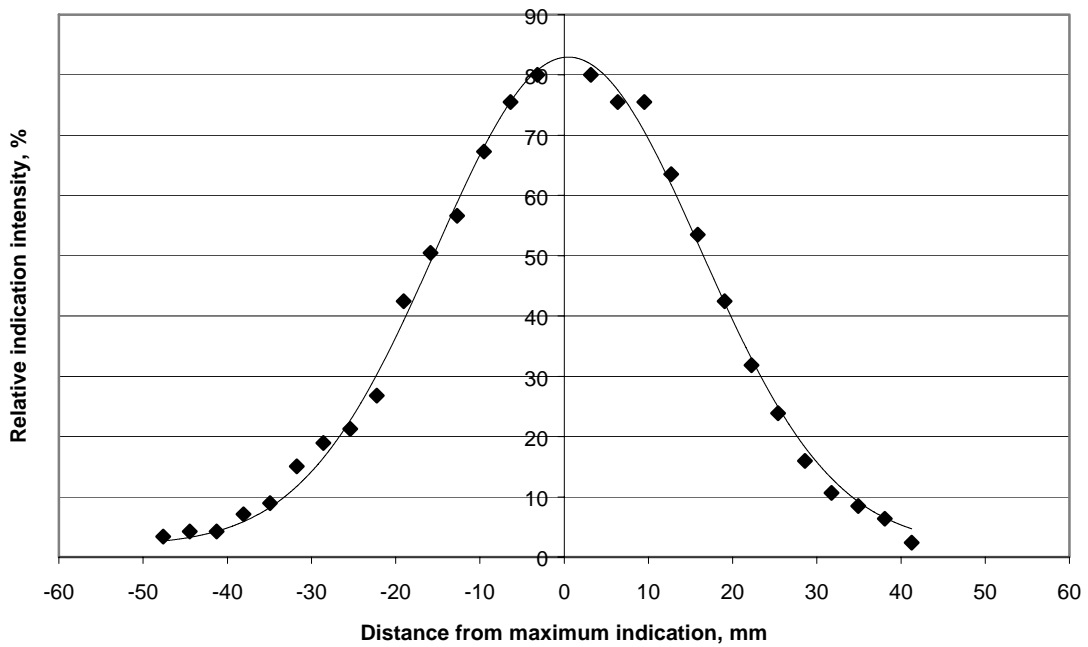


a. 76.2-mm penetration.

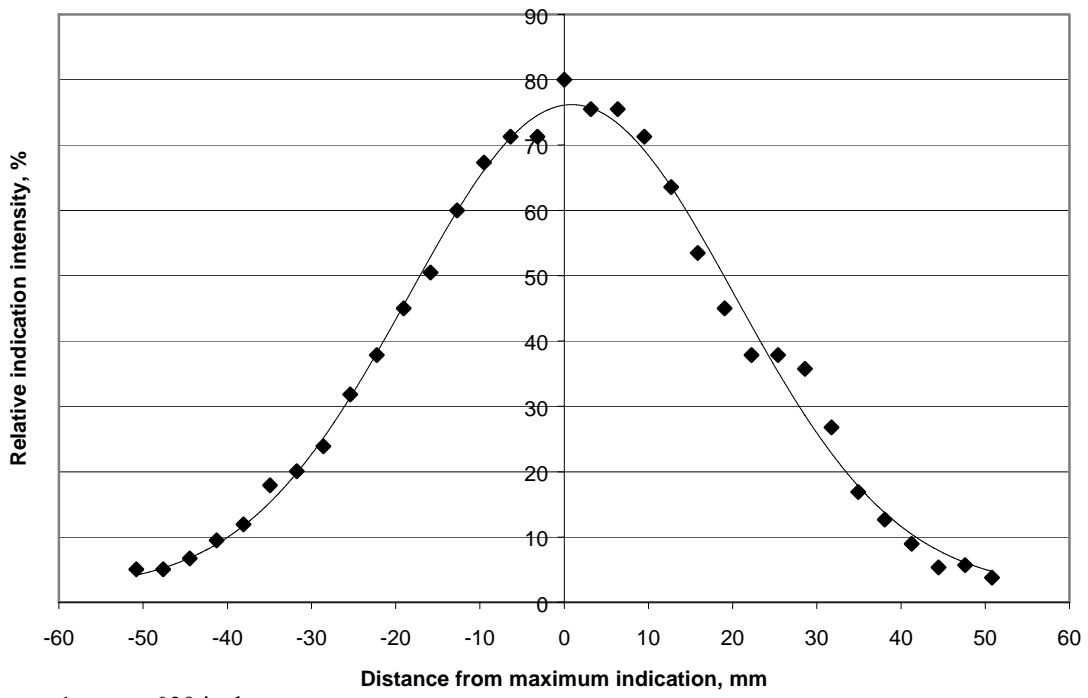


b. 127-mm penetration.

Figure 34. Beam diffraction results for 14-degree, 2.25-MHz, 12.7-mm diameter transducer.

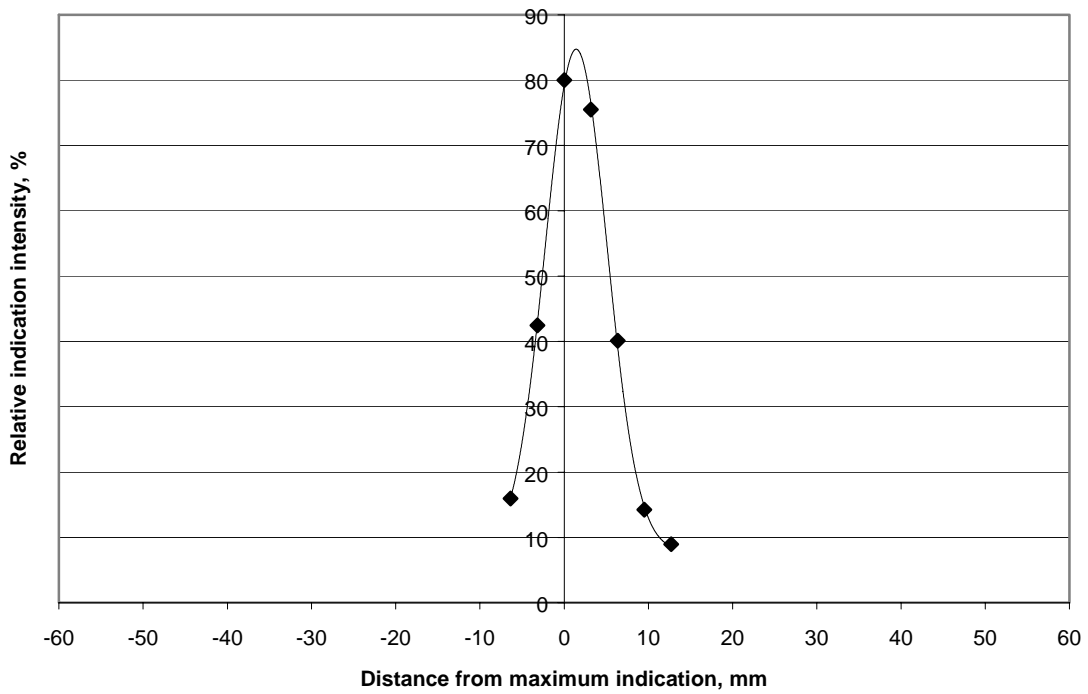


c. 177.8-mm penetration.



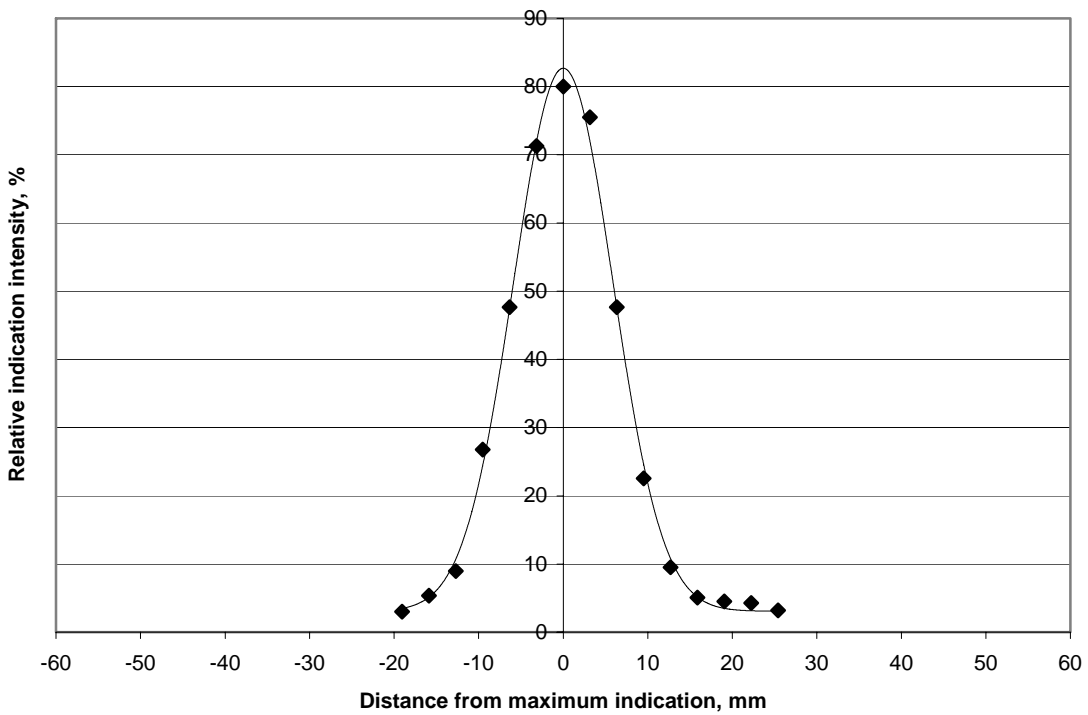
d. 228.6-mm penetration.

Figure 34. (Continued) Beam diffraction results for 14-degree, 2.25-MHz, 12.7-mm diameter transducer.



1 mm = .039 inch

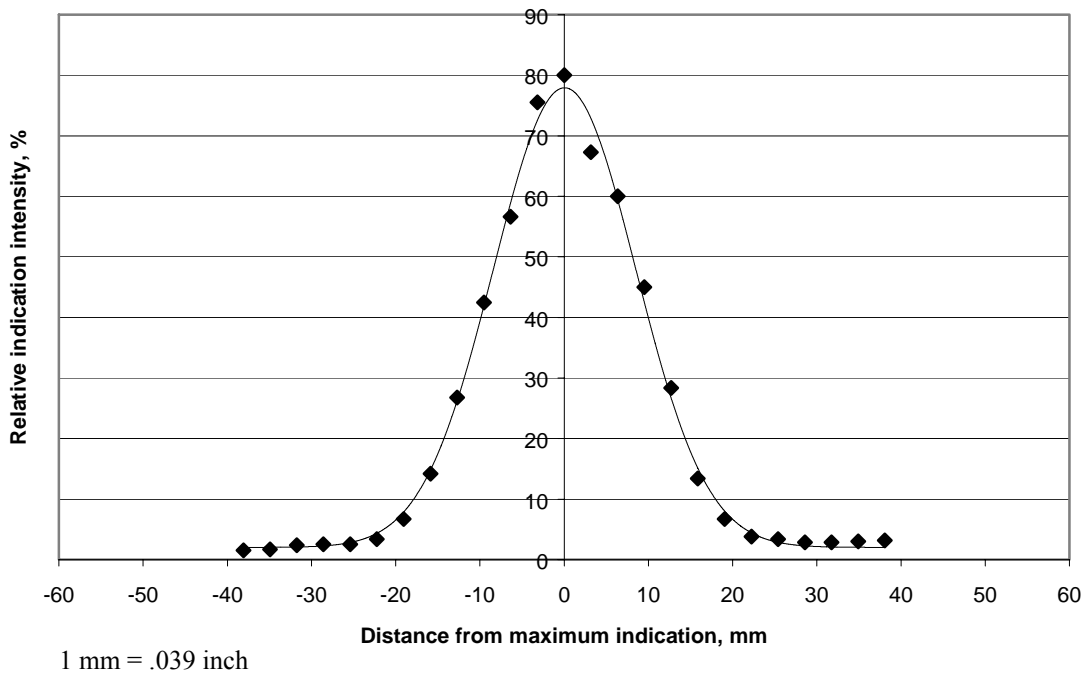
a. 76.2-mm penetration.



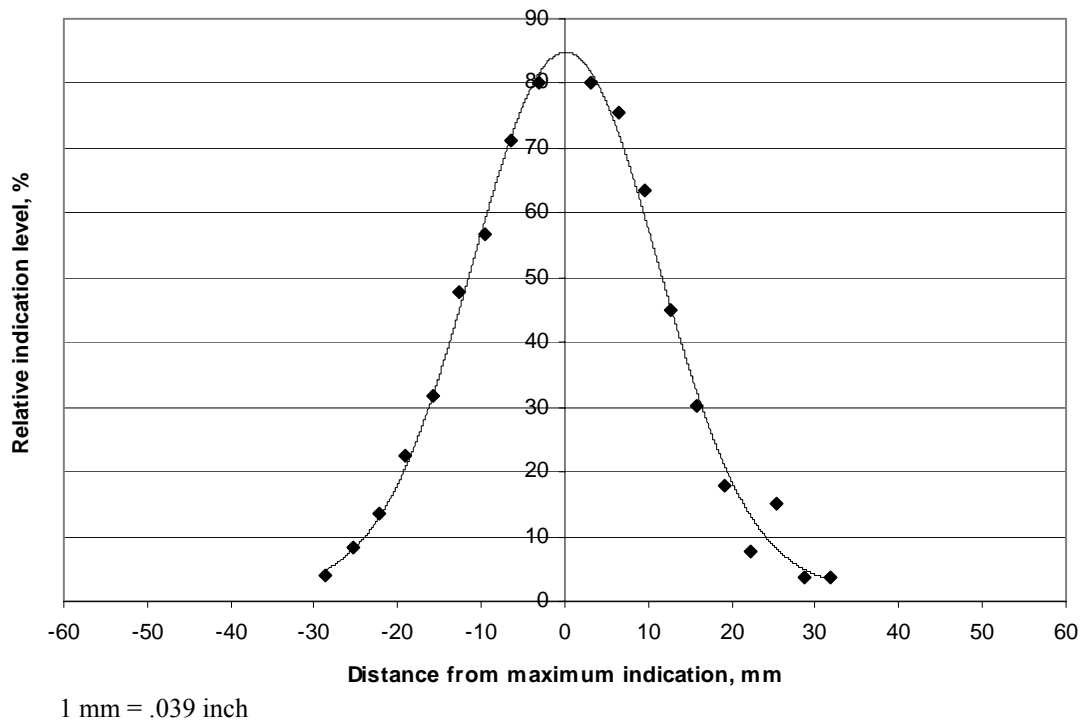
1 mm = .039 inch

b. 127-mm penetration.

Figure 35. Beam diffraction results for 8-degree, 2.25-MHz, 19-mm square transducer.



c. 177.8-mm penetration.



d. 228.6-mm penetration.

Figure 35. (Continued) Beam diffraction results for 8-degree, 2.25-MHz, 19-mm square transducer.

## 4.2. DISTANCE AMPLITUDE CORRECTION

Six transducers were again used in the distance amplitude correction testing portion of this study. These transducers represent typical transducers that might be used during a pin/hanger inspection. An indication level at 80 percent screen height was collected for each transducer at each sound path distance. Figures 36 through 41 summarize the experimental distance amplitude correction results. In addition, a best-fit exponential curve is also shown for each test.

As can be seen from the data in figures 36 through 41, there is really very little difference in the distance amplitude correction curve for the various transducers. This would indicate that the loss of signal strength is primarily dependent upon the material being tested and less so on the characteristics of the ultrasonic transducer. Also note the good agreement, within the sensitivity of the test, between the exponential curve and the experimental data. Again, this would be expected, given the manner in which the ultrasonic signal is introduced into the test specimen.

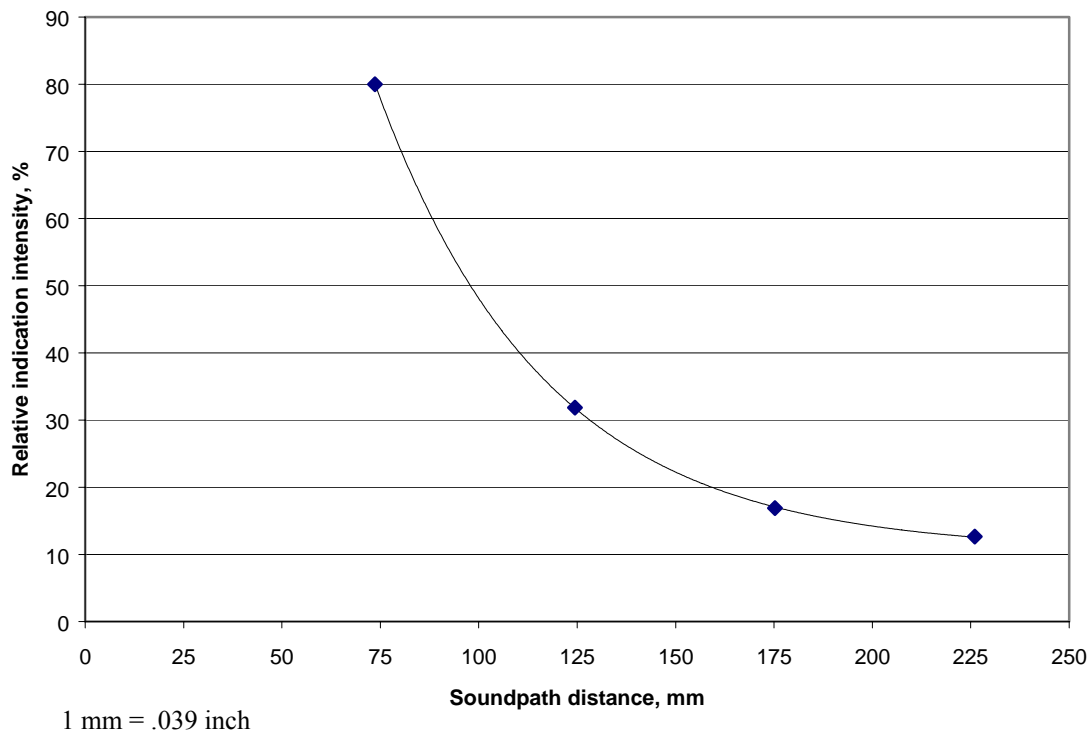


Figure 36. Distance amplitude correction curve for 8-degree, 5-MHz, 12.7-mm diameter transducer.

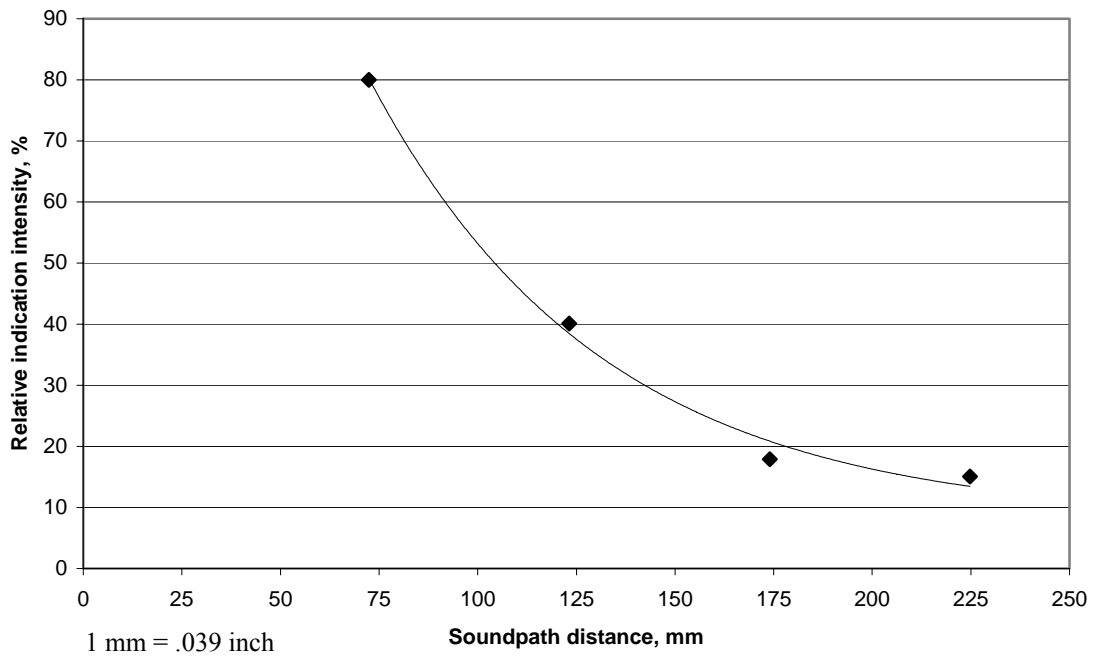


Figure 37. Distance amplitude correction curve for 0-degree, 5-MHz, 12.7-mm diameter transducer.

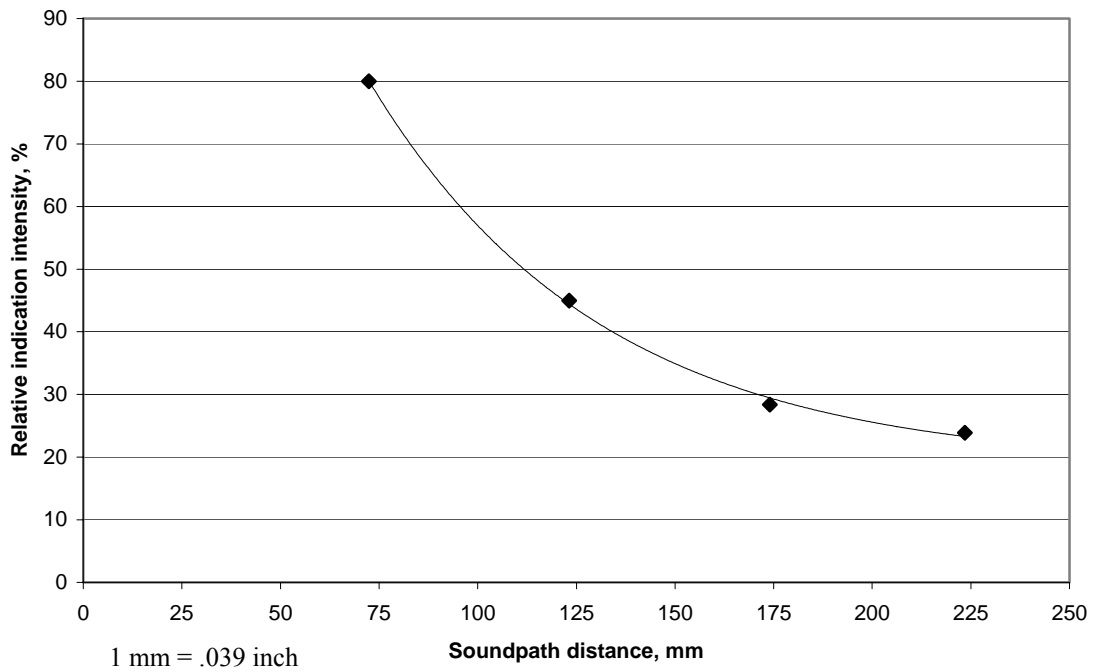


Figure 38. Distance amplitude correction curve for 0-degree, 2.25-MHz, 25.4-mm diameter transducer.

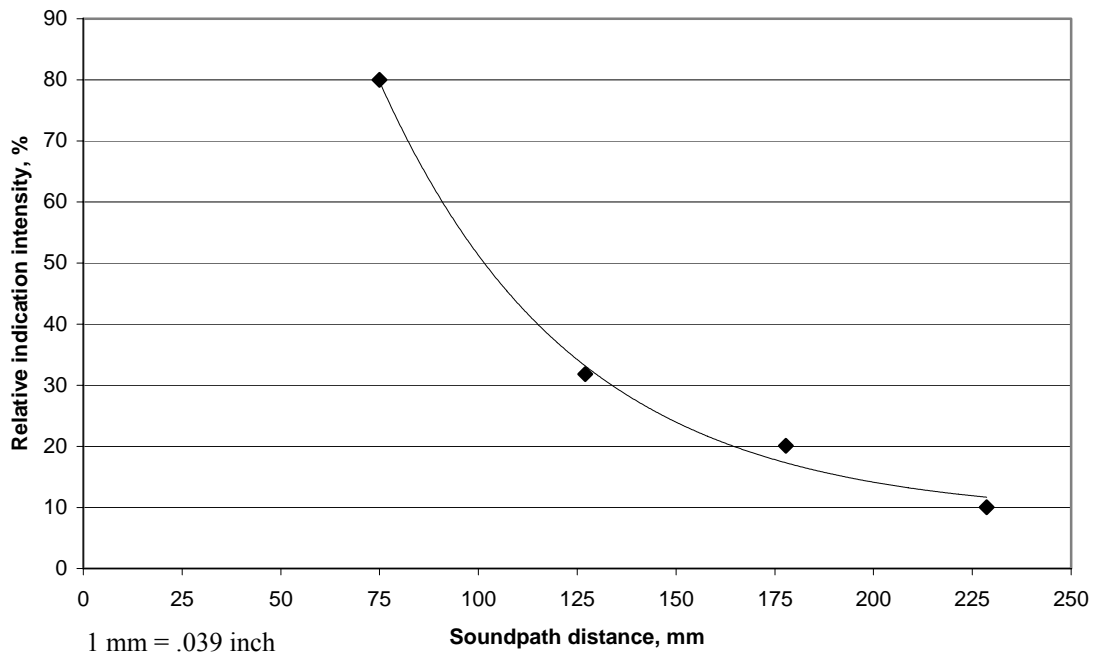


Figure 39. Distance amplitude correction curve for 11-degree, 2.25-MHz, 12.7-mm diameter transducer.

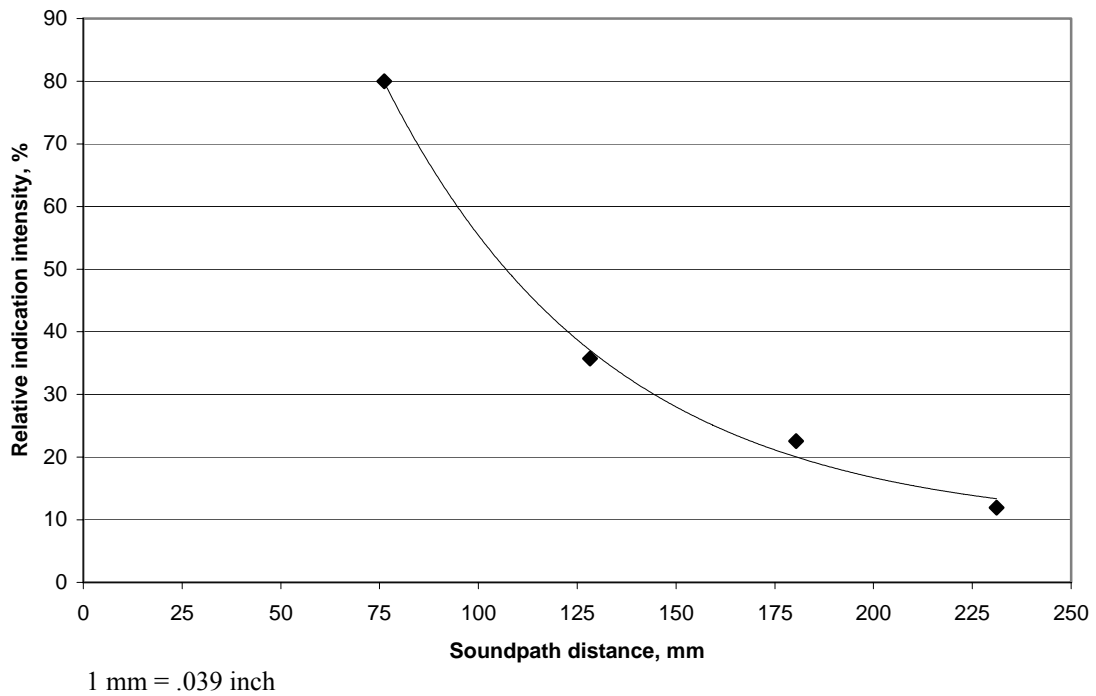


Figure 40. Distance amplitude correction curve for 14-degree, 2.25-MHz, 12.7-mm diameter transducer.

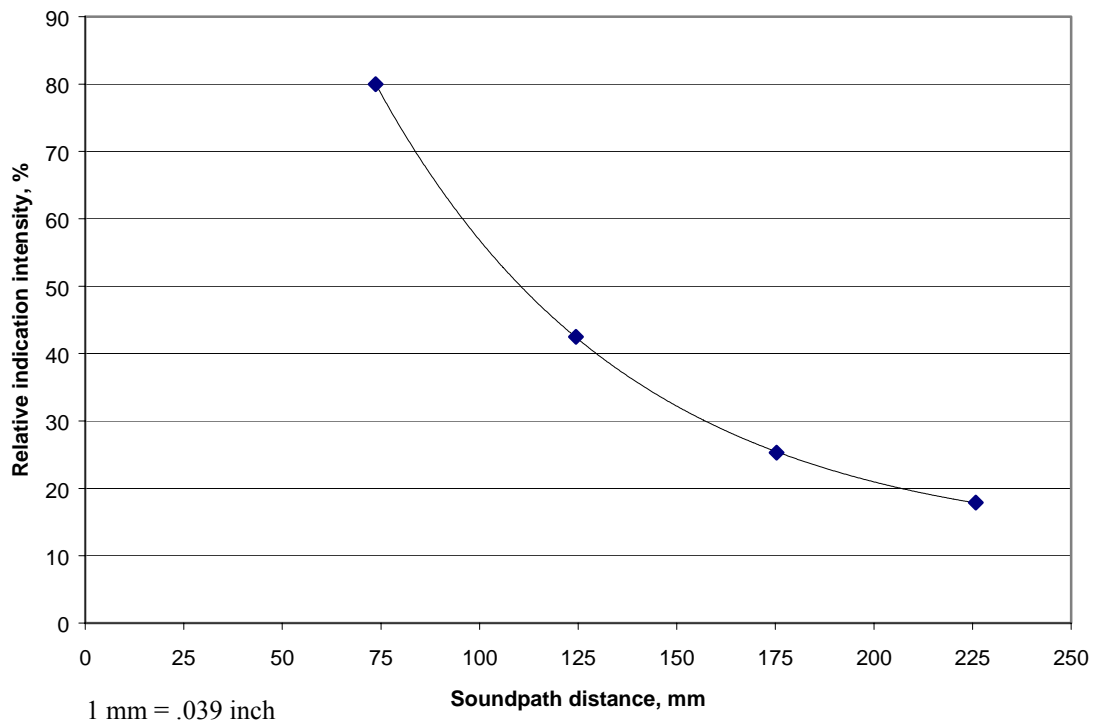


Figure 41. Distance amplitude correction curve for 8-degree, 2.25-MHz, 19-mm square transducer.

### **4.3. ANGLE AND STRAIGHT BEAM SENSITIVITY TO CRACKS**

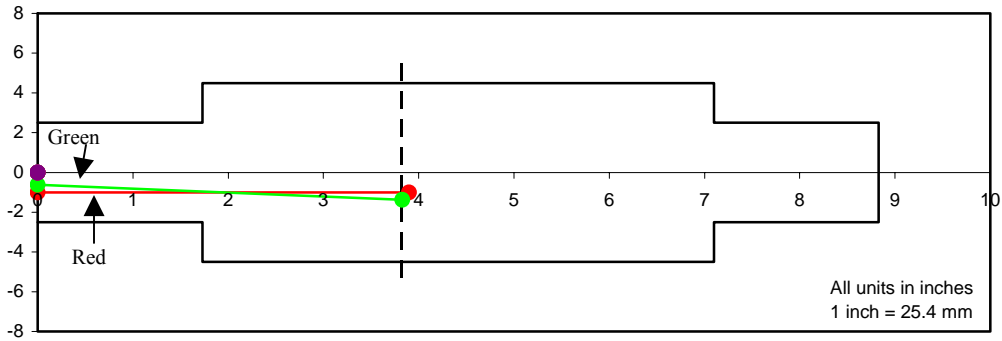
As mentioned previously, to study the sensitivity of angle and straight beam transducers to cracks, “normal” pin inspection procedures were completed on each of the pins with manufactured cracks. From these results one can infer the relative sensitivity of each transducer to the cracks found in these specimens. The data for each of the pins are summarized in figures 42 through 46. Each figure gives the raw inspection data and a graphical representation of the scan results. Parts B and E of each figure show the centerline path of the ultrasonic beam as it traveled from the transducer to the indication. Parts C and F of each figure summarize the location of peak signal strength (indicated by the large dot) and the range about the circumference over which the typical signal was observed. Note that in parts B and E of each figure, the dotted line represents the known location of the cracks. As can be seen from the data, regardless of the transducer used, the inspector was relying on the beam spread to identify each crack. This may not always be the case in a typical pin inspection. Also of interest is the fact that for the smallest defect, the straight beam transducer was not able to reliably detect the crack. Further, the crack could only be identified when the inspector was aware that a crack existed. This finding illustrates the importance of selecting the correct transducer for each inspection.

Note	Scan angle, deg	Indication level, dB	Reference level, dB	Reading location, hh:mm	Beginning of signal location, hh:mm	End of signal location, hh:mm	Distance to index, inches	Sound path distance, inches	Axial distance, inches	Radial distance, inches
1	0	73	47	7:30	7:30	7:30	1	3.9	3.9	1.00
2	11	57	47	7:30	7:00	8:00	5/8	3.9	3.83	1.37

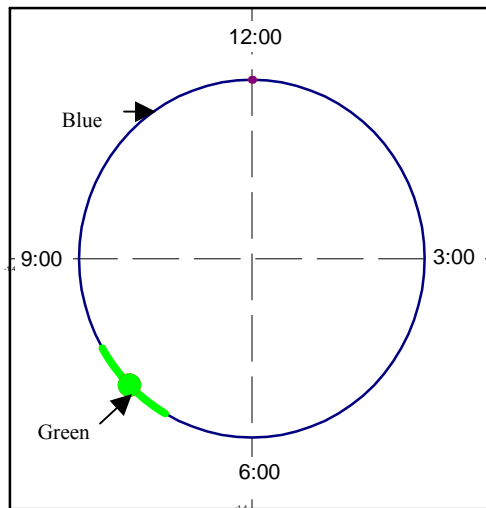
Unit conversion: 1 inch = 25.4 mm

Red →  
Green →

a. Raw inspection data for end 1 scanning.



b. Pin elevation for end 1 scanning.



c. Pin cross section for end 1 scanning.

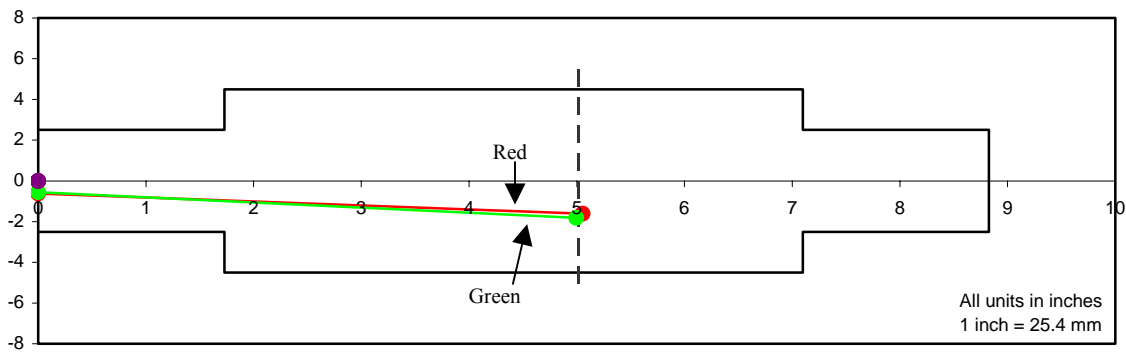
Figure 42. Pin 1 testing results.

Red →  
Green →

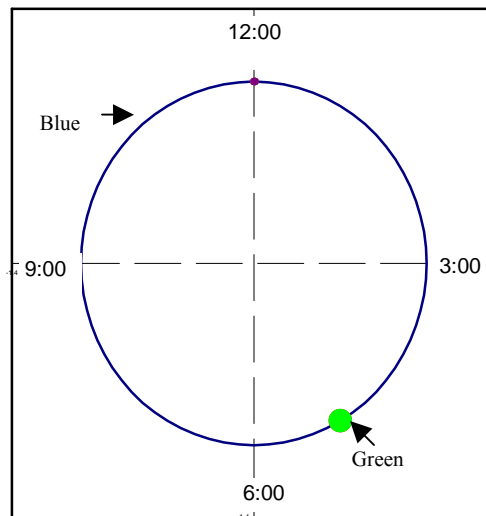
Note	Scan angle, deg	Indication level, dB	Reference level, dB	Reading location, hh:mm	Beginning of signal location, hh:mm	End of signal location, hh:mm	Distance to index, inches	Sound path distance, inches	Axial distance, inches	Radial distance, inches
1	11	63	47	5:00	5:00	5:00	5/8	5.15	5.06	1.61
2	14	59	43	5:00	5:00	5:00	9/16	5.15	5.00	1.81

Unit conversion: 1 inch = 25.4 mm

d. Raw inspection data for end 2 scanning.



e. Pin elevation for end 2 scanning.



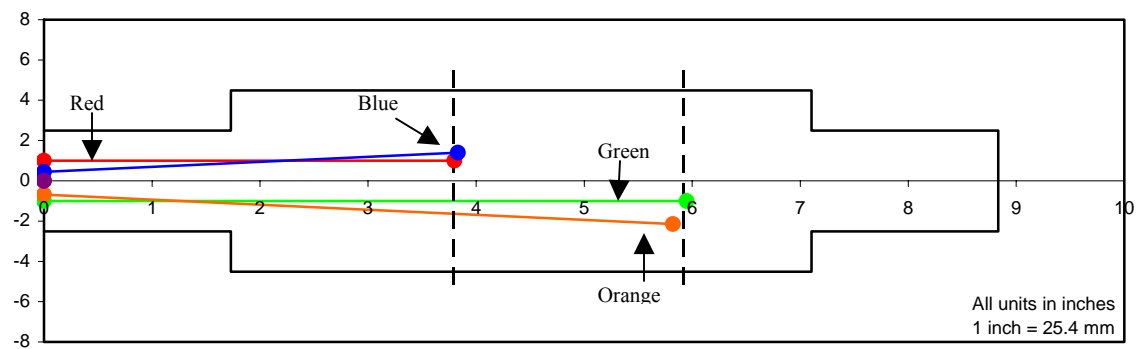
f. Pin cross section for end 2 scanning.

Figure 42. (Continued) Pin 1 testing results.

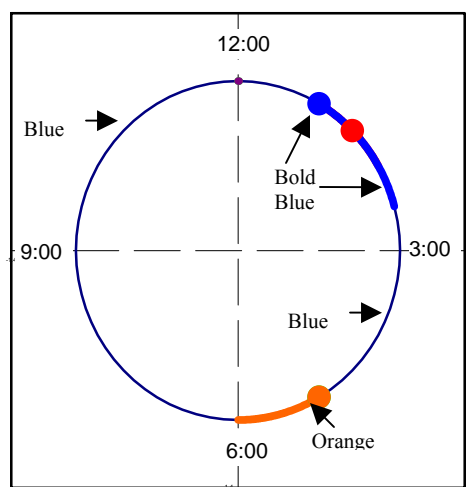
	Note	Scan angle, deg	Indication level, dB	Reference level, dB	Reading location, hh:mm	Beginning of signal location, hh:mm	End of signal location, hh:mm	Distance to index, inches	Sound path distance, inches	Axial distance, inches	Radial distance, inches
Red	1	0	58	47	1:30	1:00	2:00	1	3.80	3.80	1.00
Orange	2	0	58	47	5:00	5:00	5:00	1	5.95	5.95	1.00
Blue	3	14	43	43	1:00	1:00	2:30	7/16	3.95	3.83	1.39
Green	4	14	51	43	5:00	5:00	6:00	11/16	6.00	5.80	2.14

Unit conversion: 1 inch = 25.4 mm

a. Raw inspection data for end 1 scanning.



b. Pin elevation for end 1 scanning.



c. Pin cross section for end 1 scanning.

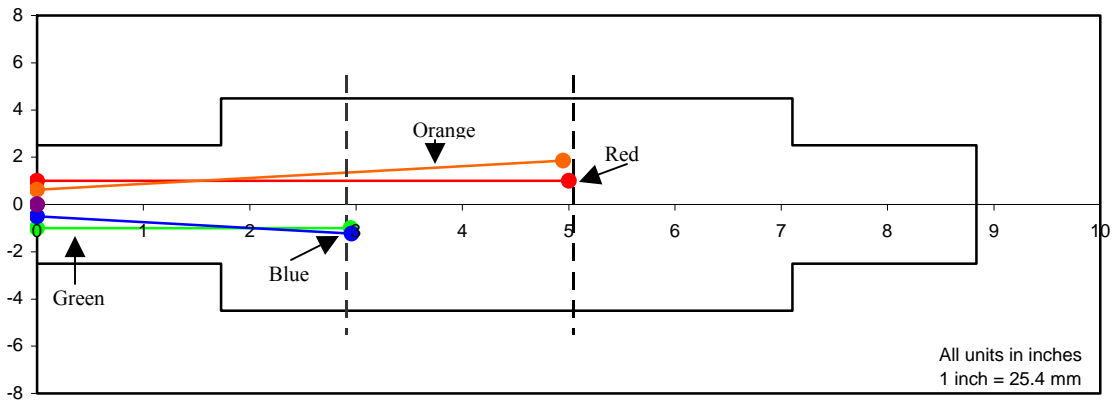
Figure 43. Pin 2 testing results.

Note	Scan angle, deg	Indication level, dB	Reference level, dB	Reading location, hh:mm	Beginning of signal location, hh:mm	End of signal location, hh:mm	Distance to index, inches	Sound path distance, inches	Axial distance, inches	Radial distance, inches
1	0	57	47	10:30	9:30	11:00	1	5.00	5.00	1.00
2	0	55	47	7:00	7:00	7:00	1	2.95	2.95	1.00
3	14	39	43	6:30	6:30	7:00	1/2	3.05	2.96	1.24
4	14	49	43	10:00	9:00	11:00	5/8	5.10	4.95	1.86

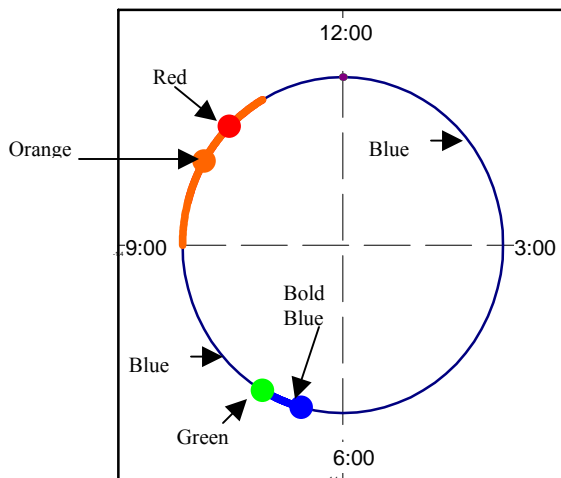
Unit conversion: 1 inch = 25.4 mm

Red →  
 Green →  
 Blue →  
 Orange →

d. Raw inspection data for end 2 scanning.



e. Pin elevation for end 2 scanning.



f. Pin cross section for end 2 scanning.

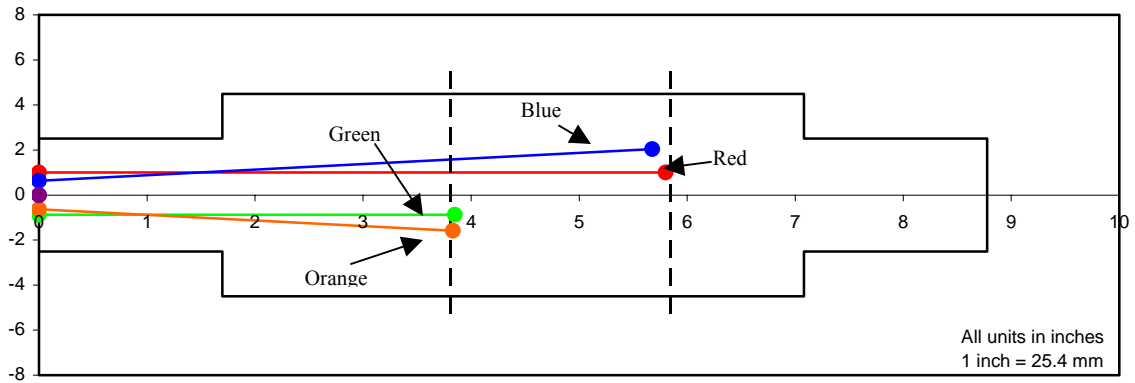
Figure 43. (Continued) Pin 2 testing results.

Note	Scan angle, deg	Indication level, dB	Reference level, dB	Reading location, hh:mm	Beginning of signal location, hh:mm	End of signal location, hh:mm	Distance to index, inches	Sound path distance, inches	Axial distance, inches	Radial distance, inches
1	0	32	58	11:00	10:30	11:30	1	5.80	5.80	1.00
2	0	42	58	5:00	4:30	6:00	7/8	3.85	3.85	0.88
3	14	38	43	10:30	10:00	11:30	5/8	5.85	5.68	2.04
4	14	36	43	4:30	4:00	6:00	5/8	3.95	3.83	1.58

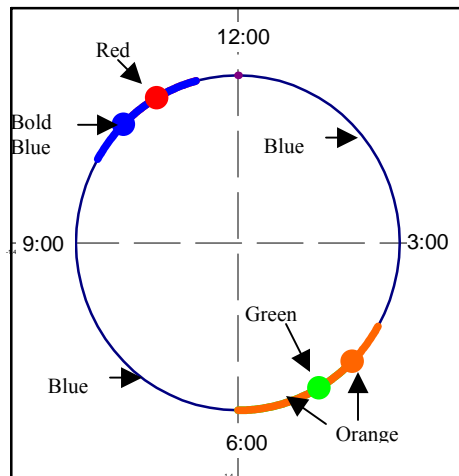
Unit conversion: 1 inch = 25.4 mm

Red →  
 Green →  
 Orange →  
 Blue →

a. Raw inspection data for end 1 scanning.



b. Pin elevation for end 1 scanning.



c. Pin cross section for end 1 scanning.

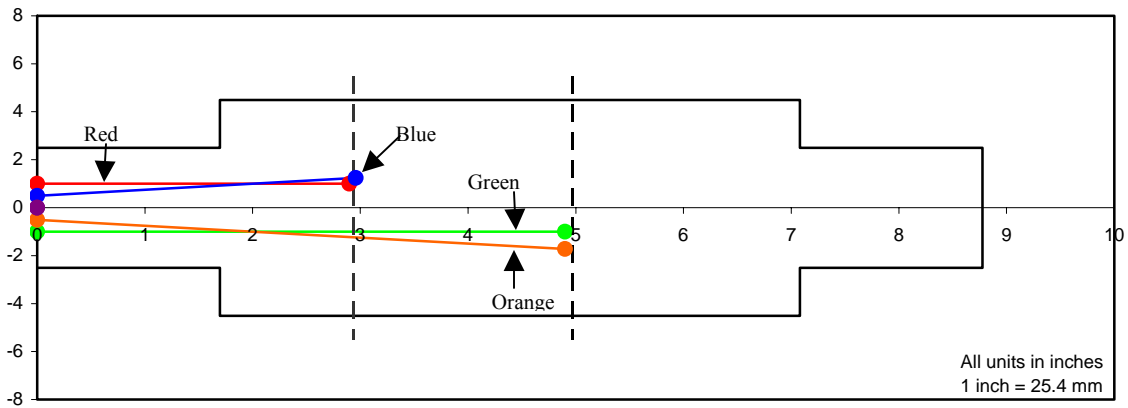
Figure 44. Pin 3 testing results.

Note	Scan angle, deg	Indication level, dB	Reference level, dB	Reading location, hh:mm	Beginning of signal location, hh:mm	End of signal location, hh:mm	Distance to index, inches	Sound path distance, inches	Axial distance, inches	Radial distance, inches
1	0	37	58	12:30	12:00	2:00	1	2.90	2.90	1.00
2	0	45	58	7:00	6:00	8:00	1	4.90	4.90	1.00
3	14	34	43	1:00	12:15	2:00	1/2	3.05	2.96	1.24
4	14	35	43	6:30	6:00	7:30	1/2	5.05	4.90	1.72

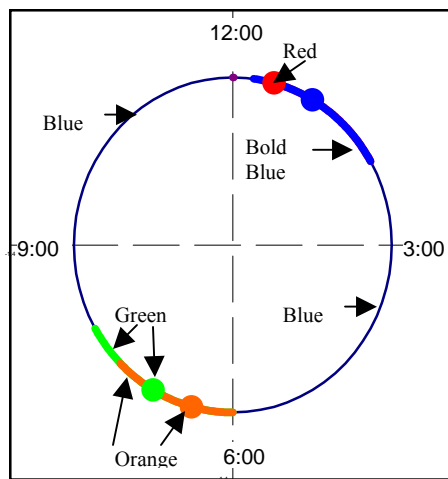
Unit conversion: 1 inch = 25.4 mm

Red →  
 Green →  
 Blue →  
 Orange →

d. Raw inspection data for end 2 scanning.



e. Pin elevation for end 2 scanning.



f. Pin cross section for end 2 scanning.

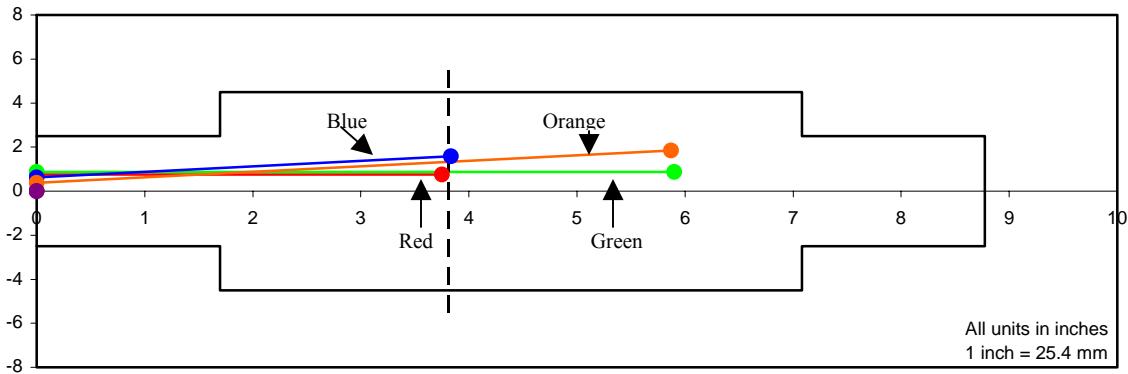
Figure 44. (Continued) Pin 3 testing results.

Note	Scan angle, deg	Indication level, dB	Reference level, dB	Reading location, hh:mm	Beginning of signal location, hh:mm	End of signal location, hh:mm	Distance to index, inches	Sound path distance, inches	Axial distance, inches	Radial distance, inches
1	0	36	58	1:00	12:30	2:00	3/4	3.75	3.75	0.75
2	0	65	58	1:00	1:00	1:00	7/8	5.90	5.90	0.88
3	14	40	43	12:30	12:00	12:30	5/8	3.95	3.83	1.58
4	14	50	43	1:00	1:00	1:30	3/8	6.05	5.87	1.84

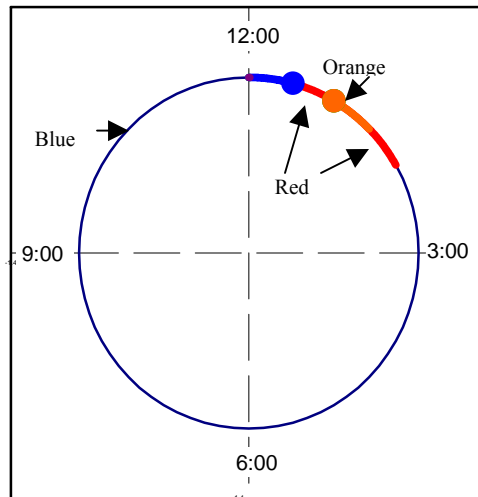
Unit conversion: 1 inch = 25.4 mm

Red →  
 Green →  
 Blue →  
 Orange →

a. Raw inspection data for end 1 scanning.



b. Pin elevation for end 1 scanning.



c. Pin cross section for end 1 scanning.

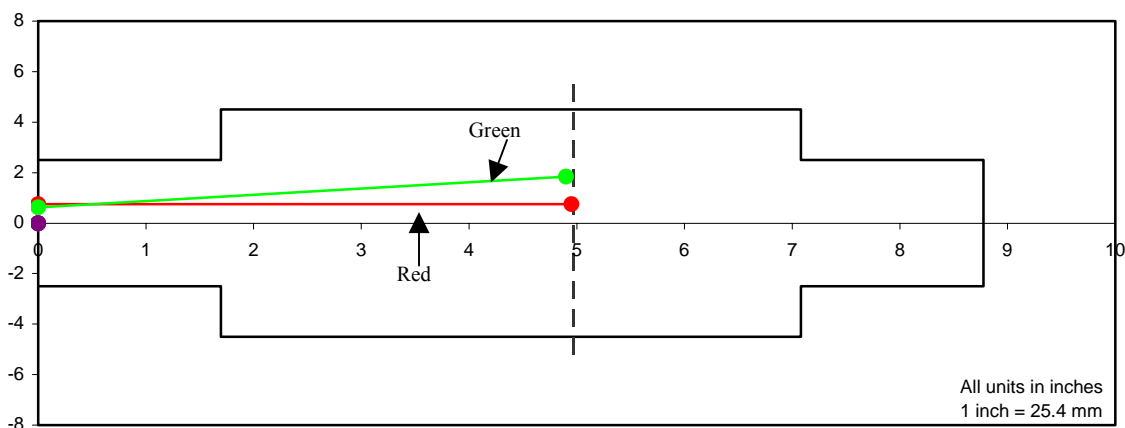
Figure 45. Pin 4 testing results.

Red →  
Green →

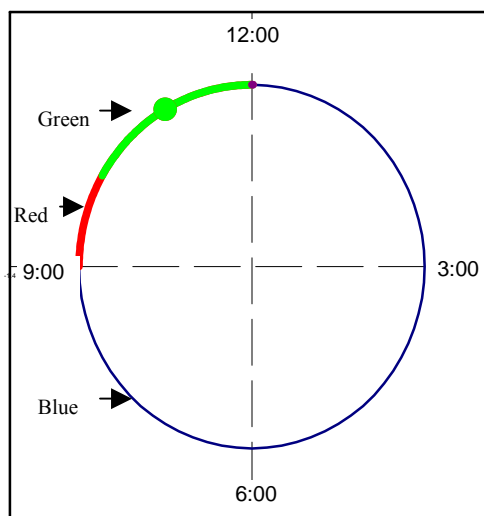
Note	Scan angle, deg	Indication level, dB	Reference level, dB	Reading location, hh:mm	Beginning of signal location, hh:mm	End of signal location, hh:mm	Distance to index, inches	Sound path distance, inches	Axial distance, inches	Radial distance, inches
1	0	30	58	11:00	9:00	12:00	3/4	4.95	4.95	0.75
2	14	42	43	11:00	10:00	12:00	5/8	5.05	4.9	1.85

Unit conversion: 1 inch = 25.4 mm

d. Raw inspection data for end 2 scanning.



e. Pin elevation for end 2 scanning.



f. Pin cross section for end 2 scanning.

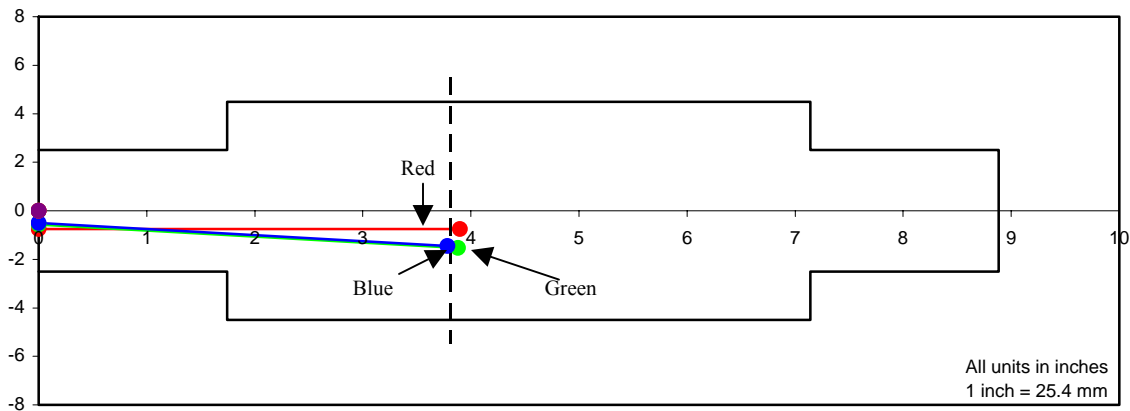
Figure 45. (Continued) Pin 4 testing results.

Red  
Green  
Blue

Note	Scan angle, deg	Indication level, dB	Reference level, dB	Reading location, hh:mm	Beginning of signal location, hh:mm	End of signal location, hh:mm	Distance to index, inches	Sound path distance, inches	Axial distance, inches	Radial distance, inches
1	0	24	56	6:30	5:45	7:00	3/4	3.90	3.90	0.75
2	14	39	43	6:00	5:30	6:30	9/16	4.00	3.85	1.53
3	14	36	43	7:00	7:00	7:00	1/2	3.90	3.78	1.44

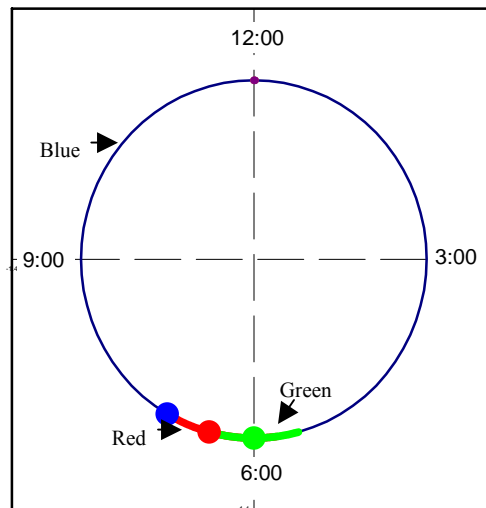
Unit conversion: 1 inch = 25.4 mm

a. Raw inspection data for end 1 scanning.



All units in inches  
1 inch = 25.4 mm

b. Pin elevation for end 1 scanning.



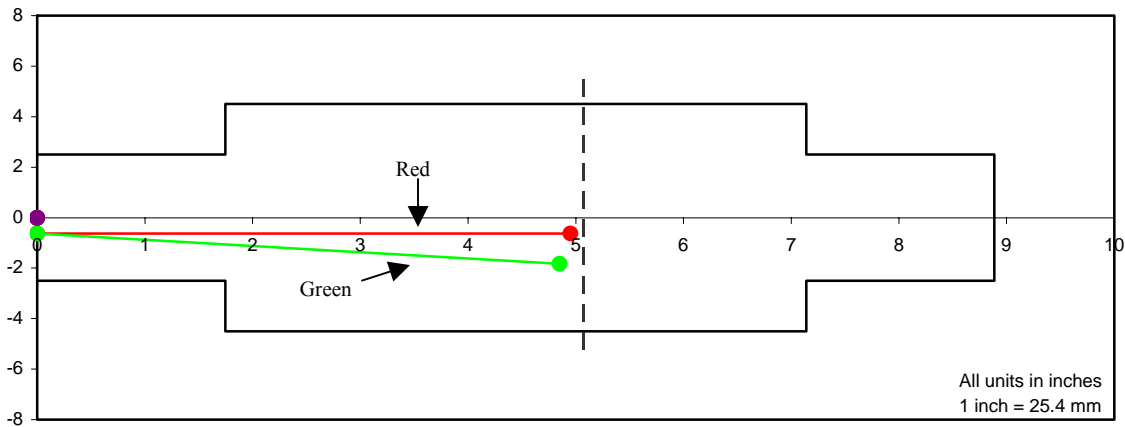
c. Pin cross section for end 1 scanning.

Figure 46. Pin 5 testing results.

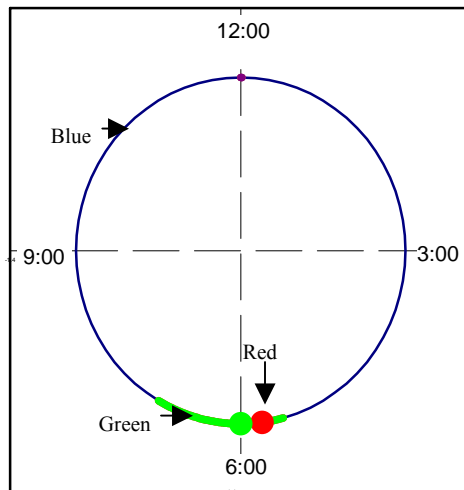
Note	Scan angle, deg	Indication level, dB	Reference level, dB	Reading location, hh:mm	Beginning of signal location, hh:mm	End of signal location, hh:mm	Distance to index, inches	Sound path distance, inches	Axial distance, inches	Radial distance, inches
1	0	29	58	5:45	5:30	7:00	5/8	4.95	4.95	0.63
2	14	40	43	6:00	5:30	7:00	5/8	5	4.85	1.83

Unit conversion: 1 inch = 25.4 mm

d. Raw inspection data for end 2 scanning.



e. Pin elevation for end 2 scanning.



f. Pin cross section for end 2 scanning.

Figure 46. (Continued) Pin 5 testing results.

#### 4.4. DEFECT SIZING

To study the ability of manual ultrasonic testing to evaluate crack sizes, the five previously described manufactured pins, with known defect sizes, were used. Further, immersion tank ultrasonic testing was also completed to provide additional data for evaluating the conventional ultrasonic test results. The results included in table 1 summarize the depth of the crack into the pin and the width of the crack around the circumference. Tables 2 and 3 give the error and the absolute value of the error, based on the as-built dimensions, for each technique. As can be seen from this data, the manual ultrasonic sizing tended to overestimate the crack size. On the other hand, the immersion tank ultrasonic sizing tended to overestimate the size of smaller cracks but underestimated the size of larger cracks. The overestimation that occurred in the immersion tank testing was most likely the result of the calibration techniques used and various geometrical constraints. The underestimation of large defects can most likely be attributed to cotter pin effects. Regardless of the technique used, for defects of similar size and shape, the sizing results are relatively consistent indicating the repeatability of the two techniques.

Table 1. Defect size data.

Specimen	Flaw Number	As-built		Immersion tank UT		Manual UT	
		Depth, inches	Width, inches	Depth, inches	Width, inches	Depth, inches	Width, inches
Pin 1	1	0.125	0.249	0.150	0.280	0.094	0.380
Pin 2	1	0.250	0.514	0.320	0.170	0.380	0.690
Pin 2	2	0.250	0.514	0.325	0.269	0.310	0.690
Pin 3	1	0.500	1.000	0.486	0.372	0.780	1.250
Pin 3	2	0.500	1.000	0.458	0.469	0.750	0.880
Pin 4	1	0.750	0.748	0.620	0.321	0.750	0.660
Pin 5	1	1.000	0.993	0.880	0.910	0.930	0.875

1 inch = 25.4 mm

Table 2. Defect sizing error.

Specimen	Flaw Number	Immersion tank UT		Manual UT	
		Depth, %	Width, %	Depth, %	Width, %
Pin 1	1	20.0	12.0	-25.0	53.0
Pin 2	1	28.0	-67.0	52.0	34.0
Pin 2	2	30.0	-48.0	24.0	34.0
Pin 3	1	-2.8	-63.0	56.0	25.0
Pin 3	2	-8.4	-53.0	50.0	-12.0
Pin 4	1	-17.0	-57.0	0.0	-12.0
Pin 5	1	-12.0	-80.0	-7.0	-12.0

Table 3. Absolute value of defect sizing error.

Specimen	Flaw Number	Immersion tank UT		Manual UT	
		Depth, %	Width, %	Depth %	Width %
Pin 1	1	20.0	12.0	25.0	53.0
Pin 2	1	28.0	67.0	52.0	34.0
Pin 2	2	30.0	48.0	24.0	34.0
Pin 3	1	2.8	63.0	56.0	25.0
Pin 3	2	8.4	53.0	50.0	12.0
Pin 4	1	17.0	57.0	0.0	12.0
Pin 5	1	12.0	8.4	7.0	12.0
Average		17.0	44.0	31.0	26.0
Standard deviation		10.0	24.0	23.0	16.0

#### 4.5. ACOUSTIC COUPLING

Photographs of the setups used during the acoustic coupling testing are shown in figures 47, 49, and 51 with the corresponding results given in figures 48, 50, and 52. As can be seen in figure 47, a 14-degree transducer in the pulse-echo format was first used to investigate the presence of acoustic coupling. Note in figure 48 the indication near the “5” gradation along the horizontal scale. As can be seen in the series of scans, as the load decreases, the intensity of the signal decreases; suggesting that the indication is load dependent. In short, the amount of sound transmitted across the interface between the pin and the test frame is dependent upon the magnitude of the applied load.

As can be seen in figure 49, the second test investigating acoustic coupling utilized two 0-degree transducers in the pitch-catch format. For this testing, if the receiving transducer picks up a signal, then it is clear that a signal from the transmitter is crossing the interface between the pin and the test frame. As can be seen in figure 50, this is the case and is, as before, load dependent. Similarly, the setup shown in figure 51 with corresponding data in figure 52 further illustrates the presence of acoustic coupling under a decreasing load.

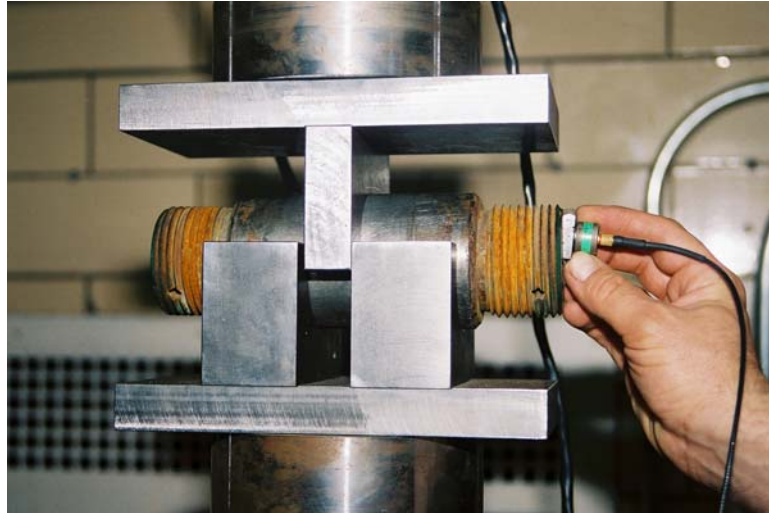
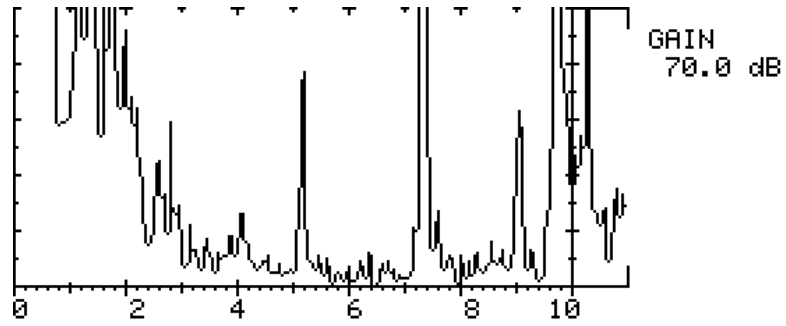
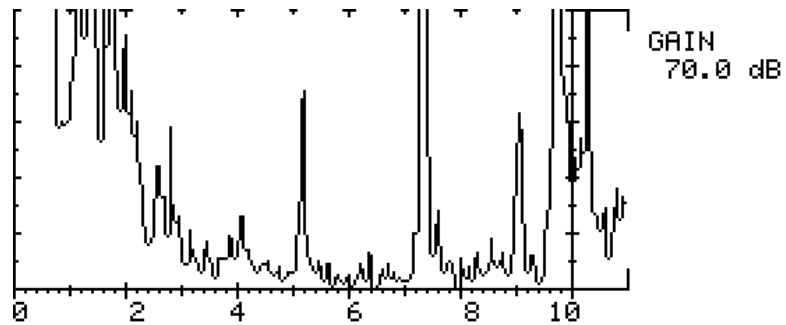


Figure 47. Photograph of pulse-echo setup using 14-degree transducer.



1 KN = 225 pounds

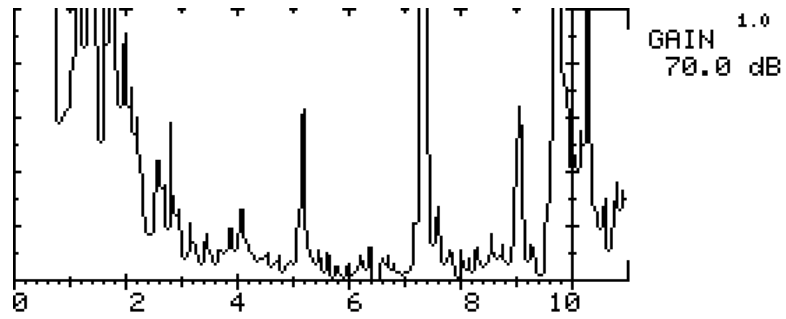
a. Load step 1: 88.96 Kilonewton (KN).



1 KN = 225 pounds

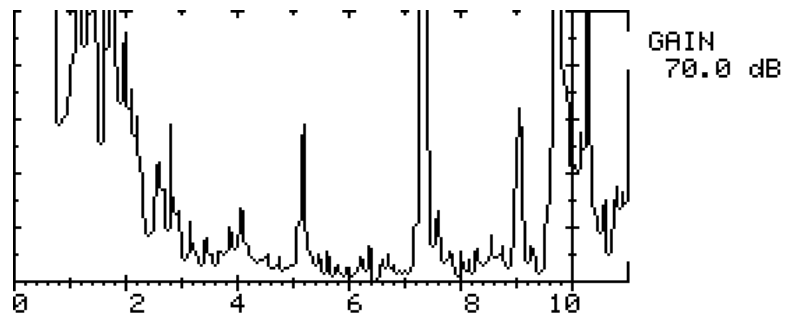
b. Load step 2: 84.51 KN.

Figure 48. UT scan utilizing pulse-echo technique with a 14-degree transducer.



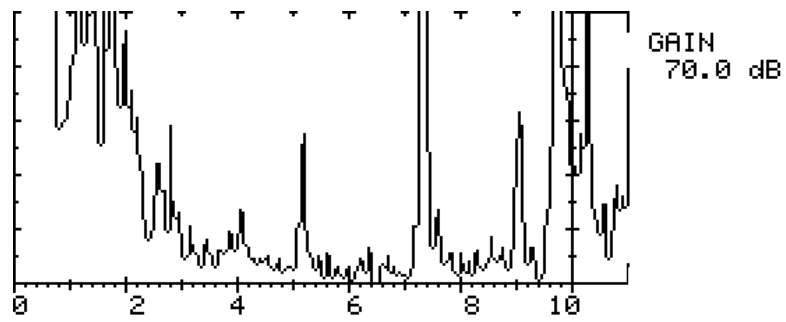
1 KN = 225 pounds

c. Load step 3: 80.07 KN.



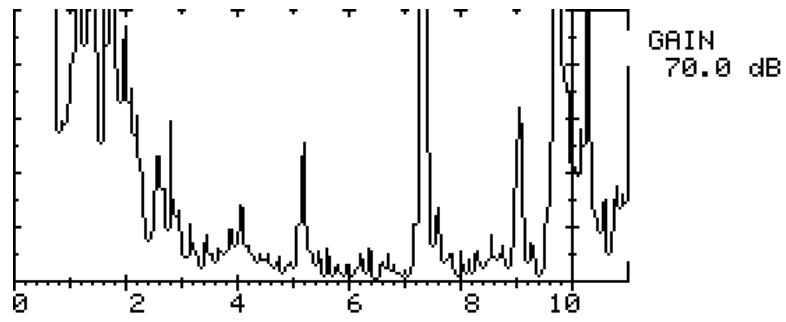
1 KN = 225 pounds

d. Load step 4: 75.62 KN.



1 KN = 225 pounds

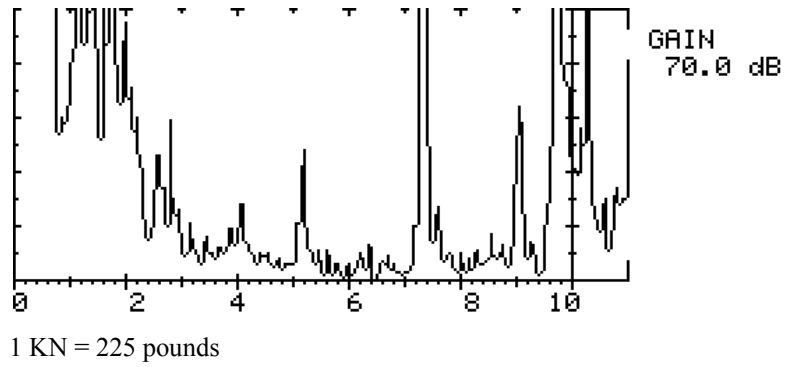
e. Load step 5: 71.17 KN.



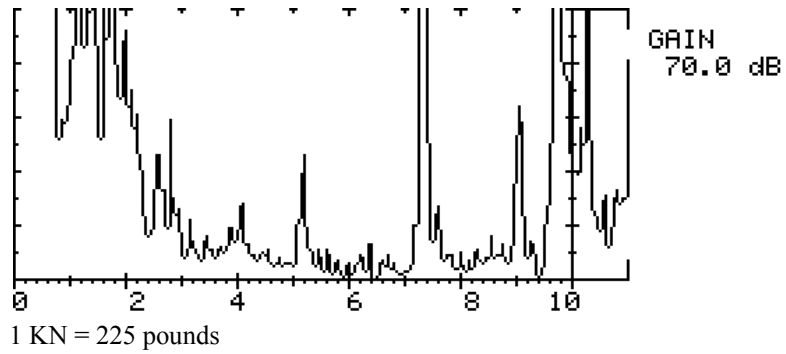
1 KN = 225 pounds

f. Load step 6: 66.72 KN.

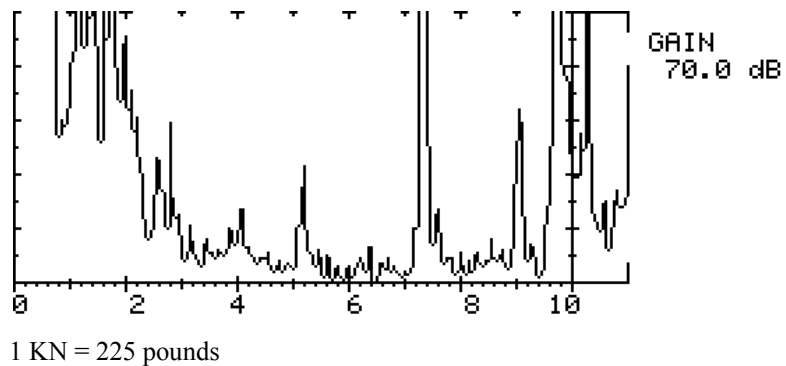
Figure 48. (Continued) UT scan utilizing pulse-echo technique with a 14-degree transducer.



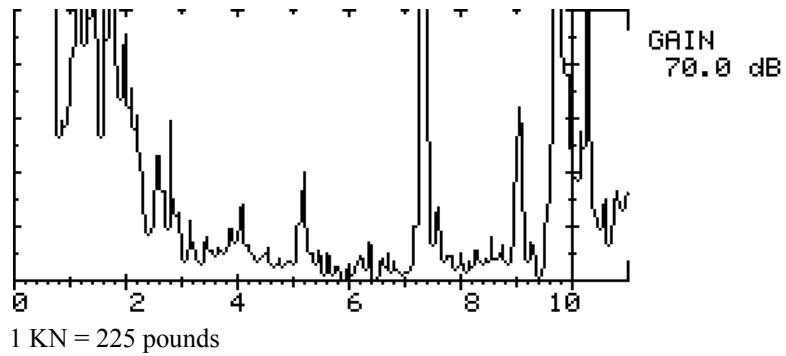
g. Load step 7: 62.28 KN.



h. Load step 8: 57.83.

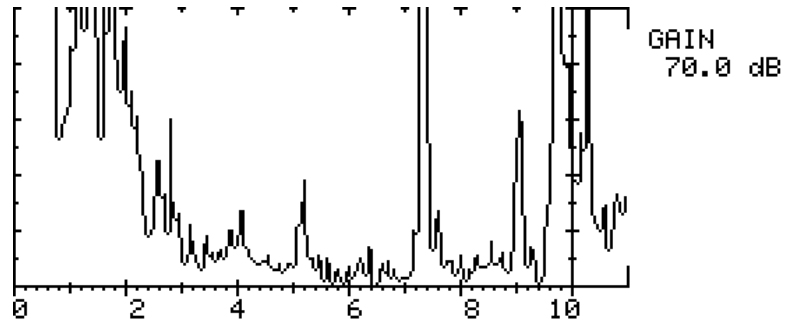


i. Load step 9: 53.38 KN.



j. Load step 10: 48.93 KN.

Figure 48. (Continued) UT scan utilizing pulse-echo technique with a 14-degree transducer.



1 KN = 225 pounds

k. Load step 11: 44.48 KN.

Figure 48. (Continued) UT scan utilizing pulse-echo technique with a 14-degree transducer.

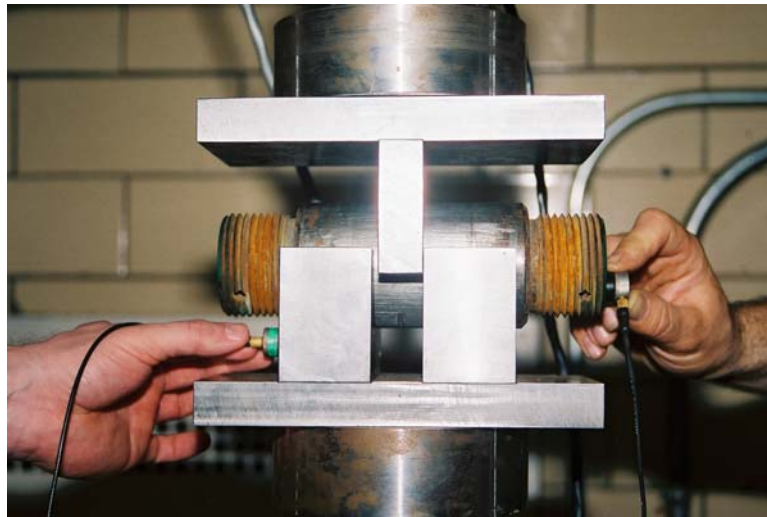
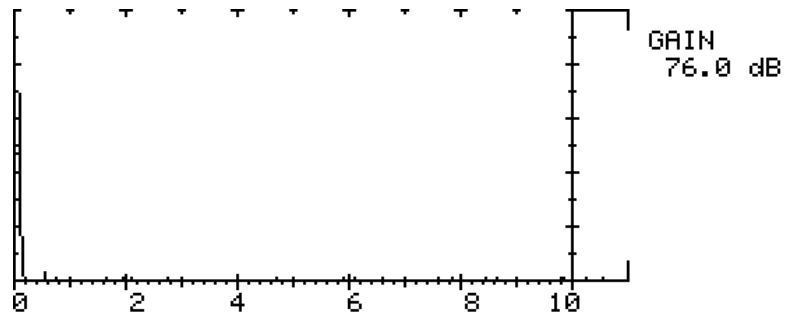


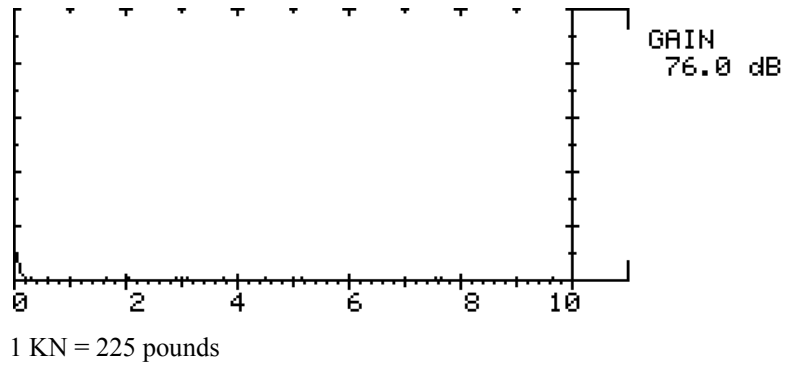
Figure 49. Photograph of pitch-catch setup using 0-degree transducers.



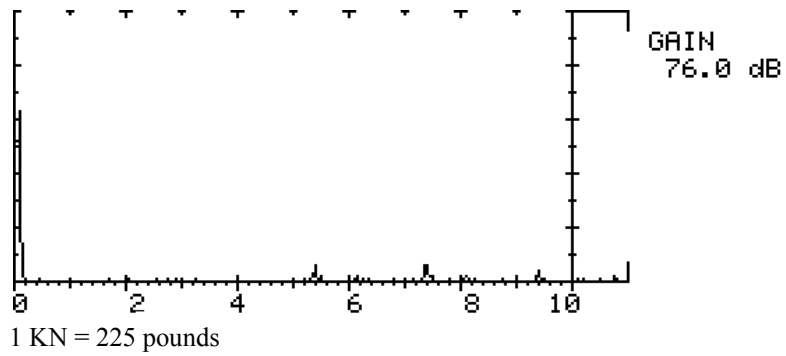
1 KN = 225 pounds

a. Load step 1: 0.00 KN.

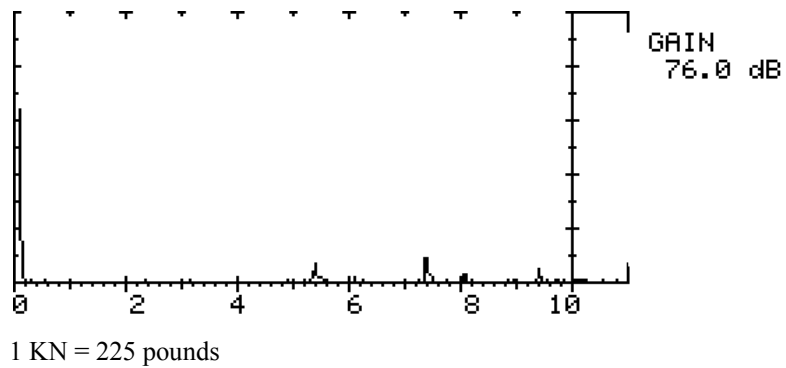
Figure 50. UT scan utilizing pitch-catch technique using 0-degree transducers.



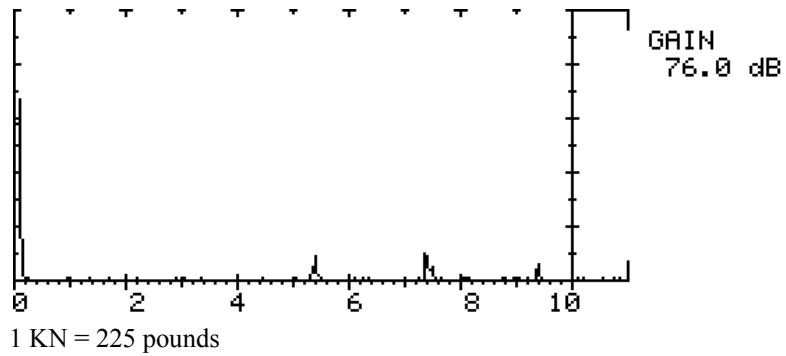
b. Load step 2: 8.89 KN.



c. Load step 3: 13.34 KN.

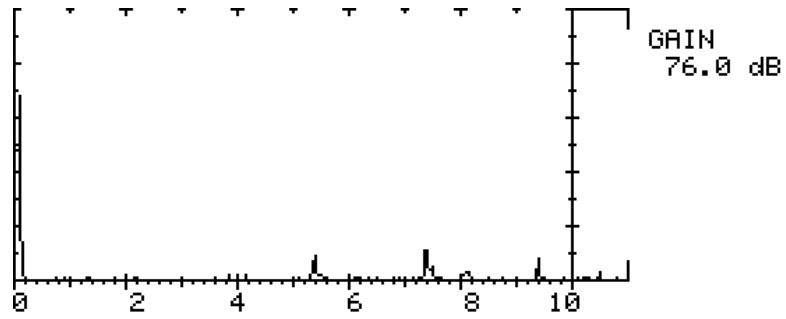


d. Load step 4: 17.79 KN.



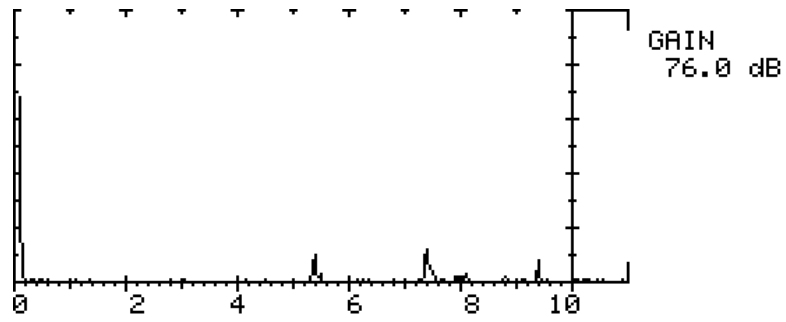
e. Load step 5: 22.24 KN.

Figure 50. (Continued) UT scan utilizing pitch-catch technique using 0-degree transducers.



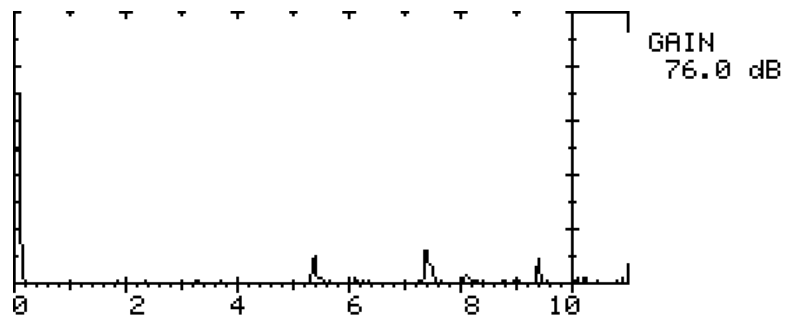
1 KN = 225 pounds

f. Load step 6: 26.69 KN.



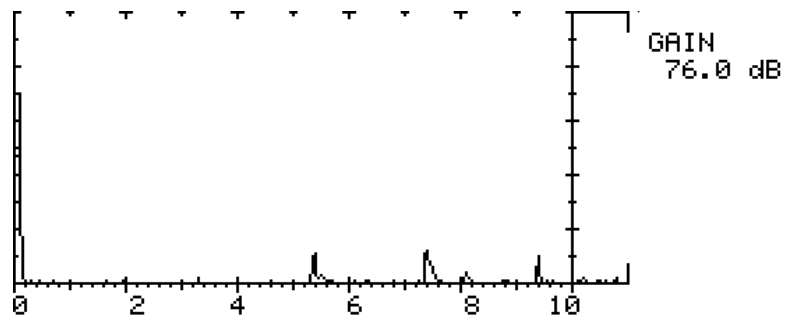
1 KN = 225 pounds

g. Load step 7: 31.14 KN.



1 KN = 225 pounds

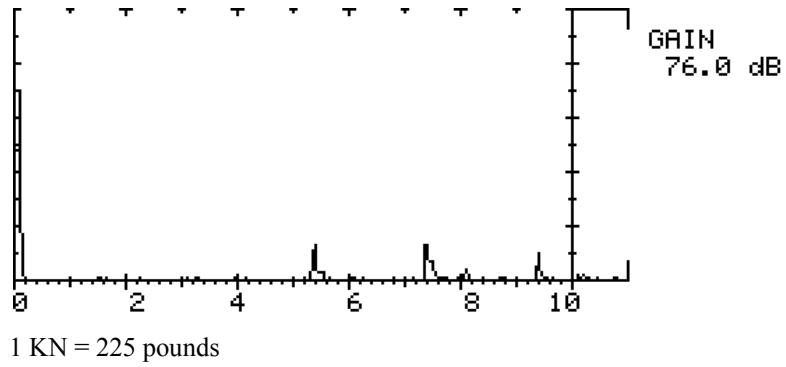
h. Load step 8: 35.59 KN.



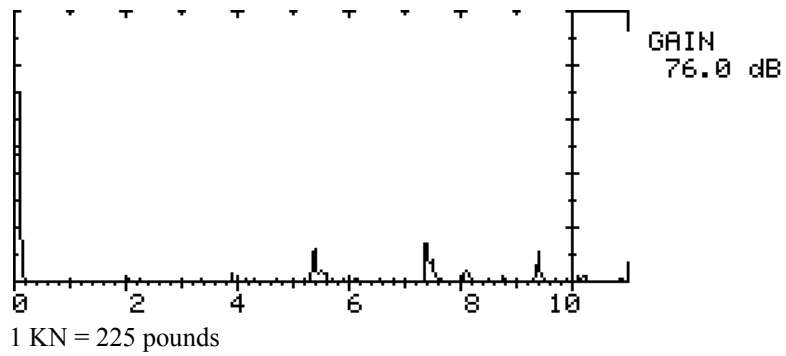
1 KN = 225 pounds

i. Load step 9: 40.03 KN.

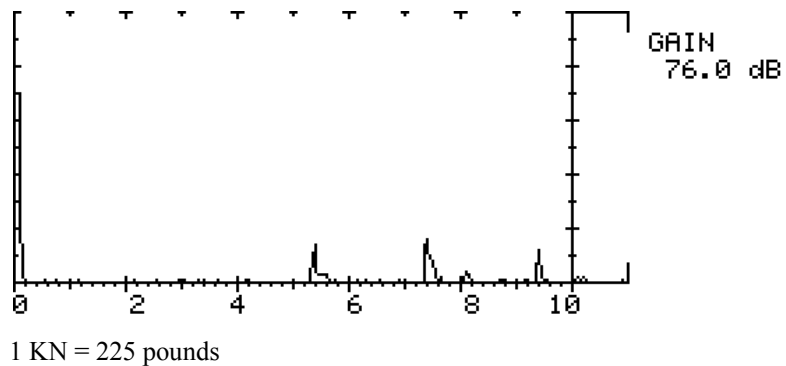
Figure 50. (Continued) UT scan utilizing pitch-catch technique using 0-degree transducers.



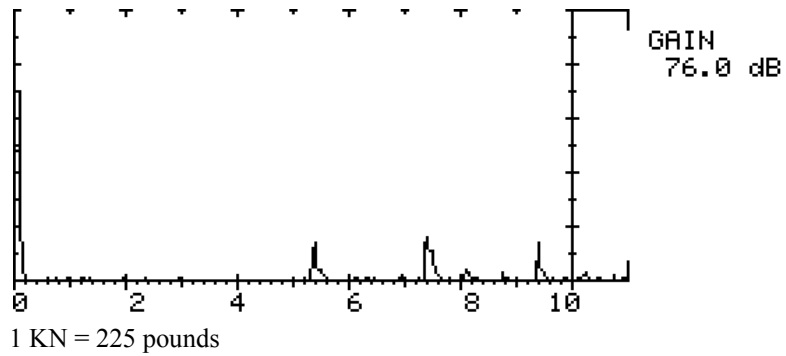
j. Load step 10: 44.48 KN.



k. Load step 11: 48.93 KN.

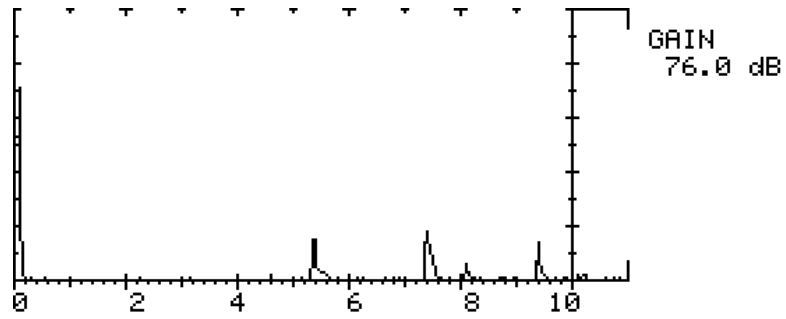


l. Load step 12: 53.38 KN.



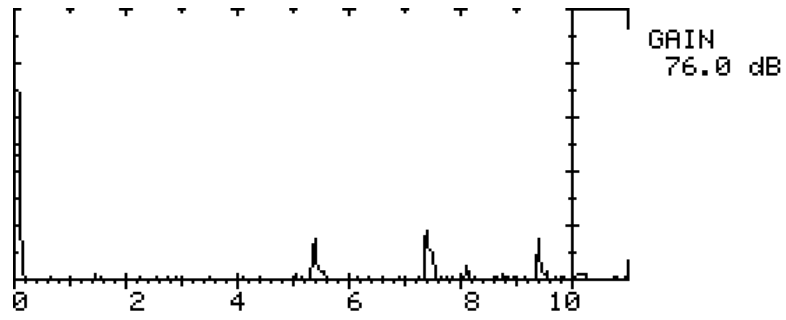
m. Load step 13: 57.82 KN.

Figure 50. (Continued) UT scan utilizing pitch-catch technique using 0-degree transducers.



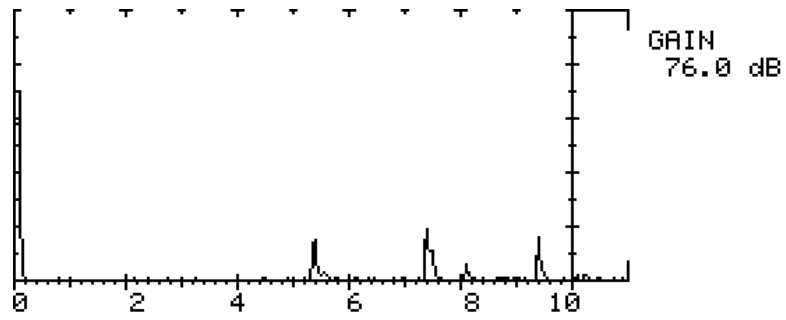
1 KN = 225 pounds

n. Load step 14: 62.28 KN.



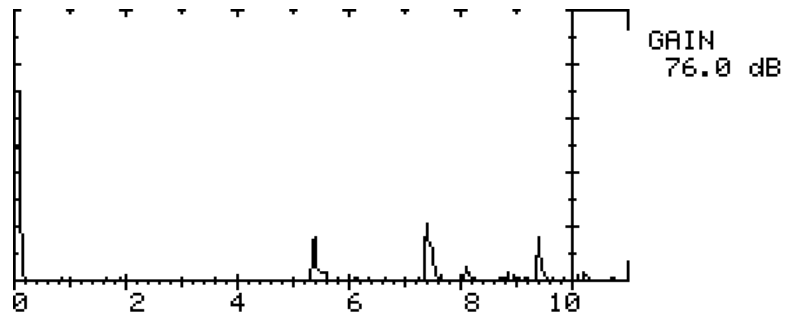
1 KN = 225 pounds

o. Load step 15: 66.72 KN.



1 KN = 225 pounds

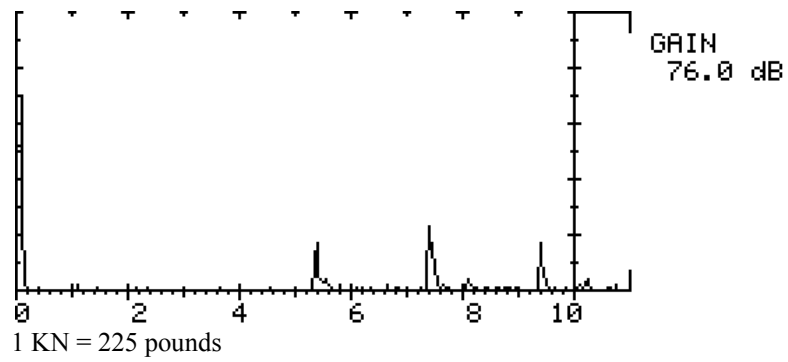
p. Load step 16: 71.17 KN.



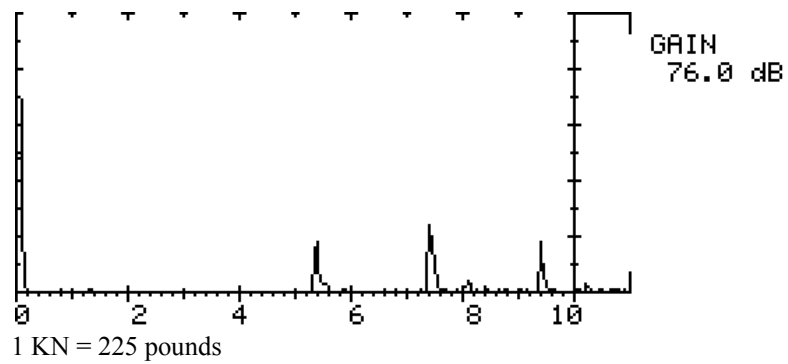
1 KN = 225 pounds

q. Load step 17: 75.62 KN.

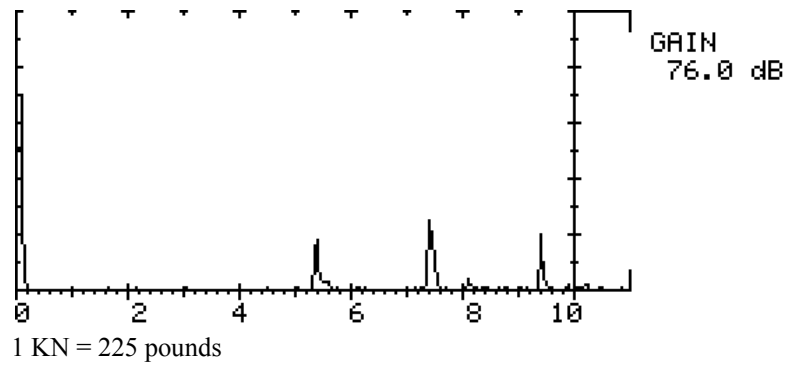
Figure 50. (Continued) UT scan utilizing pitch-catch technique using 0-degree transducers.



r. Load step 18: 80.07 KN.



s. Load step 19: 84.52 KN.



t. Load step 20: 88.96 KN.

Figure 50. (Continued) UT scan utilizing pitch-catch technique using 0-degree transducers.

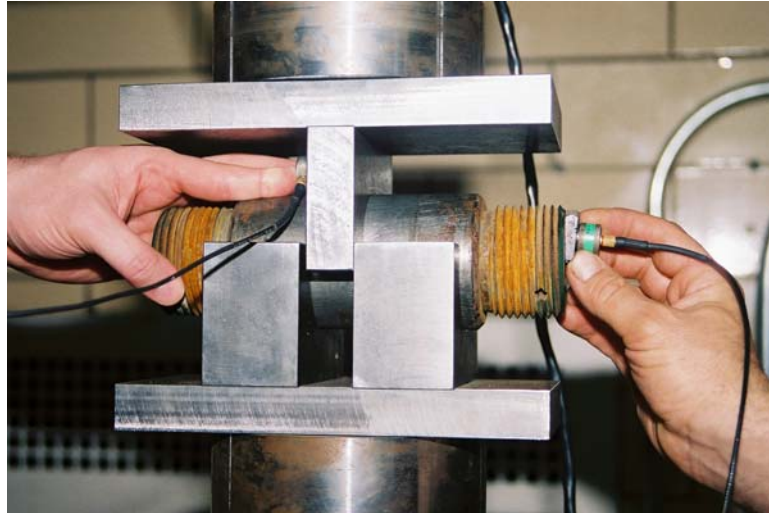
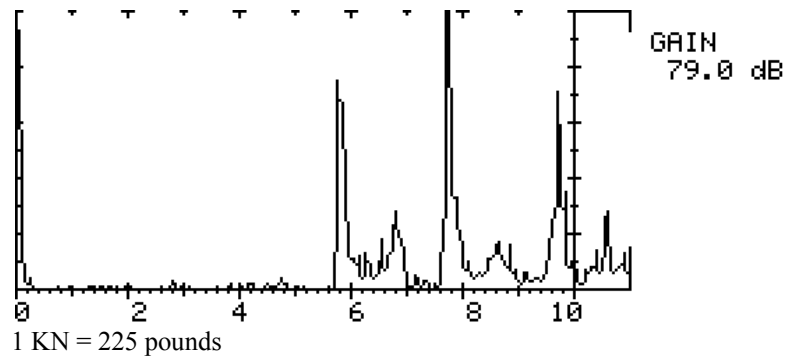
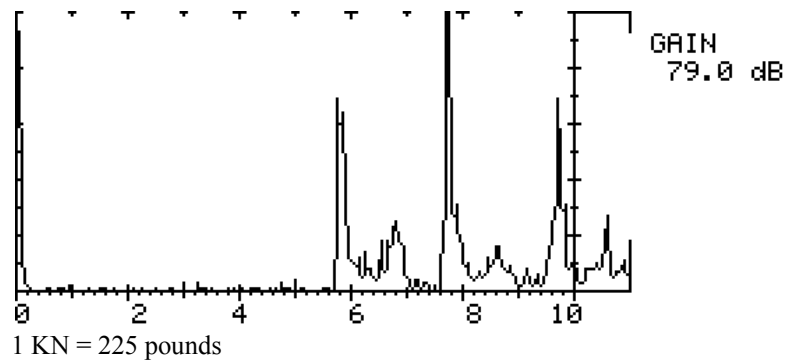


Figure 51. Photograph of pitch-catch setup using 0-degree receiving and 14-degree transmitting transducers.

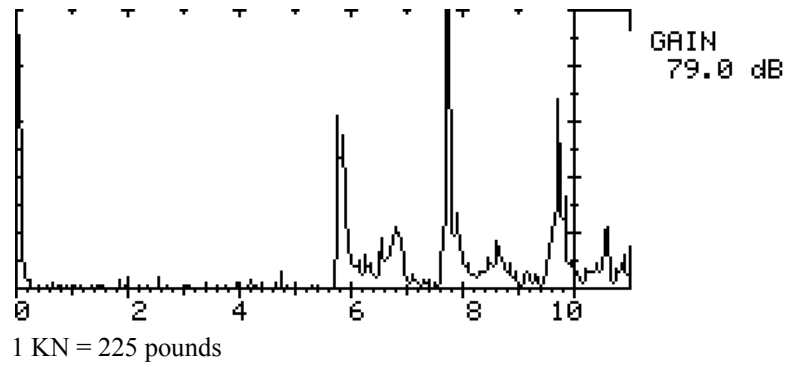


a. Load step 1: 88.96 KN.

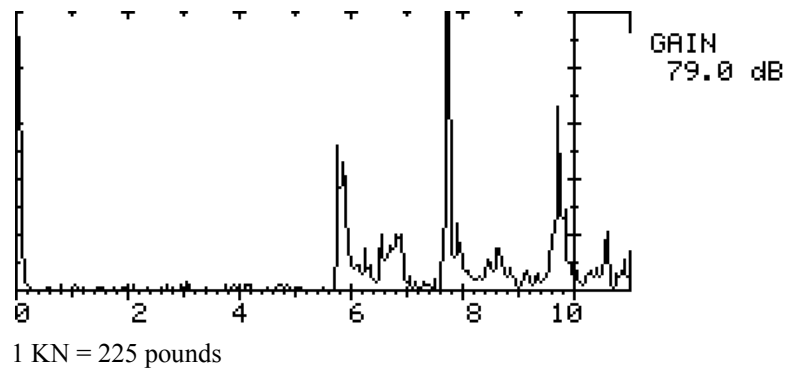


b. Load step 2: 84.52 KN.

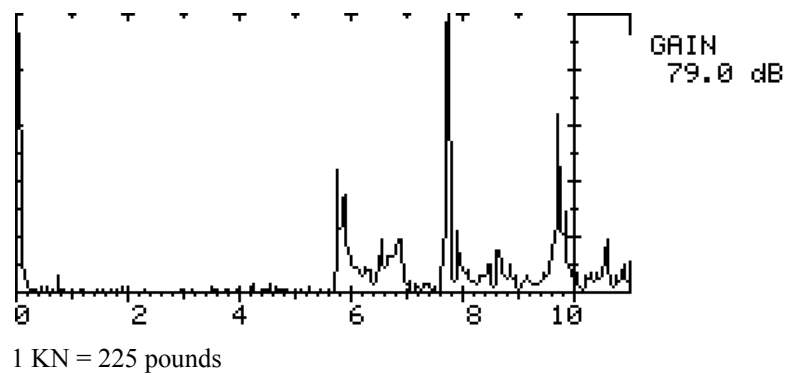
Figure 52. UT scan utilizing pitch-catch technique using 0-degree and 14-degree transducers.



c. Load step 3: 80.07 KN.

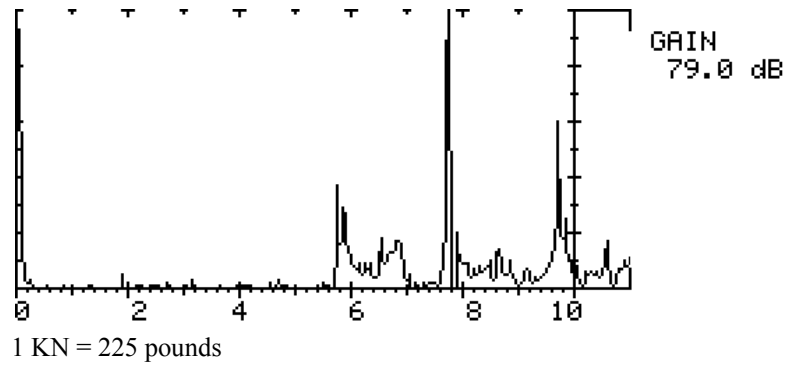


d. Load step 4: 75.62 KN.

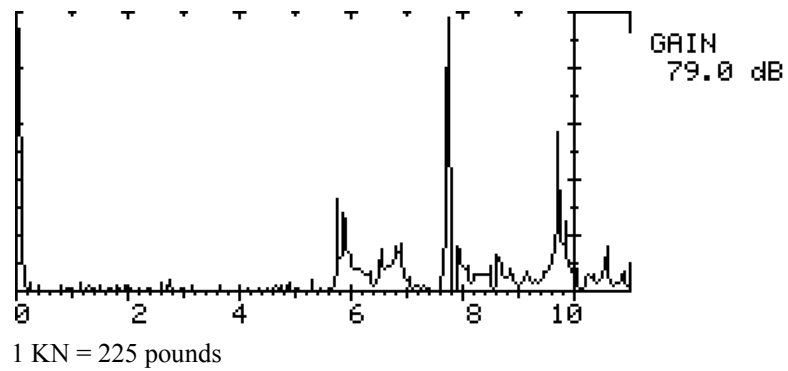


e. Load step 5: 71.17 KN.

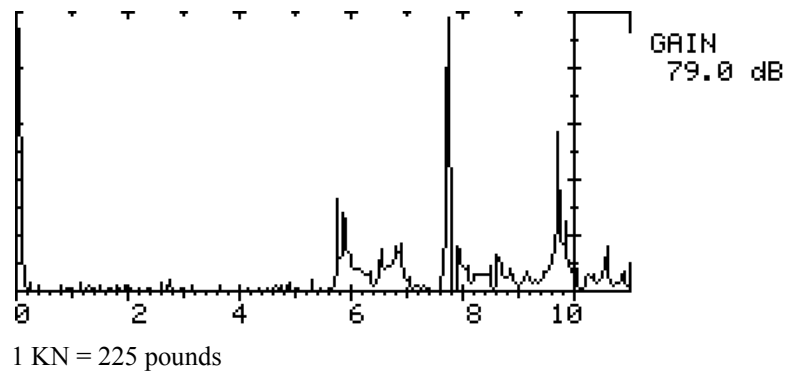
Figure 52. (Continued) UT scan utilizing pitch-catch technique using 0-degree and 14-degree transducers.



f. Load step 6: 66.72 KN.

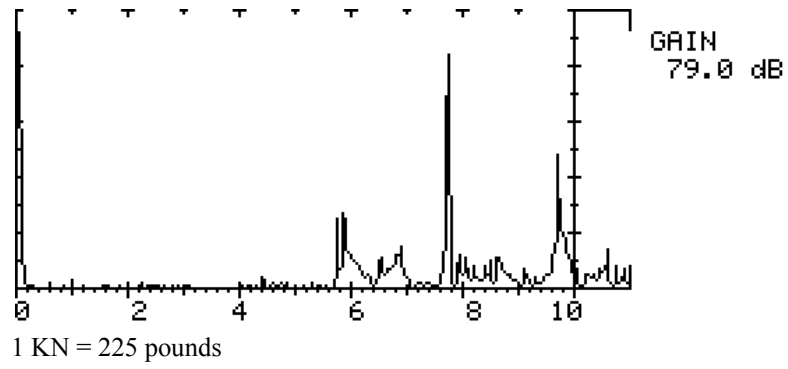


g. Load step 7: 62.28 KN.

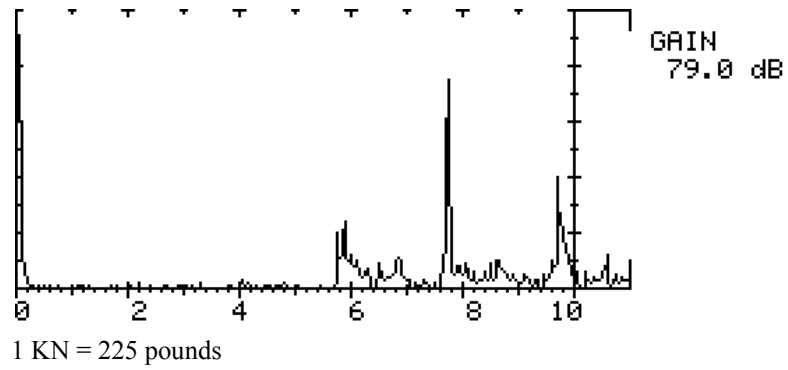


h. Load step 8: 57.83 KN.

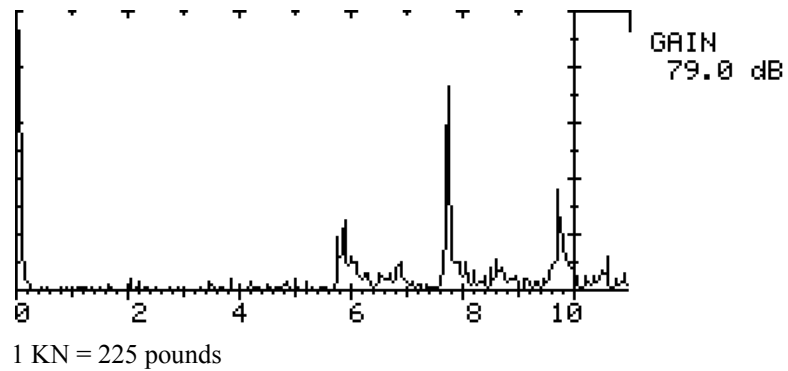
Figure 52. (Continued) UT scan utilizing pitch-catch technique using 0-degree and 14-degree transducers.



i. Load step 9: 53.38 KN.

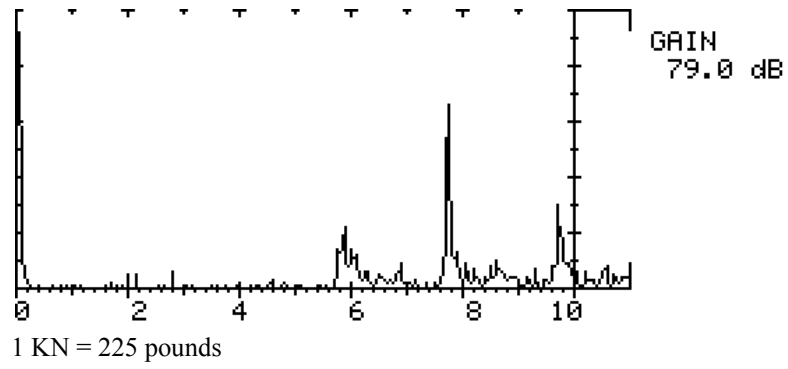


j. Load step 10: 48.93 KN.

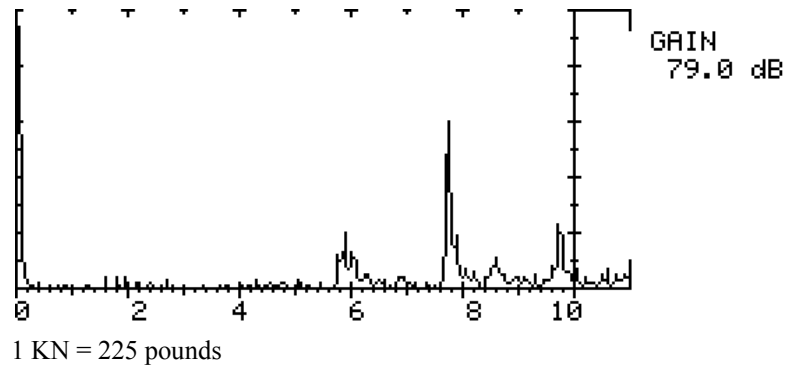


k. Load step 11: 44.48 KN.

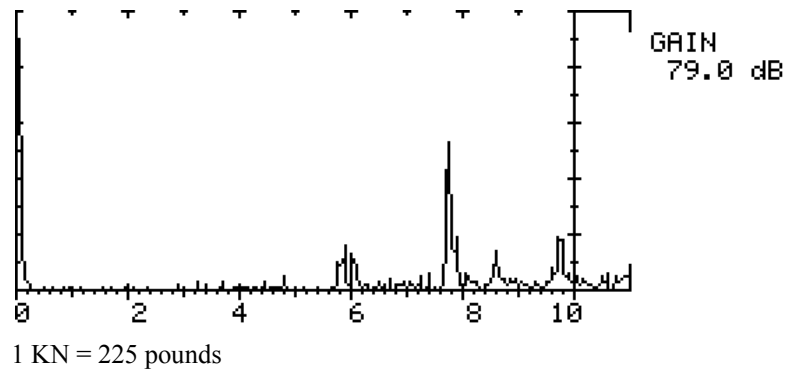
Figure 52. (Continued) UT scan utilizing pitch-catch technique using 0-degree and 14-degree transducers.



l. Load step 12: 40.03 KN.

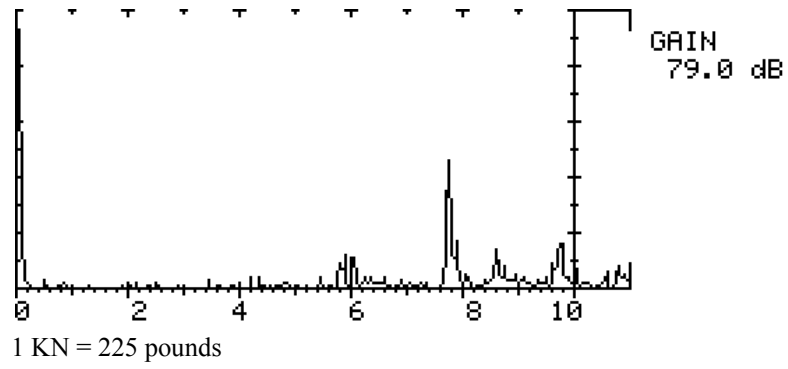


m. Load step 13: 35.59 KN.

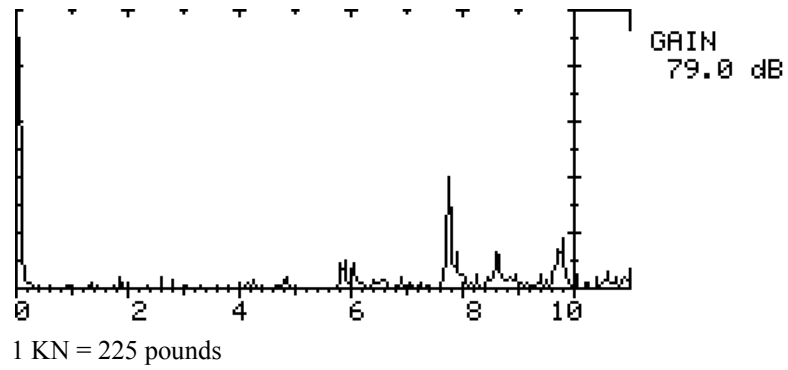


n. Load step 14: 31.14 KN.

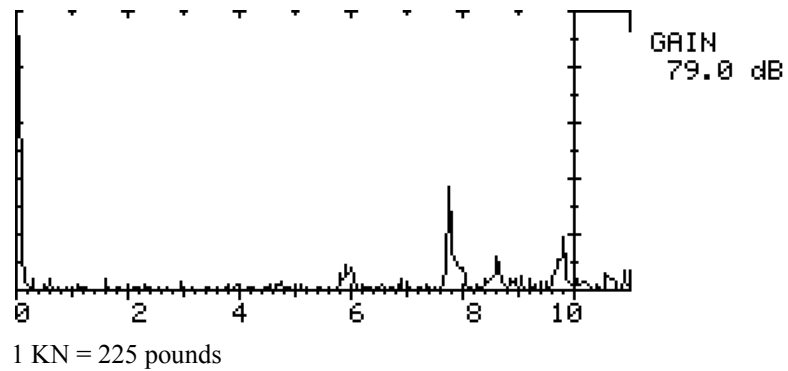
Figure 52. (Continued) UT scan utilizing pitch-catch technique using 0-degree and 14-degree transducers.



o. Load step 15: 26.69 KN.

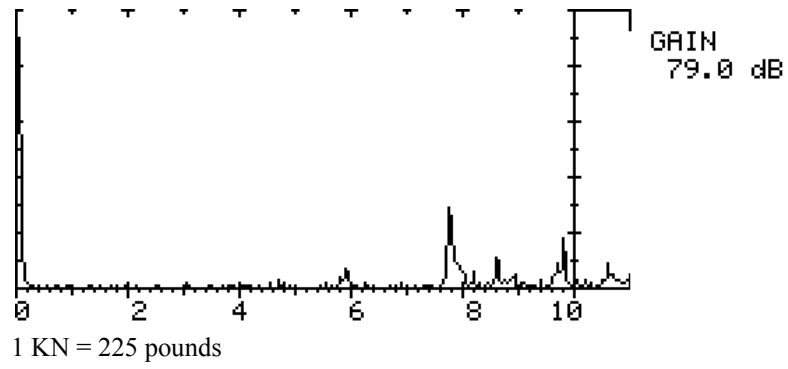


p. Load step 16: 22.24 KN.

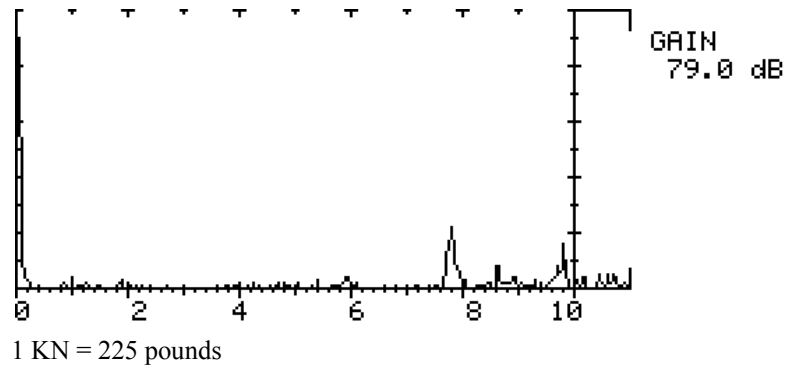


q. Load step 17: 17.79 KN.

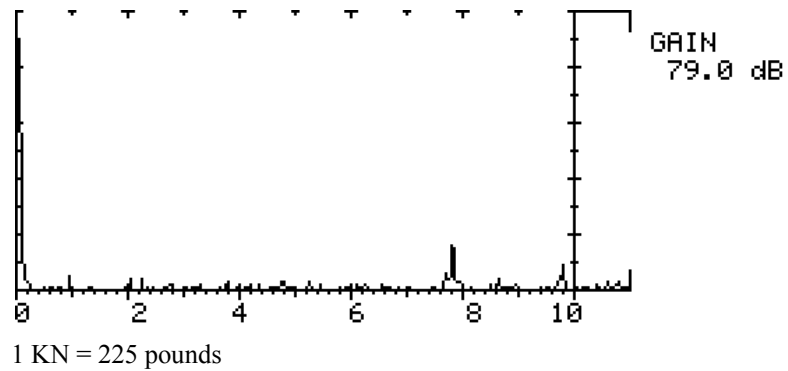
Figure 52. (Continued) UT scan utilizing pitch-catch technique using 0-degree and 14-degree transducers.



r. Load step 18: 13.34 KN.

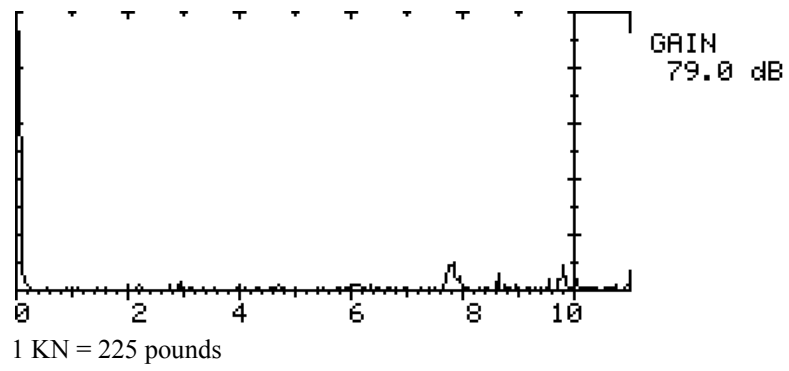


s. Load step 19: 8.90 KN.



t. Load step 20: 4.45 KN.

Figure 52. (Continued) UT scan utilizing pitch-catch technique using 0-degree and 14-degree transducers.



u. Load step 21: 0.00 KN.

Figure 52. (Continued) UT scan utilizing pitch-catch technique using 0-degree and 14-degree transducers.



## **5. CONCLUDING REMARKS**

The information presented herein should be useful for State departments of transportation and organizations providing ultrasonic testing services. Although not all-inclusive, this document summarizes the important aspects of ultrasonic testing of pins and can enhance the more effective use of inspection resources and inspection results. In addition, the laboratory testing completed as part of this study should be useful in understanding the mechanics of ultrasonic testing. Further, the concrete and indisputable evidence of acoustic coupling should allow ultrasonic testing results to be interpreted more accurately.